Extreme Measures:

Mechanisms driving changes in climate extremes in Australia

By

Lisa Victoria Alexander BSc (Hons), MSc

A thesis submitted in partial fulfillment of the
requirements for the degree of Doctor of Philosophy

School of Geography and Environmental Science
Monash University

February 2009

To be is to do

Socrates

To do is to be

Sartre

Do be do be do

Sinatra

Monash Research Graduate School

Declaration for thesis based or partially based on conjointly published or unpublished work

General Declaration

In accordance with Monash University Doctorate Regulation 17 / Doctor of Philosophy and Master of Philosophy (MPhil) regulations the following declarations are made:

I hereby declare that this thesis contains no material which has been accepted for the award of any other degree or diploma at any university or equivalent institution and that, to the best of my knowledge and belief, this thesis contains no material previously published or written by another person, except where due reference is made in the text of the thesis.

This thesis includes three original papers published or in press in peer reviewed journals and one submitted unpublished publication. These sections are identified and listed in the table below along with my contribution to the work. The ideas, development and writing up of all the papers in the thesis were the principal responsibility of myself, the candidate, working within the School of Geography and Environmental Science under the supervision of Prof. Amanda Lynch.

Thesis chapter	**Publication title**	**Publication status**	**Nature and extent of candidate's contribution**
2	Alexander LV, Hope P, Collins D, Trewin B, Lynch A, Nicholls N. 2007. Trends in Australia's climate means and extremes: a global context. *Australian Meteorological Magazine* **56**: 1-18.	Published	Formulation of research problem and the context of the research in the wider literature: data gathering, statistical analysis, production of figures, interpretation of results and writing.
C	Alexander LV, Power S. 2009. Severe storms inferred from 150 years of sub-daily pressure observations along Victoria's "Shipwreck Coast". *Australian Meteorological Magazine*	Accepted subject to minor revisions	Formulation of research problem and the context of the research in the wider literature: data quality control, analysis and writing.
3	Alexander LV, Uotila P, Nicholls N, Lynch A. Diagnosing the synoptic influences driving changes in climate extremes over southern Australia during the last century. 2009. *Journal of Climate*.	Submitted	Formulation of research problem and the context of the research in the wider literature: quality control and homogenisation of observations, analysis of synoptic patterns in relation to extreme events, interpretation of results and writing.
5	Alexander LV, Arblaster JM. 2008. Assessing trends in observed and modelled climate extremes over Australia in relation to future projections. *International Journal of Climatology* DOI: 10.1002/joc.1730	Published (on-line)	Formulation of research problem and the context of the research in the wider literature: description and analysis of observations in relation to model output.

Signed: _____ Date: _____

Declaration for Publication 1

Declaration by candidate

In the case of "Alexander LV, Hope P, Collins D, Trewin B, Lynch A, Nicholls N. 2007. Trends in Australia's climate means and extremes: a global context. *Australian Meteorological Magazine* **56**: 1-18", the nature and extent of my contribution to the work was the following:

Nature of contribution	Extent of contribution (%)
Formulation of research problem and the context of the research in the wider literature: data gathering, statistical analysis, production of figures, interpretation of results and writing.	60%

The following co-authors contributed to the work. Co-authors who are students at Monash University must also indicate the extent of their contribution in percentage terms:

Name	Nature of contribution
Pandora Hope	Formulation of research problem and the context of the research in the wider literature: data gathering, statistical analysis, interpretation of results and writing.
Dean Collins	Formulation of research problem and the context of the research in the wider literature: provision of updated observations and interpretation of results.
Blair Trewin	Formulation of research problem and the context of the research in the wider literature: interpretation of results.
Amanda Lynch	Formulation of research problem and the context of the research in the wider literature: interpretation of results.
Neville Nicholls	Formulation of research problem and the context of the research in the wider literature: interpretation of results.

Candidate's Signature		**Date**

Declaration by co-authors

The undersigned hereby certify that:

(1) the above declaration correctly reflects the nature and extent of the candidate's contribution to this work, and the nature of the contribution of each of the co-authors.
(2) they meet the criteria for authorship in that they have participated in the conception, execution, or interpretation, of at least that part of the publication in their field of expertise;
(3) they take public responsibility for their part of the publication, except for the responsible author who accepts overall responsibility for the publication;
(4) there are no other authors of the publication according to these criteria;
(5) potential conflicts of interest have been disclosed to (a) granting bodies, (b) the editor or publisher of journals or other publications, and (c) the head of the responsible academic unit; and
(6) the original data are stored at the following location(s) and will be held for at least five years from the date indicated below:

Location(s)	**Monash University**

Signature 1		**Date**
Signature 2		
Signature 3		
Signature 4		
Signature 5		

Declaration for Publication 2

Declaration by candidate

In the case of "Alexander LV, Power S. 2009. Severe storms inferred from 150 years of sub-daily pressure observations along Victoria's "Shipwreck Coast". *Australian Meteorological Magazine*", the nature and extent of my contribution to the work was the following:

Nature of contribution	Extent of contribution (%)
Formulation of research problem and the context of the research in the wider literature: data quality control, analysis and writing.	90%

The following co-authors contributed to the work. Co-authors who are students at Monash University must also indicate the extent of their contribution in percentage terms:

Name	Nature of contribution
Scott Power	Formulation of research problem and the context of the research in the wider literature: interpretation of results.

Candidate's Signature		**Date**

Declaration by co-authors

The undersigned hereby certify that:

(1) the above declaration correctly reflects the nature and extent of the candidate's contribution to this work, and the nature of the contribution of each of the co-authors.
(2) they meet the criteria for authorship in that they have participated in the conception, execution, or interpretation, of at least that part of the publication in their field of expertise;
(3) they take public responsibility for their part of the publication, except for the responsible author who accepts overall responsibility for the publication;
(4) there are no other authors of the publication according to these criteria;
(5) potential conflicts of interest have been disclosed to (a) granting bodies, (b) the editor or publisher of journals or other publications, and (c) the head of the responsible academic unit; and
(6) the original data are stored at the following location(s) and will be held for at least five years from the date indicated below:

Location(s)	**Monash University**

Signature 1		**Date**

Declaration for Publication 3

Declaration by candidate

In the case of "Alexander LV, Uotila P, Nicholls N, Lynch A. Diagnosing the synoptic influences driving changes in climate extremes over southern Australia during the last century. 2009. *Journal of Climate*", the nature and extent of my contribution to the work was the following:

Nature of contribution	**Extent of contribution (%)**
Formulation of research problem and the context of the research in the wider literature: quality control and homogenisation of observations, analysis of synoptic patterns in relation to extreme events, interpretation of results and writing.	70%

The following co-authors contributed to the work. Co-authors who are students at Monash University must also indicate the extent of their contribution in percentage terms:

Name	**Nature of contribution**
Petteri Uotila	Formulation of research problem and the context of the research in the wider literature: construction of SOM algorithm software, analysis and interpretation of results.
Neville Nicholls	Formulation of research problem and the context of the research in the wider literature: interpretation of results.
Amanda Lynch	Formulation of research problem and the context of the research in the wider literature.

Candidate's Signature		**Date**

Declaration by co-authors

The undersigned hereby certify that:

(1) the above declaration correctly reflects the nature and extent of the candidate's contribution to this work, and the nature of the contribution of each of the co-authors.
(2) they meet the criteria for authorship in that they have participated in the conception, execution, or interpretation, of at least that part of the publication in their field of expertise;
(3) they take public responsibility for their part of the publication, except for the responsible author who accepts overall responsibility for the publication;
(4) there are no other authors of the publication according to these criteria;
(5) potential conflicts of interest have been disclosed to (a) granting bodies, (b) the editor or publisher of journals or other publications, and (c) the head of the responsible academic unit; and
(6) the original data are stored at the following location(s) and will be held for at least five years from the date indicated below:

Location(s)	**Monash University**

Signature 1		**Date**
Signature 2		
Signature 3		

Declaration for Publication 4

Declaration by candidate

In the case of "Alexander LV, Arblaster JM. 2008. Assessing trends in observed and modelled climate extremes over Australia in relation to future projections. *International Journal of Climatology* DOI: 10.1002/joc.1730", the nature and extent of my contribution to the work was the following:

Nature of contribution	Extent of contribution (%)
Formulation of research problem and the context of the research in the wider literature: description and analysis of observations in relation to model output.	50% of published work (90% of section presented in thesis).

The following co-authors contributed to the work. Co-authors who are students at Monash University must also indicate the extent of their contribution in percentage terms:

Name	Nature of contribution	Extent of contribution (%) for student co-authors only
Julie Arblaster	Formulation of research problem and the context of the research in the wider literature: description and analysis of model output in relation to future climate projections.	

Candidate's Signature		**Date**

Declaration by co-authors

The undersigned hereby certify that:

(1) the above declaration correctly reflects the nature and extent of the candidate's contribution to this work, and the nature of the contribution of each of the co-authors.
(2) they meet the criteria for authorship in that they have participated in the conception, execution, or interpretation, of at least that part of the publication in their field of expertise;
(3) they take public responsibility for their part of the publication, except for the responsible author who accepts overall responsibility for the publication;
(4) there are no other authors of the publication according to these criteria;
(5) potential conflicts of interest have been disclosed to (a) granting bodies, (b) the editor or publisher of journals or other publications, and (c) the head of the responsible academic unit; and
(6) the original data are stored at the following location(s) and will be held for at least five years from the date indicated below:

Location(s)	**Monash University**

Signature 1		**Date**

List of Acronyms

AAO Antarctic Oscillation

APN Asia-Pacific Network

AR4 Fourth Assessment Report (of the **IPCC**)

BoM Bureau of Meteorology

CCl Commission for Climatology

CMIP3 Coupled Model Intercomparison Project phase 3

ENSO El Niño-Southern Oscillation

ETCCDI Expert Team on Climate Change Detection and Indices

GCM Global Climate Model/General Circulation Model

IOCI Indian Ocean Climate Initiative

IPCC Intergovernmental Panel on Climate Change

IPO Inter-decadal Pacific Oscillation

ISCCP International Satellite Cloud Climatology Project

JSC Joint Scientific Committee

MSLP Mean sea-level pressure

NCC National Climate Centre (of **BoM**)

NOAA National Oceanic and Atmospheric Administration

NSD National Shipwrecks Database of Australia

OLS Ordinary Least Squares Regression

PCMDI Program for Climate Model Diagnosis and Intercomparison

PDF Probability Distribution Function

RCM Regional Climate Model

SAM Southern Hemisphere Annular Mode

SAR Second Assessment Report (of the **IPCC**)

SLP Station level pressure

SOM Self-Organising Maps

SRES Special Report on Emissions Scenarios

SST Sea Surface Temperature

SSTA Sea Surface Temperature anomalies

TAR Third Assessment Report (of the **IPCC**)

UTC Coordinated Universal Time

WCRP World Climate Research Programme

WMO World Meteorological Organisation

Table of Contents

List of Tables

Table 5.2: Observed and simulated decadal OLS trends calculated over the 1957 to 1999 period for each index (**Table 5.1**) averaged across Australia using grid boxes containing observations from **Fig. 5.2** and **Fig. 5.3**. Bold signifies trends are significant at 5% level. Observations are shown with 2 standard errors in the trend calculation estimated using Restricted Maximum Likelihood (*Trenberth et al.* 2007) while 10 to 90% confidence intervals are shown in brackets for the model data by randomly resampling the bootstrapped trends (see text) across all model runs to give an estimate of the uncertainty from using multiple model simulations. Units as **Table 5.1** (per decade).

Table 5.3: As **Table 5.2** but showing OLS trends and 10% and 90% confidence intervals for each model used in this study. For models where the ensemble mean is calculated from multiple simulations, the confidence intervals are calculated using all ensemble members.

List of Figures

Fig. 2.4: Seasonal trends (%/decade) in mean rainfall for 1910-2005 (LHS) and 1951-2005 (RHS). Only statistically significant trends are shown in colour. Maps are overlaid with annual trends (%/decade) at each station location with sufficient high quality data represented by upward (downward) triangles for increasing (decreasing) trends for (a)-(h) seasonal maximum 1-day precipitation totals (RX1day). The size of the triangle reflects the magnitude of the trend. Bold indicates statistically significant change.

Fig. 2.5: Triangles represent annual trends (°C/year) in mean maximum (minimum) temperature at high-quality Australian station locations (*Trewin* 2001) plotted against trends in the hottest (coldest) maximum (minimum) daily temperature (°C/year) at those stations for (a) and (b) summer and (c) and (d) winter between 1957 and 2005. Red triangles indicate where the absolute seasonal trend in the warmest ((a) and (c)) or coldest ((b) and (d)) day at a station is greater than the absolute seasonal trend in mean maximum ((a) and (c)) or minimum temperature ((b) and (d)) at that station *i.e*. where the magnitude of the trend in the extremes is greater than the magnitude of the mean trend. The line of best fit calculated using total least squares regression is shown in red, s is the slope of the line and r is the spatial correlation.

Fig. 2.6: Seasonal trends (%/decade) in 10^{th} and 90^{th} percentile indices (**Table 2.1**) with respect to seasonal trends (%/decade) in the median (denoted on the x-axes by TN50p for minimum temperature and TX50p for maximum temperature) for (a)-(d) Dec-Feb, (e)-(h) Mar-May, (i)-(l) Jun-Aug and (m)-(p) Sep-Nov. Each symbol represents a station. The line of best fit calculated using total least squares regression is shown in red, s is the slope of the line and r is the spatial correlation.

Fig. 2.7: Annual trends (%/year) at Australian stations for (a) R95p and (b) R99p plotted against annual trends (%/year) in mean precipitation between 1910 and 2005. The line of best fit calculated using total least squares regression is shown in red, s is the slope of the line and r is the spatial correlation.

Fig. 2.8: Trends (%/year) in (a) R10mm, (b) R95p, (c) R99p and (d) RX5day on the y-axis plotted against trends (%/year) in annual total precipitation > 1mm for global stations from *Alexander et al.* (2006) with at least 40 years of non-missing data. Each symbol represents a station. The line of best fit calculated using total least squares regression is shown in red,

s is the slope of the line and r is the spatial correlation using the percentage trends. Australian stations are represented by blue asterisks.

Fig. C.1: Satellite image over Victoria at 0225 UTC (1325 EDST) on 3rd February 2005 corresponding to the severe storm index at Cape Otway. Satellite image originally processed by the Bureau of Meteorology from the geostationary satellite GOES-9 operated by the National Oceanographic and Atmospheric Administration for the Japan Meteorological Agency. Image obtained from http://www.bom.gov.au/announcements/sevwx/vic/2005feb/index.shtml.

Fig. C.2: Weather log from 7th March 1866 which reads "Midnight barometer 29.002. N.W.6. Minimum 30°. Dense mist and rain. Fine dull cloudy. Severe gale in the night from N.W.". The ships Bitter Beer (schooner) and Pomona (ketch) were likely wrecked when caught in this gale, described in the NSD as "one of the fiercest gales ever experienced on the Victorian Coast".

Fig. C.3: An example of an incorrectly recorded value in the original handwritten archive (and hence wrongly digitised). The 3pm mean sea level pressure reading of 1024.5 hPa (white circle) has been incorrectly recorded in the observation column (green circle) rather than the station level pressure reading of 1014.5 hPa (red circle). This produced an 11 hPa increase in the storm index in a 6 hour period rather than the correct 1 hPa increase.

Fig. C.4: Pressure tendencies (09:00 to 15:00) for Cape Otway for each day in June 1870. The dotted lines represent the 1st and 99th percentiles of the 6-hour pressure tendencies (**Table C.1**) described in the text. A severe storm event is defined on 27th June.

Fig. C.5: Bars represent the number of severe storms per year at Cape Otway, 1865-2006, the blue line is a 21-term binomial filter representing decadal fluctuations in the data and the red line is the linear fit to the data. The trend is significant at the 5% level.

Fig. 3.1: Location of stations (◊) used in this study. Some metropolitan centres (x) are also marked for reference. Macquarie Island (54.5S, 158.94E) and Heard Island (53.02S, 73.39E) were also digitized but are not marked on the map.

Fig. D.4: Rainfall intensity (mm/day) associated with dynamical cloud regimes from **Fig. D.1a** for (a) Sydney, (b) Melbourne, (c) Adelaide and (d) Perth.

Fig. D.5: Correlations of detrended timeseries averaged across Australia of (a) annual maximum daily maximum temperature, (b) Daily rainfall intensity, (c) annual maximum 5-day rainfall and (d) Southern Ocean cyclone density with detrended timeseries of annual sea surface temperatures from HadISST (*Rayner et al.* 2003). Black lines enclose regions where correlations are significant at 5% level.

Fig. D.6: As **Fig D.5** but for warm nights across Australia for the period 1957-2006.

Fig. 4.1: Seasonal SSTA patterns ('nodes') from HadISST1.1 derived using Self-Organising Maps (SOM). Each node is shown alongside the probability distribution function of the associated NINO4 index value for the seasons where this node occurs. The number of times, *n*, that each node appears within the SOM between 1950 and 2006 when the NINO4 index is also available is shown above each map.

Fig. 4.2: Timeseries of seasonal SSTA from HadISST1 as categorized by the 8 SOM nodes defined in **Fig. 4.1**. Each symbol represents a different season. Lines are shaded blue where at least 3 consecutive seasons most closely resembled node 1 (strong La Niña) and orange where they most closely resembled node 8 (strong El Niño).

Fig. 4.3: Anomalies are shown for cool nights (TN10p), warm nights (TN90p) and maximum 1-day precipitation totals (RX1day) during each SOM node. Units for temperature indices are percentage deviations from expected value *i.e*. 10% and precipitation extremes are shown as the normalized deviations (by removing the mean and dividing by the standard deviation) from average. Colours are shown such that green/blues (yellow/red) reflect a cooler/wetter (warmer/drier) climate.

Fig. 4.4: As **Fig. 4.3** but for cool days (TX10p), warm days (TX90p) and maximum consecutive 5-day precipitation totals (RX5day).

Fig. 4.5: Differences in the value of each index from this study (except RX1day) between SOM node 1 and node 8 (left hand side) and node 3 and node 6 (right hand side). Colour bars are presented such that green/blue (yellow/red) indicate that the node named first in the title is cooler/wetter (warmer/drier) than the node named second. Crosses indicate gridboxes where the difference between the nodes shown is significant at the 5% level using a Kolmogorov-Smirnoff (K-S) test.

Fig. 4.6: Seasonal SSTA patterns ('nodes') derived using SOMs from (LHS) observed SST-forced CAM3 runs and (RHS) observed SST-forced CAM3 run including "climate of the 20th century" atmospheric forcing.

Fig. 4.7: The difference (°C) between the response of TXx to strong La Niña (node 1) minus strong El Niño (node 8) for (a) observations, (b) SST-forced CAM3 run and (c) SST-forced CAM3 run including "climate of the 20th century" atmospheric forcing. Greens/blues (yellows/reds) indicate that the response is cooler (warmer) during La Niña. Crosses indicate where the response is statistically significantly different (at the 5% level using a K-S test).

Fig. 4.8: Differences in precipitable water measurements during strong La Niña events (node 1) and strong El Niño events (node 8) for (a) the SST-forced CAM3 run including "climate of the 20th century" atmospheric forcing and (b) observations from the ISCCP dataset (described in **Section D**).

Fig. E.1: Changes in mean temperature (left column) and precipitation (right column) for observations (a, b), 20thC simulations (c, d) and 21stC SRES A1B simulations (e, f). Twentieth Century changes are represented as trends from 1957-1999, while future changes are differences of 2080-2099 minus 1980-1999. Stippling in e) and f) indicates regions where the multimodel mean change divided by the intermodel standard deviation of the change is greater than one, a measure of the consistency of the multimodel response. The same nine models for which extremes indices were analysed are used to form the multimodel means here. Figure produced by Julie Arblaster and presented in *Alexander and Arblaster* (2008).

Fig. 5.7: The relationship between two different definitions of the *heat wave duration*, *warm nights* and *consecutive dry days* indices (**Table 5.1**) across Australia. Each triangle represents the annual trend calculated between 1957 and 1996 for each index at Australian stations. The red line represents the line of best fit using total least squares regression, s is the slope of the line and r is the spatial correlation between all points.

Acknowledgements

I acknowledge the help and support of my supervisors, Prof. Amanda Lynch, Prof. Neville Nicholls and Prof. Nigel Tapper. I thank them for imparting their expertise and knowledge to me and I would particularly like to thank Amanda for giving me the opportunity and financial support to pursue this thesis, Neville for always being available, willing and able to answer my questions and Nigel for his support and guidance.

I could not have completed this work over the last 3 years without the camaraderie, scientific debate and technical support that has been given to me by the Regional Climate Group at Monash University: Rebecca Abramson, Michelle D'Amico, Jo Brown, Jill Gallucci, Klaus Görgen, Sue Mackay, Andrew Marshall, Lee Tryhorn and Petteri Uotila.

Particular thanks also to my co-authors at the Bureau of Meteorology: Julie Arblaster, Dean Collins, Pandora Hope, Scott Power and Blair Trewin. Without your expertise this would not have been possible.

Thanks also go to Lynda Chambers, Christian Jakob, Dörte Jakob, David Karoly, Ian Macadam, Jerry Meehl, Rob Smalley and Claudia Tebaldi for their useful discussions and help at various points along the way. Also thanks to John Cornally-Reilly and Guilia Cesario from the Bureau of Meteorology for organizing access to historical Cape Otway weather records and to the staff at the National Archives for being so accommodating with the viewing of manuscripts. Permission to reproduce the images from the Cape Otway meteorological log books was kindly given by the National Archives of Australia: MP660/1. Modelling groups are acknowledged for making their simulations available for the analysis in Chapter 5, the Program for Climate Model Diagnosis and Intercomparison (PCMDI) for collecting and archiving the CMIP3 model output, and the WCRP's Working Group on Coupled Modelling (WGCM) for organizing the model data analysis activity. Thanks also to the staff and students of the Schools of Geography and Environmental Science and Mathematical Sciences for making my time at Monash most enjoyable.

And finally love and thanks to my family for supporting me and telling me they are proud of me and to my partner Ian for always being patient. I couldn't have done it without you.

A. Thesis Summary

Changes in the frequency and/or severity of extreme climate events have the potential to have profound societal and ecological impacts and observations suggest that in some parts of the world such changes are already occurring. The primary objective of this thesis was to identify and analyse the mechanisms which are driving changes in climate extremes in Australia in order to be better prepared for possible future changes. Multiple research tools, methods and data were employed including station observations, reanalyses data, satellite data and model output to address fundamental questions about how climate extremes have changed in Australia over the observational period, whether interactions between and changes in large-scale mechanisms are driving observed trends, and if changes are related to anthropogenic factors.

Major results were:

1. Across Australia, trends in extremes of both temperature and precipitation were very highly correlated with mean trends indicating an over-arching mechanism driving both. Analysis of the rate of change of extremes and means across Australia as a whole showed most stations have greater absolute trends in extremes than means. There was also some evidence that the trends of the most extreme events of both temperature and precipitation are changing more rapidly in relation to corresponding mean trends than are the trends for more moderate extreme events. The relationships between means and extremes of precipitation on an annual basis in Australia were consistent with all other global regions studied.

2. There have been significant reductions in the frequency of rain bearing synoptic systems affecting southern Australia over the past century, associated with significant decreases in the frequency of severe storms in south-east Australia.

3. Changes in climate extremes are affected to a large extent by variations in global sea surface temperatures. This is particularly true of maximum temperature extremes over Australia which showed significantly different responses to opposite phases of the El Niño-Southern Oscillation *i.e*. strong La Niña events compared to

strong El Niño events. A global climate model forced with observed SSTs was unable to reproduce these observed responses.

4. Multiple simulations from nine global coupled climate models showed that when averaged across Australia the magnitude of trends and interannual variability of temperature extremes were well simulated by most models particularly for the warm nights index. The majority of models also reproduced the correct sign of trend for precipitation extremes although there was much more variation between the individual model runs. However, very few model runs showed significant skill at reproducing the observed spatial pattern of trends in temperature and precipitation extremes, although a pattern correlation measure showed that spatial noise could not be ruled out as dominating these patterns.

5. Trends in warm nights in Australia were consistent with an anthropogenic response but inconsistent with natural-only forcings. This indicates that there is a discernable human signature on the observed warming of minimum temperature extremes across Australia.

1. Introduction and aims of this PhD

The vulnerability of communities to climate variability and change is likely to depend more on changes in the intensity and frequency of extreme weather and climate events than on changes in the mean climate (*Lynch and Brunner* 2007). It is expected that the extremes of climate variables will change at a faster rate than the mean climate (*IPCC* 2001, *Katz* 1999, **Fig 1.1**). In some regions, extremes have already shown amplified responses to changes in means (*Folland et al.* 2001). Significant changes in temperature and precipitation extremes have been noted almost everywhere on the globe; annual occurrences of warm nights have significantly increased, occurrences of cold nights have significantly decreased and precipitation intensity has increased in the past half century (*Alexander et al.* 2006). Global estimates of the potential destructiveness of hurricanes and the numbers and proportion of tropical cyclones reaching categories 4 and 5 appear to have increased since the 1970s (*Webster et al.* 2005; *Emanuel* 2005), in addition to increased trends in sea surface temperatures and other variables that may influence tropical storm development (*Hoyos et al.* 2006). However, in spite of this the number of tropical cyclones in the Australian region appears to have decreased (*Nicholls et al.* 2009). Although there have been significant advances in extremes research over the past 15 years (*Nicholls and Alexander* 2007), gaps still remain especially in relation to the detection and attribution of changes in extremes. If we *understand what processes drive changes in extremes* this would provide an invaluable aid to scientists and policymakers to help improve forecasting, mitigation and/or adaptation strategies.

Therefore, the **primary objective** of this PhD thesis is to:

identify and analyse key mechanisms driving observed changes in climate extremes in Australia

Mechanisms are likely to include coupled ocean-atmosphere processes such as the El Niño-Southern Oscillation (ENSO), large scale circulation changes, sea surface temperatures (SSTs), cloud type and/or amount and land cover change. Complex interactions and changes in these processes may be related to natural climate variability or enhanced anthropogenic factors or both. One of the main obstacles to a study of climate

extremes is lack of access to the required observational data. Datasets of daily temperature and precipitation already exist for Australia (*Trewin* 2001; *Haylock and Nicholls* 2000) and observational data have recently become available which would allow the study of large scale pressure changes over Australia back to the end of the 19th century. In addition, satellite datasets are available which can be used to detect changes over Australia in cloud regimes (*Rossow and Schiffer* 1991). Reanalysis data which have already been used to look at southern hemisphere cyclone formation (*Trenberth* 1991; *Simmonds and Keay* 2000) can provide information on the large scale processes and synoptic patterns driving Australian climate extremes through clustering techniques such as Self-Organising Maps (SOMs: *Cassano et al.* 2006; *Lynch et al.* 2006). This study makes use of all of these datasets to investigate the mechanisms which drive long term changes in climate extremes with the aim of determining whether changes in large scale circulation patterns are implicated as a driver of extreme events. Links between changes in these patterns and anthropogenic influences will be investigated using state of the art climate models. Therefore, to provide a research framework for this objective, the following three primary questions will be addressed:

1. **How have climate extremes of temperature, precipitation and storminess changed in Australia during the observational record?** *Chapter 2 and Chapter 3*
2. **Are interactions between and changes in large-scale mechanisms driving observed trends in climate extremes?** *Chapter 3 and Chapter 4*
3. **Can state of the art climate models adequately represent observed changes in climate extremes?** *Chapter 4 and Chapter 5*

To attain these objectives we have built on and updated current research of trends in Australian extremes. A breadth of research documenting Australian temperature and precipitation extremes already exists (*e.g. Hennessy et al.* 1999; *Plummer et al.* 1999; *Collins et al.* 2000; *Haylock and Nicholls* 2000; *Manton et al.* 2001; *Griffiths et al.* 2005; *Gallant et al.* 2007; *Chambers and Griffiths* 2008) but the mechanisms which are driving these changes are less well understood. Furthermore, most studies have focussed on the analysis of extremes variables (most typically temperature and precipitation) separately. Regional studies across Australia and the Asia-Pacific area have shown significant increases in occurrences of hot days, warm nights and heat-waves and decreases in

occurrences of cool days and cold nights (*e.g.* *Collins et al.* 2000; *Manton et al.* 2001; *Tryhorn and Risbey* 2006) over the past few decades. **Fig. 1.2** shows how the probability distribution function (PDF) for winter temperatures in Melbourne has shifted in recent decades; the increase in mean minimum temperature of less than 1°C has been accompanied by a reduction of more than 50% in the numbers of very cold nights (*Nicholls and Alexander* 2007). While changes in precipitation extremes in Australia are more regionally dependent (*e.g.* *Hennessy et al.* 1999; *Haylock and Nicholls* 2000), we will show that there is some evidence that the trends of the most extreme events of both temperature and precipitation are changing more rapidly in relation to corresponding mean trends than are the trends for more moderate extreme events (**Chapter 2**). Over the past century there has been a significant decrease in the frequency and intensity of extreme precipitation events in southwest Western Australia and a significant increase in the proportion of total rainfall from extreme events in eastern Australia (*Haylock and Nicholls* 2000).

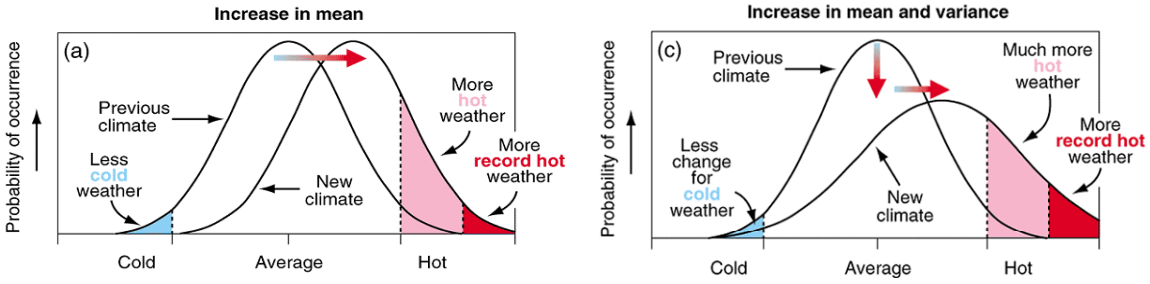

Fig. 1.1: Schematic showing the effect on temperatures when the mean increases (left panel) and when both the mean and variance increase (right panel) for a normal distribution of temperature. Source *IPCC* (2001).

Drying over Western Australia is perhaps the most extensively researched of these extremes. It has been attributed to various causes including land use change (*Pitman et al.* 2004; *Timbal and Arblaster* 2006), changes in sea surface temperatures (*Ummenhofer et al.* 2008) and decreases of Antarctic sea ice (*IOCI* 2005). However, the most recent evidence from the Indian Ocean Climate Initiative (IOCI) suggests it is a shift in large scale circulation patterns which has moved the preferred location of winter storm tracks and caused the rainfall deficit (*Hope et al.* 2006; *Frederiksen and Frederiksen* 2007). While there is an understanding of the effect that the modulation of large scale circulation *e.g.* the Southern Hemisphere Annular Mode (SAM) has on changes of the mean climate

(*Thompson and Solomon* 2002), the links between this and the effects on extreme events are still not fully understood.

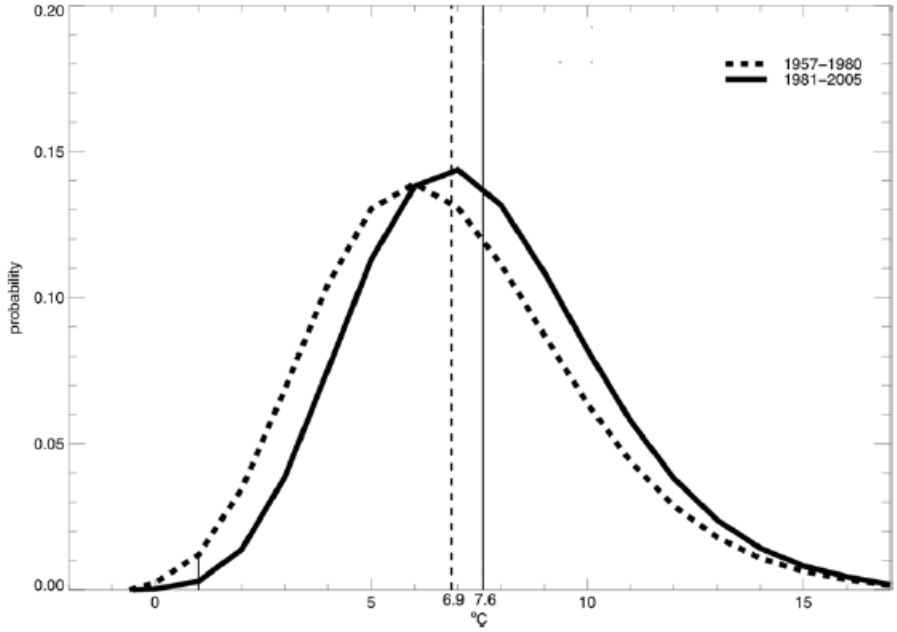

Fig. 1.2: Illustration of the changing probability distribution function (PDF) of Melbourne winter (JJA) minimum temperatures between 1957-1980 (dashed line) and 1981-2005 (solid line).

1.1 Significance/Innovation

Anthropogenic climate change is likely to shift extremes towards conditions that will stress vulnerable systems such as Australia's unique flora, fauna and ecosystems (*Fitzharris et al.* 2007; *Hughes et al.* 2003; *Chambers et al.* 2006). Extreme precipitation changes have the potential to prolong droughts and increase floods, hence affecting water supply quality and quantity. Extremes such as storms and flooding can have large impacts, not only through their immediate affects such as loss of life and property but also through residual effects such as insurance premium increases, increased health risk and loss of adaptive capacity (*Lynch and Brunner* 2007; *Nicholls and Alexander* 2007).

There is growing evidence that only the inclusion of anthropogenic as well as natural climate change can account for the global changes in extremes that have already been observed (*e.g. Kiktev et al.* 2003; *Christidis et al.* 2005) and under future enhanced greenhouse gas forcing the frequency of these extreme events is likely to increase (*e.g. Hegerl et al.* 2004; *Tebaldi et al.* 2006). However, there is also evidence that some

observed regional responses can be accounted for by natural climate variability (*Cai et al.* 2005; *Scaife et al.* 2008). The study of trends in climate extremes requires long running timeseries that are free from artificial influences or 'inhomogeneities' while the study of the atmospheric processes that drive these trends require high spatial and temporal resolution data that are unlikely to be free from such inconsistencies. This study aims not to treat these separate sources as mutually exclusive but rather to utilize all available data sources to provide a *whole and unique picture* of changes in extremes across Australia and their driving mechanisms.

The **unique aspects of the work** compared with previous analyses are:-

a) it will draw on previously unanalysed data which have only recently become available *i.e*. sub-daily station pressure and cloud regime data over Australia;

b) a multi-method approach will be adopted that will synthesize station observations, satellite data, reanalysis data and model simulations to significantly improve our understanding of the evolution of large scale synoptic patterns over Australia in order to determine how changes can impact extremes of temperature, precipitation and 'storminess' (that is, wind and storm tracks).

The use of multiple data sources over a variety of timescales will provide a uniquely comprehensive insight into the large scale mechanisms driving changes in extremes over Australia.

1.2 Approach/Methodology

1.2.1 Research tools and datasets

In this section, we note selected examples to highlight the range of datasets that were at our disposal and to illustrate the availability of long (in some cases over a century) records of multi-parameter “extremes”.

1.2.1.1 *In-situ* observations

High quality daily temperature (*Trewin* 2001) and precipitation (*Haylock and Nicholls* 2000) data from the Bureau of Meteorology (BoM) observing stations were available in near-real time (*i.e*. almost up to the current date) and were analysed for changes in and interactions between trends in mean and extreme events, placing these results in a global context. These data also contributed to the creation of a gridded dataset of temperature and precipitation indices (*Alexander et al.* 2006) which was used for comparison with global climate model output. Recently digitised sub-daily pressure data since the end of the 19th century from approximately 50 observing stations in Australia were also obtained from BoM. These data were quality controlled and interpolated to create the first long-term Australia-wide daily mean sea level pressure dataset. From this, synoptic regimes were identified for Australia and trends in these patterns over the last century were analysed in addition to trends in 'storminess' at individual stations for about 150 years in some cases. A global sea surface temperature dataset, HadISST1 (*Rayner et al.* 2003), constructed from *in-situ* ship, fixed and drifting buoy measurements, was used to analyse the influence of large scale modes of SST variability on observed temperature and precipitation extremes across Australia and the globe.

1.2.1.2 Reanalyses datasets

Reanalysis data such as NCEP/NCAR (*Kalnay et al.* 1996) and ERA-40 (*Uppala et al.* 2005) have generally been used to identify synoptic patterns in climate research (*e.g. Lynch et al.* 2006; *Cassano et al.* 2006). They are useful because of their complete global coverage since the 1950s and high temporal resolution (6 hours) and have been used successfully to document Southern Hemisphere cyclone formation (*Trenberth* 1991; *Simmonds and Keay* 2000). Although they suffer from heterogeneities particularly before 1960 and around the late 1970s (*Kistler et al.* 2001) when used in conjunction with the other sources of data they have provided a useful benchmark for comparison. Several clustering techniques are available such as Self-Organising Maps (*e.g. Lynch et al*. 2006), simulated annealing clustering (*e.g. Philipp et al.* 2006) or K-Means clustering (*Anderberg* 1973) to enable identification of synoptic regimes and investigate links with changes in extreme events identified from both the reanalyses and in-situ datasets.

1.2.1.3 Satellite data

For the first time, "dynamical" cloud regimes have been identified for Australia using International Satellite Cloud Climatology Project (ISCCP; *Rossow and Schiffer* 1991) data, available at 250km resolution, 3–hourly timescale from July 1983 to December 2004 (*Jakob and Tseliodis* 2003; *Rossow et al.* 2005). In addition to being able to create cloud climatologies for Australia and to analyse changes in cloud type and amount using ISCCP data, these regimes were compared to various extremes of temperature and precipitation to identify patterns driving the observed change.

1.2.1.4 Model simulations

To diagnose the mechanisms driving changes in Australian climate extremes requires the use of climate models. In addition models can be used to determine the anthropogenic component of observed changes in other climate extremes using optimal detection/fingerprinting techniques (*e.g. Allen and Tett* 1999; *Tett et al.* 1999) or objective bootstrapping methods (*e.g. Kiktev et al.* 2003) using natural-only, anthropogenic or all forcings experimental design.

A set of experiments from the CCSM3 climate model (*Collins et al.* 2006b) forced with observed sea surface temperatures (SSTs) and different atmospheric forcings were used to investigate the effect of large scale phenomenon such as El Niño-Southern Oscillation (ENSO) on trends and variability of climate extremes. The output from these experiments was compared to the observed response of temperature extremes to varying SSTs. The resolution of the version of CCSM3 that was used was 128 by 64 horizontal grid cells (approximately 2.8 degree resolution) with 26 levels in the vertical.

In addition, 22 runs from nine state of the art climate models were available from the World Climate Research Programme's (WCRP) Coupled Model Intercomparison Project phase 3 (CMIP3) at the Program for Climate Model Diagnosis and Intercomparison (PCMDI) in California. Ten extremes indices, calculated from daily data and based on the definitions of *Frich et al.* (2002), were available with 5 temperature-based indices (*e.g*. heat wave duration, occurrence of frosts) and 5 precipitation-based indices (*e.g*. heavy precipitation events, consecutive dry days).

Christidis et al. (2005) is, thus far, the only formal detection and attribution study globally that has convincingly associated a trend in temperature extremes with a human influence. While some regional studies in Australia have convincingly argued that anthropogenic forcings play a role in the drying of south-west Western Australia (*e.g.* *Timbal and Arblaster* 2006) most studies relate to mean rather than extreme change. For this reason, the output from a series of climate model experiments was analysed to test the hypothesis that changes in climate extremes in Australia are human-induced.

1.2.2 Research Tasks

The primary objective "Identify and analyse key mechanisms which are driving observed changes in climate extremes in Australia" was addressed by using the datasets and research tools described above and by addressing three primary questions as follows:-

- How have climate extremes of temperature, precipitation and storminess changed in Australia during the observational record? *Chapter 2 and Chapter 3*

Data need to undergo rigorous quality control before being used in any extremes analysis since values are likely to show up as extreme when incorrectly recorded. In addition inhomogeneities (that is artificial changes which cannot be explained by changes in climate) need to be accounted for or removed prior to any analysis. For various climate variables we did this as follows:-

a. Temperature and precipitation

Daily temperature and precipitation station data across Australia have already had extensive quality control applied (*Trewin* 2001; *Haylock and Nicholls* 2000) although there may still be issues regarding incorrectly recorded accumulations for precipitation (*Viney and Bates* 2004). Some recent work has already attempted to address these issues (*Gallant et al.* 2007).

Recent intensive collaboration by the World Meteorological Organisation (WMO), Expert Team on Climate Change Detection and Indices (ETCCDI) has facilitated the identification and calculation of a suite of 27 climate extremes indices for most regions of

the world (*Alexander et al.* 2006). As part of this thesis, these indices were updated and analysed for Australia between 1957-2005 for temperature and 1910-2005 for precipitation to assess how the extremes of these variables relate to trends in the mean. This allowed us to answer questions about how the distributions of temperature and rainfall are changing across Australia. In addition, recent work performed on a global scale using these climate indices (*Alexander et al.* 2006) allowed the results to be put into a global context to determine whether changes seen in Australia were remarkable compared to other regions of the world.

b. Mean sea level pressure

The mean sea-level pressure (MSLP) dataset was developed as a new dataset, and provides a unique look at long-term changes in synoptic patterns and extreme storm events over Australia (since the early 20th century). However, the station dataset required a high degree of "hands-on" quality control before it could be used. Although the earliest observations dated back to 1859, it was not until 1907 that a reasonable number of stations had enough data to analyse. These data were raw and in most cases had been keyed directly from original manuscripts without quality control. Gravity and index corrections were not performed on the raw data and, depending on barometer type, could be quite large (up to several hPa). In addition, an extensive search of original manuscripts at the BoM archive and the National Archives of Australia was required to account for changes in the type and location of the barometer at individual sites in conjunction with sophisticated statistical techniques to identify artificial climate shifts. Other studies in the Northern Hemisphere, particularly the European Union project, EMULATE, which was set up to categorise synoptic variability over Europe since about 1850, have had experience in addressing these sorts of problems (*Ansell et al*. 2006). We drew on the quality control techniques employed by EMULATE and other studies (*e.g. Alexandersson et al.* 2000; *Bärring and von Storch* 2004; *Alexander et al.* 2005; *Zou et al*. 2006) from which it was then possible to classify storm events from daily pressure tendencies (*i.e*. the difference in hPa between subsequent pressure readings) at individual stations. Pressure tendencies have been shown to be a good proxy for wind speed (*WASA Group* 1998) and are more reliable as they are less affected by inhomogeneities from changing instrumentation. Probability distribution functions were defined for the quality controlled pressure tendencies at each station from which a threshold was identified above which events were classified as "extreme". These

thresholds could then be employed as a quality control measure for the data. Timeseries of extreme storm events were then analysed using the most up to date statistical techniques to determine if there has been any change in the frequency or intensity of events.

- Are interactions between and changes in large-scale mechanisms driving observed trends in climate extremes? *Chapter 3 and Chapter 4*

We investigated large scale mechanisms over Australia and their interactions by using the pressure dataset described above in addition to reanalyses data to identify synoptic patterns using existing techniques (*e.g.* *Lynch et al.* 2006; *Cassano et al.* 2006) and by identifying cloud regimes (clusters) from ISCCP data (*Jakob and Tseliodis* 2003; *Rossow et al.* 2005). This enabled us to determine if particular cloud clusters were systematically linked to particular synoptic types and if this was the case whether the occurrences of extremes also map to certain circulation types and in turn an associated cloud cluster. In addition, because of the strong influence of ENSO on the climate of Australia, global patterns of SST variability were identified using the same clustering algorithm used to classify synoptic pressure patterns, to analyse the effect that these large scale modes have on temperature and precipitation extremes across the country. Finally, the anthropogenic component of changes in these extremes was assessed using multiple runs from two global climate models with different forcings.

To classify synoptic MSLP and SST patterns, a technique called Self-Organising Maps (SOM) was used. The SOM algorithm (*Kohonen* 2001) applies an unsupervised learning process to map input data onto the elements of a regular one- or two-dimensional array and hence provides an efficient means of interpreting and visualizing large data sets. The way the SOM algorithm was used here most directly compares to cluster analysis except that the SOM approach is characterized by a tendency to categorize data by preserving its probability density (*Cassano et al.* 2006). Using the ERA-40 reanalysis product, daily averaged fields of mean sea level pressure (MSLP) for the time period 1958-2001 were retrieved. Daily averaged fields from the newly created observed MSLP dataset were also calculated for the period 1907-2006. From these, synoptic patterns were derived by applying the SOM algorithm and using all days through the year. The observed SOM was mapped to the ERA-40 SOM in order to create spatially and temporally complete MSLP synoptic patterns over Australia for the past century. Frequency distributions and trends

were then calculated for all the synoptic types and these were linked to changes in extreme events. For the SST data, the SOM algorithm was used in a similar way only this time using the 1° latitude x 1° longitude HadISST dataset. Eight patterns of seasonal SST anomalies were identified which showed that phases of ENSO modulated the majority of global SST variability. The influence of these patterns of variability on global temperature and precipitation extremes was analysed.

For the cloud regimes, for each 280km grid square within a region defined around Australia, cloud top pressure, optical thickness (τ) and cloud amount were extracted from the ISCCP data for every 3-hourly period since 1983. To allow for the different dynamical regimes that exist between tropical and extratropical Australia, the country was split into two regions with clusters defined for each one although most of our focus was on the extratropical region. Since optical thickness can only be calculated with the visible channel, two daytime periods were investigated (morning to early afternoon and mid afternoon to early evening) to allow for the differences in convective situations that occur during the day. A K-Means clustering algorithm (*Anderberg* 1973) was implemented to search for possible patterns or "clusters" to identify the cloud regimes within the region. Once the cloud regimes were identified it was possible to make direct links between trends in these and the various synoptic types defined from the pressure and reanalyses datasets and how these were associated with changes in the range of climate extremes described in the previous section. This allowed us to tell if there were certain regimes which were driving most of the changes in extreme events.

On a global scale, previous work has been moderately successful at detecting a discernible anthropogenic influence on temperature and precipitation extremes (*Kiktev et al.* 2003; *Kiktev et al.* 2007). However recent studies on regional scales show that trends in climate extremes for individual seasons and regions are often dominated by natural variability (*e.g. Scaife et al.* 2008) so the same treatment cannot be applied to seasonal and regional changes as has been applied in the past to global (*i.e*. radiative) changes. Although there is good evidence globally (*e.g. Kiktev et al.* 2003; *Christidis et al.* 2005) that changes in temperature extremes can only be explained by both natural and anthropogenic forcings, to our knowledge a formal detection study of changes in extremes over Australia had yet to be performed. Two of the models from the CMIP3 archive had data available for analysis with natural-only and anthropogenic-only as well as all-forcings runs. The output from

these climate models was analysed using an *objective pattern similarity* technique (using bootstrapping) that allowed for the objective comparison of observed and temporal trend patterns for various extremes using natural-only, anthropogenic-only and all forcings runs. This technique has been used successfully in previous global extremes studies (*Kiktev et al.* 2003; *Kiktev et al.* 2007).

- Can state of the art climate models adequately represent observed changes in climate extremes? *Chapter 4 and Chapter 5*

In addition to using the CMIP3 archive to analyse the anthropogenic influence on changes in extremes across Australia, this resource was also used to assess the general performance of state of the art climate models in simulating observed changes in extremes over Australia. Multiple simulations from nine global climate models were assessed for their ability to reproduce observed trends in temperature and precipitation extremes over Australia. Observed trends over the 1957 to 1999 period were compared with individual and multi-modelled trends calculated over the same period. These data were used to determine whether individually or collectively global climate models were able to reproduce both the magnitude and spatial pattern of trends over Australia. Due to the noise superimposed on long-term trends, estimates obtained from analysis of timeseries include a stochastic component. The associated uncertainty in the modelled trend estimates was assessed using a bootstrap procedure with multiple evaluations of "perturbed" trends for the model timeseries. The resulting multiple fields of bootstrapped trend patterns were randomly sampled to estimate Probability Density Functions (PDFs) of similarity between the actual and reproduced trends. From the pattern similarity PDFs for each climate extreme considered, we tested the null hypothesis that the model patterns had no positive skill in reproducing observed trends. The null hypothesis was rejected at the 5% level if a zero measure of similarity fell within the lower 5%-tail of the PDF. If more than 5% of the PDF was to the right of zero, then the ensemble mean showed positive skill at simulating the observed trend patterns at the 5% level.

The SOM algorithm was also employed to classify SST variability from two experiments of the CCSM3 model and to compare the resulting patterns with those patterns obtained from observations. The observed and modelled responses of extreme maximum temperatures over Australia to strong El Niño and La Niña events were compared.

1.3 National Benefit

Given the uniqueness of some of the datasets being created and used and the multi-method approach, the results of this research have allowed for a much improved understanding of the mechanisms which have lead to changes in climate extremes in Australia. In addition we have been able to answer objectively whether changes in extremes in Australia are human-induced to some extent. This is fundamental if governments and policymakers are to receive appropriate advice on the impacts and vulnerability of certain communities and regions to extreme climate change.

1.4 Structure of this thesis

Each chapter of this thesis aims to address the three primary questions posed to meet the primary objective as follows. An introductory section (labelled “A”, “B” etc.) precedes each of main chapters (labelled “1”, “2” etc.). The aim of the introductory sections is to act as a bridge between each of the main chapters and to give more informal background information to the specific scientific questions which are dealt with in the main chapters to answer the primary objective.

B. A land of droughts and flooding rains

Australia, described in Dorothea Mackellar's 1904 poem "My Country" as a land of "drought and flooding rains", may be better placed than most, given its variable climate, to adapt to changes in climate extremes. In the last 10 years, southeastern Australia has experienced a prolonged period of drought, most of the rainfall decline occurring in autumn (*Murphy and Timbal* 2008). While this dry spell is of a similar severity to one that occurred at the beginning of the 20th century, the recent dry has been exacerbated by much warmer temperatures in the present day compared to a century ago. In tandem with periods of drought, there have also been significant flooding incidences and in the eastern part of the country the multi-decadal variability of these events is modulated both by the El Niño-Southern Oscillation (ENSO) and the inter-decadal Pacific Oscillation (IPO) index (*Kiem et al.* 2003). This dual modulation of ENSO processes appears to have the effect of reducing and elevating flood risk on multi-decadal timescales. However, even though some systems may have evolved to be resilient to this variability, climate change might shift extremes towards conditions that will stress vulnerable systems such as Australia's unique ecosystems (*Pittock et al*. 2001; *Hughes et al.* 2003; *Fitzharris et al.* 2007). There is growing evidence that only the inclusion of anthropogenic as well as natural climate change can account for the global changes in extremes that have been observed in recent decades (*e.g*. *Kiktev et al*. 2003; *Christidis et al.* 2005) and under enhanced greenhouse gas forcing the frequency of some of these extreme events is likely to change (*e.g*. *Hegerl et al.* 2004; *Tebaldi et al.* 2006). *Folland et al*. (2001) concluded that in some regions both temperature and precipitation extremes have already shown amplified responses to changes in means.

The impacts of most extremes are typically felt at a local or regional scale so regional studies of climate extremes are of the highest priority for most countries for assessing potential climate impacts. However, given that climate change signals in climate extremes are difficult to detect at a regional scale, to understand fully how the climate varies and the extent to which humans have influenced the climate system requires a global approach. This in turn requires a consistent approach for analysis. The Intergovernmental Panel on Climate Change (IPCC) Second Assessment Report (SAR) in 1995 concluded that although there was no evidence globally that extreme weather events or climate variability

had increased, data and analyses were "poor and not comprehensive" although changes in extreme weather events were observed in some regions where sufficient data were available (*Nicholls et al.* 1996a). One reason for such ambiguity was that while there were studies of regional changes in climate extremes, the lack of consistency in the definition of extremes between analyses meant that it was impossible to provide a comprehensive global picture. These ambiguities in the SAR conclusions led to a number of workshops and globally co-ordinated efforts which have made significant progress in our analysis of extremes (*Nicholls and Alexander* 2007). Groups such as the World Meteorological Organisation (WMO) CCl/CLIVAR/JCOMM Expert Team on Climate Change Detection and Indices (ETCCDI)[1], the European Climate Assessment (ECA) and the Asia-Pacific Network (APN), in addition to their primary aim of filling in data gaps, have aimed to provide a framework for defining and analysing observed climate extremes so that the results from different countries can be combined seamlessly. It was early realised that countries were more likely to exchange information on seasonal and/or annual climate indices *e.g*. heatwave duration, heavy precipitation events than they were to release raw daily or sub-daily meteorological observations. In addition, temperature and precipitation were the most widely available long-term climate variables so most global studies have focused on analysis of these data. The first study to attempt a global analysis of temperature and precipitation extremes under the auspices of the ETCCDI was that of *Frich et al.* (2002) who showed that there had been significant changes in extreme climate indices, such as reductions in frost days and increases in warm nights and heavy rainfall events over the last 50 years. This approach has also been pivotal in "data mining" in regions where previously little or no data had been readily available, developing ongoing capacity in these data sparse regions and enhancing international collaboration (*Peterson and Manton* 2008). Modelling groups have also now taken a similar approach through the Joint Scientific Committee (JSC)/CLIVAR Working Group on Coupled Models so that observations and model output can be compared consistently. *Tebaldi et al.* (2006) was the first study to use the multi-model approach to assess potential future changes in climate extremes showing that the 21st century would bring global changes in temperature extremes consistent with a warming climate. While that study also showed that global changes in precipitation extremes were consistent with a wetter world with greater precipitation intensity, the consensus and significance amongst the models was weaker

[1] Previously known as the Expert Team on Climate Change Detection, Monitoring and Indices (ETCCDMI), see http://www.clivar.org/organization/etccdi/etccdi.php for details.

when regional patterns were considered. This indicates the importance of combining global results with more regionally relevant studies to assess the impacts of these changes. These and other multi-national efforts such as *Alexander et al.* (2006) meant that by the time of the IPCC's Third Assessment Report (TAR) and Fourth Assessment Report (AR4) in 2001 and 2007 respectively, much stronger conclusions could be drawn about how extremes had changed and how they might change in the future. This was largely due to increased data coverage and the availability of longer timeseries which enabled better detection of changes by enhancing the signal to noise ratio. In addition, because of the availability of global datasets, studies such as that of *Christidis et al.* (2005) were for the first time able to detect a discernible human influence on recent trends in global temperature extremes. By AR4, it was "likely" that there would be increases in droughts, intense tropical cyclones and extreme high sea level, "very likely" that warm spells and heavy precipitation events would increase and "virtually certain" that there would be more warm nights and fewer cold nights at the end of the 21st century compared to the end of the 20th century (*IPCC* 2007).

In light of this, the next chapter of this thesis employs the ethos of the ETCCDI and other international groups by analysing a standard set of temperature and precipitation extremes derived from daily data for Australia and presenting the results in a global context.

2. Trends in Australia's climate means and extremes: a global context

Summary

Using a standard set of annual and seasonal climate extremes indices derived from daily temperature and precipitation data, relationships between mean and extreme trends across Australia and the globe were analysed. Extremes indices were calculated using station data from Australian high quality daily temperature and precipitation datasets and pre-existing high quality datasets of climate extremes for the globe. Spatial correlations were calculated between the trends in means and extremes both annually and seasonally for maximum and minimum temperature and precipitation across Australia and annually for precipitation across the rest of the globe. In Australia, trends in extremes of both temperature and precipitation were very highly correlated with mean trends. Annually, the spatial correlation between trends in extremes and trends in the mean was stronger for maximum temperature than for minimum temperature. However, this situation was reversed in winter, when minimum temperatures showed the stronger correlations. Analysis of the rate of change of extremes and means across Australia as a whole showed most stations have greater absolute trends in extremes than means. There was also some evidence that the trends of the most extreme events of both temperature and precipitation are changing more rapidly in relation to corresponding mean trends than are the trends for more moderate extreme events. The annual relationships between means and extremes of precipitation in Australia were consistent with all other global regions studied.

2.1 Introduction

Trends in Australian temperature and precipitation extremes have been examined extensively *e.g*. *Hennessy et al*. (1999); *Plummer et al*. (1999); *Collins et al*. (2000); *Haylock and Nicholls* (2000); *Manton et al*. (2001); *Griffiths et al*. (2005) and *Gallant et al*. (2007). These studies reported widespread increases in warm temperature extremes and decreases in cold temperature extremes while trends in rainfall extremes show more regionally dependent variations. The relationships between means and extremes of temperature have been examined across Australia by *Trewin* (2001) and *Griffiths et al*. (2005). *Griffiths et al*. (2005) found changes in mean temperatures between 1961 and 2003 to be a good indicator for changes in a range of temperature extremes. That analysis extended across southeast Asia, Australia and the south Pacific, but the spatial distribution across Australia was relatively sparse. *Trewin* (2001) used a larger selection of stations and found that the lower (cold) tails of both the minimum and maximum temperature distributions were warming faster than the upper (warm) tails.

Most studies, however, have focussed on the analysis of temperature and precipitation extremes separately. Assessing trends in precipitation and temperature concurrently allows statements to be made about the drivers of some of these trends, given the high correlation between the two across much of Australia. For most of Australia the correlation between mean temperature and precipitation is negative and statistically significant (*Power et al.* 1998). This correlation is strongly dictated by maximum daily temperatures. Correlations between rainfall and minimum temperature vary regionally – in many places there is no statistically significant correlation; in the southern half of the continent statistically significant correlations are positive, while in the north they are negative. However, partial correlations between precipitation and minimum temperature, after the relationship between minimum and maximum temperature has been removed, reveal statistically significant positive correlations across most of Australia south of about 20°S. Correlations between the Australia-wide average annual precipitation and temperature are consistent with the wide-spread spatial responses described above (*Nicholls et al*. 1997; *Power et al*. 1998).

The breadth of Australian observational studies was made possible by the availability of high quality daily datasets that have undergone extensive checks for temporal inconsistencies. This study aims to use these datasets in order to assess simple measures of the relationship between means and extremes of temperature and precipitation at all the stations across Australia. Variations in this signature on the regional and seasonal scale will be assessed. Extremes were selected from the standardised set used in *Alexander et al.* (2006) to allow a comparison of the annual relationship between means and extremes across Australia with the rest of the globe.

First the data and methods used are described, followed by a discussion of the results and conclusions.

2.2 Data and Methods

While inland Australia has a relatively sparse geographical coverage of climate recording stations, for the data that are available there has been a long history of assessing data quality and subsequent homogenisation to minimise the effect of changes in exposure or observing practices (*Lavery et al.* 1992; *Torok and Nicholls* 1996; *Trewin* 2001; *Della-Marta et al.* 2004). Two sources of readily available Australian data were used in this study. These are the Bureau of Meteorology's National Climate Centre (NCC) interpolated grids of monthly temperature and precipitation and a subset of station data used in the calculation of these grids which also contain information on daily timescales. For global analysis, precipitation stations used by *Alexander et al.* (2006) which have sufficient non-missing data were used.

2.2.1 Gridded fields

The 0.25x0.25 degree gridded fields of monthly maximum and minimum temperature and precipitation were obtained from the NCC. The gridded data are based on station data, interpolated using a two-dimensional Barnes analysis. For precipitation we used a gridded dataset based on the homogeneous rainfall series described in *Lavery et al.* (1997), while *Jones* (1998) provides details about the temperature grids. The gridded data were used to create maps to describe the coarse spatial variability in the seasonal trends to allow an easy

visual comparison with trends in the extreme indices at station locations. The daily datasets are now available at http://www.bom.gov.au/climate/change/datasets/datasets.shtml while analyses based on the homogenous monthly datasets are available at http://www.bom.gov.au/climate/change.

2.2.2 Station data

For Australian station records, temperature data have been adjusted for inhomogeneities at the daily timescale from 1957 onwards by taking account of the magnitude of discontinuities for different parts of the frequency distribution for each variable/station combination (*Trewin* 2001). Stations used in this study were updated from the high-quality list used by *Trewin* (2001) although 3 stations have been removed from the analysis – Nhill, Sale and Wilcannia – since these stations are known to have inhomogeneities at or around 1996 after which no homogeneity adjustments have been applied. Prior to 1957, the amount of digitized daily temperature data is limited, and most of the digital data that do exist have only become available recently. For stations which do have pre-1957 data, flat monthly homogeneity adjustments have been made prior to 1957 due to a lack of digitized daily comparison data, thereby increasing the potential for undetected inhomogeneities to exist in the extremes. Australian precipitation data came from a high quality precipitation dataset (*Haylock and Nicholls* 2000). Subsequent studies have shown that multi-day rainfall in some instances has been incorrectly recorded as daily values, particularly just after the weekend (*Viney and Bates* 2004). However, analysis of the extremes in rainfall for a subset of stations has not shown any significant trend differences between rainfall gathered during the whole week and rainfall gathered between Tuesday and Friday (personal communication Dörte Jakob). Therefore no stations were rejected from the analysis for this reason. For global stations, the high-quality indices dataset that was developed on behalf of the WMO CCl/CLIVAR Expert Team on Climate Change Detection and Indices (ETCCDI) was used. The dataset includes 27 indices derived from daily data for 2223 temperature and 5948 precipitation observing stations across the globe. Details of the indices can be found at http://cccma.seos.uvic.ca/ETCCDI/.

2.2.3 Extreme indices calculation

Extremes indices for Australia have already been calculated from these daily station data for the global study of *Alexander et al*. (2006) but have been updated here using all available data up to 2005. Indices were calculated using standard software which was produced on behalf of the ETCCDI by the Climate Research Branch of the Meteorological Service of Canada. Two versions of the software are available, *FclimDex* written in Fortran and *RclimDex* written in the statistical software package R, although both provide identical results. The use of a standardised methodology to calculate climate indices allows the results to be compared directly with other regional analyses (*e.g*. *Aguilar et al*. 2005; *Zhang et al*. 2005; *Vincent et al*. 2005; *Haylock et al*. 2006; *Klein Tank et al*. 2006; *New et al*. 2006) which in turn can be fitted seamlessly into a global analysis. Although the indices for Australia have already been used in the global study of *Alexander et al*. (2006), because of the uneven distribution of global stations, the results in that study were gridded onto a 3.5 degrees longitude × 2.75 degrees latitude grid. This makes it difficult to pinpoint small regional shifts, such as in the southwest corner of Australia, where there are strong gradients in mean rainfall. For this reason we revisit and update the analysis of Australian climate indices to 2005 at individual stations. **Table 2.1** lists the indices that have been used in this study. It should be noted that some of the indices recommended by ETCCDI are not relevant for the Australian climate (see *Collins et al*. 2000). Thus we do not analyse growing season length and annual occurrences of days where maximum temperature is less than 0°C. In addition a precipitation index measuring the number of days greater than a user-defined amount of rainfall was not considered since the indices R10mm (days above 10 mm) and R20mm (days above 20 mm) were deemed sufficient for this study. For temperature, all indices except occurrence of frost (FD), cold and warm spell duration (CSDI and WSDI), tropical nights (TR) and summer days (SU) can be calculated seasonally as well as annually. For precipitation, only the maximum 1-day and 5-day precipitation totals indices (RX1day and RX5day) were calculated on a monthly basis.

The indices have been chosen to measure the extreme ends (and in some cases the mean or total *e.g*. PRCPTOT) of the temperature and precipitation distribution but are not so extreme that they are unreliable due to the data quality or the length of record.

2.2.4 Missing data

Missing station data were accounted for using the ETCCDI recommended standard criteria (see Appendix C of the *RclimDex* user manual on the ETCCDI website at http://cccma.seos.uvic.ca/ETCCDMI/RClimDex/RClimDexUserManual.doc). Briefly, monthly indices were calculated if no more than 3 days were missing in a month and annual values were calculated if no more than 15 days were missing in a year. However an annual value was also not calculated if any month's data were missing. For percentile threshold indices *e.g.* TX10p, TN90p and duration indices *e.g.* CSDI and WSDI (see **Table 2.1**) additional criteria were applied as described in the *RclimDex* manual.

2.3 Trend and correlation calculation

As stated in the introduction, there are statistically significant correlations between mean temperature and precipitation across much of Australia. Therefore, before analysing the relationships between means and extremes of the individual variables, correlations (using a simple Pearson product-moment correlation unless otherwise stated) were calculated for area averaged values over Australia between annual, summer (DJF) and winter (JJA) mean maximum and mean minimum temperatures and mean rainfall for 1957-2005 using the high quality gridded datasets outlined above.

Also using the gridded monthly interpolated fields and monthly station data described above, we calculated linear trends for annual (Jan-Dec), and seasonal (Dec-Feb, Mar-May, Jun-Aug and Sep-Nov) mean maximum and mean minimum temperature and precipitation. Because of the rainfall variability across Australia, to make the trends consistent across the country, percentage trends were additionally calculated *i.e.* the values in a timeseries were divided by the mean over the period of record prior to the trend calculation at each grid point or station in order to represent the trends as a percentage of average. For temperature, to cover the period of homogenous record, the period 1957-2005 (49 years) was analysed and for precipitation because of its much longer record, two periods were chosen: 1910-2005 (96 years) and 1951-2005 (55 years). For station data, for the analysis of trends, at least 80% of non-missing data had to be available for all time periods studied. Seasonal data had to have at least two of the three months present otherwise the value for that year

was regarded as missing. While this is probably more appropriate for temperature data, the two-month threshold was also used for precipitation data to provide sufficient temporal and spatial coverage for analysis.

To determine how well the trends in extremes were correlated with trends in means across Australia we calculate linear trends in mean precipitation and mean maximum and minimum temperature and in the extremes indices (**Table 2.1**) over the period of interest for all the stations in our study. Linear trends were calculated using a modified version of the non-parametric Kendall tau test (*Wang and Swail* 2001) since prior assumptions do not have to be made about the distribution of the indices timeseries. In addition the method is robust to the effect of outliers in the series. The linear trends in means were calculated as the annual or seasonal trends in either precipitation or mean maximum or minimum temperature. To represent a measure of the spatial correlation between trends in means and extremes rather than a temporal correlation at each station, mean trends were correlated with the linear trends for each extreme index across all stations.

Although these correlations provide information about the relationship between two variables (*i.e*. the mean and the extreme index) they do not indicate the magnitude or rate of change of one variable in relation to the other. In the case of the absolute-threshold temperature indices *i.e*. TXx, TNn, TXn and TNx (see **Table 2.1**), it makes sense to compare trends in the mean directly with trends in the maximum or minimum values since both are measured in the same units (*i.e*. °C/year). In all other cases trends are presented here as a percentage trend of the average (described above). The indices trends were then plotted against the mean trends to not only show how the trends in the means and extremes vary at each station point but also how they vary across the country as a whole. Each scatter plot (**Figs. 2.5-2.8**) is fitted with a line of best fit using total least squares regression (*Golub and van Loan* 1996). Total least squares is recommended when there are likely to be "errors" in both the horizontal and vertical direction since it minimizes the distance from each point perpendicular to the fitted line rather than just in the *y*-direction as would be the case with ordinary least squares regression. From the slope of the best fit line we can determine if trends in extremes across Australia as a whole are the same as trends in the mean *e.g*. if the slope of the line was equal to -1.0 or 1.0, where comparable units are being used, then the absolute trends in extremes would be of the same magnitude as trends in means.

Table 2.1: The extreme temperature and precipitation indices used in this study as recommended by the ETCCDI. The full list of all recommended indices and precise definitions is given at http://cccma.seos.uvic.ca/ETCCDI/list_27_indices.html. For spell duration indicators (marked with a *), a spell can continue into the next year and is counted against the year in which the spell ends. Precipitation indices for Australia were calculated using stations from *Haylock and Nicholls* (2000) and temperature indices were calculated using stations from *Trewin* (2001).

ID	Indicator name	Indicator definitions	UNITS
TXx	Max Tmax	Monthly maximum value of daily max temperature	ºC
TNx	Max Tmin	Monthly maximum value of daily min temperature	ºC
TXn	Min Tmax	Monthly minimum value of daily max temperature	ºC
TNn	Min Tmin	Monthly minimum value of daily min temperature	ºC
TN10p	Cool nights	Percentage of time when daily min temperature < 10^{th} percentile	%
TX10p	Cool days	Percentage of time when daily max temperature < 10^{th} percentile	%
TN90p	Warm nights	Percentage of time when daily min temperature > 90^{th} percentile	%
TX90p	Warm days	Percentage of time when daily max temperature > 90^{th} percentile	%
DTR	Diurnal temperature range	Monthly mean difference between daily max and min temperature	ºC
FD0	Frost days	Annual count when daily minimum temperature < 0°C	days
SU25	Summer days	Annual count when daily max temperature > 25°C	days
TR20	Tropical nights	Annual count when daily min temperature > 20°C	days
WSDI*	Warm spell duration indicator	Annual count when at least 6 consecutive days of max temperature > 90^{th} percentile	days
CSDI*	Cold spell duration indicator	Annual count when at least 6 consecutive days of min temperature < 10^{th} percentile	days
RX1day	Max 1-day precipitation amount	Monthly maximum 1-day precipitation	mm
RX5day	Max 5-day precipitation amount	Monthly maximum consecutive 5-day precipitation	mm
SDII	Simple daily intensity index	The ratio of annual total precipitation to the number of wet days (> 1 mm)	mm/day
R10	Number of heavy precipitation days	Annual count when precipitation > 10 mm	days
R20	Number of very heavy precipitation days	Annual count when precipitation > 20 mm	days
CDD*	Consecutive dry days	Maximum number of consecutive days when precipitation < 1 mm	days
CWD*	Consecutive wet days	Maximum number of consecutive days when precipitation ≥ 1 mm	days
R95p	Very wet days	Annual total precipitation from days > 95^{th} percentile	mm
R99p	Extremely wet days	Annual total precipitation from days > 99^{th} percentile	mm
PRCPTOT	Annual total wet-day precipitation	Annual total precipitation from days ≥ 1 mm	mm

For a global perspective on the Australian results similar measures were calculated for comparison. Although we do not have access to the mean maximum and minimum temperatures for the global stations with extreme indices, the PRCPTOT precipitation indicator does give a measure of total mean precipitation at each station with which to compare the other indices. Because PRCPTOT is an annual indicator, only annual changes were considered for each index. The period 1951-2003 was used for comparison since this is when most global stations have sufficient data. Only stations which had at least 40 years of precipitation data during this period were used. Again, linear trends were calculated as a percentage of the average for each precipitation index in **Table 2.1**. The percentage trends for the precipitation indices were then plotted against the percentage trends in PRCPTOT to determine the relationship between the means and extremes of rainfall. In addition to a global analysis, 5 non-overlapping latitude bands were chosen to compare with Australian results.

2.4 The relationship between means and extremes of temperature and precipitation in Australia

There are strong relationships between temperature and rainfall in Australia which we need to bear in mind when looking at trends in the means and extremes of both. There was a strong negative correlation between spatially averaged Australia-wide rainfall and maximum temperature in all seasons (summer and winter are shown in **Table 2.2**). A statistically significant correlation between rainfall and minimum temperature was only evident in winter, when there was a strong positive relationship. These results hold true even if the linear trends were removed prior to the correlation calculation although the significant correlations were slightly stronger using the detrended data.

To gain an appreciation for the spatial variability of climate trends across Australia, maps of the trends in the gridded mean fields were plotted and overlaid with a triangle at each station location to represent the magnitude and statistical significance of the trend for each extremes index (**Figs. 2.1 – 2.4**). Only statistically significant trends in mean temperature or precipitation are shown in colour.

Table 2.2: LHS: Correlations (using a Kendall tau test) between mean rainfall, averaged over Australia, and mean maximum and minimum temperatures for 1957-2005. RHS as LHS only for detrended values. Correlations significant at the 5% level are marked in bold. Values courtesy P. Hope, Bureau of Meteorology

	With trend			Detrended		
	DJF	JJA	Ann	DJF	JJA	Ann
Tmax	**-0.63**	**-0.48**	**-0.59**	**-0.67**	**-0.52**	**-0.72**
Tmin	0.14	**0.66**	0.07	0.08	**0.67**	0.03

2.4.1 Maps – temperature

Annually averaged mean maximum and minimum temperatures are increasing across most of Australia with an associated statistically significant decrease in the annual occurrence of cold nights (**Fig. 2.1a**) and cold days (**Fig. 2.1b**). All the other temperature indices show similar spatially coherent trends commensurate with warming: reductions in frost days and cold spells and an associated significant increase in all the other temperature indices, particularly the annual occurrence of warm nights (**Fig. 2.1c**) and warm days (**Fig. 2.1d**). These results agree well with *Collins et al*. (2000) who studied changes in annual extreme temperature trends up to 1996 and other studies such as *Tryhorn and Risbey* (2006) who found a general increase in heatwaves across Australia in recent decades. At a particular location, the trend in the mean minimum temperature and cool nights (**Fig. 2.1a**) is generally slightly larger than the trend in mean maximum temperature and cool days (**Fig. 2.1b**). Spatially, the trends in mean maximum and minimum temperatures are mostly statistically significant in the east of the continent and are up to 0.4°C/decade, an increase of 1.96°C since 1957. In the southeast, the trend in cool nights is stronger than the underlying warming of mean minimum temperature. Within the southeast region there are small areas where the mean minimum temperature has been decreasing, particularly in east Gippsland and the Australian Alps and a small part of northwest New South Wales. Mean maximum temperature has significantly decreased along part of the southern coastline of Western Australia. There are also non-significant decreases in temperature in the northwest of the continent (not shown) along with small increases in the number of cool days and nights. The majority of stations, however, exhibit statistically significant increases in the

annual occurrence of warm nights even in some places where mean minimum temperature has been decreasing (**Fig. 2.1c**). Extreme maximum temperature trends (**Fig. 2.1d**) are bigger than extreme minimum temperature trends along the east coast although in other regions the converse is true.

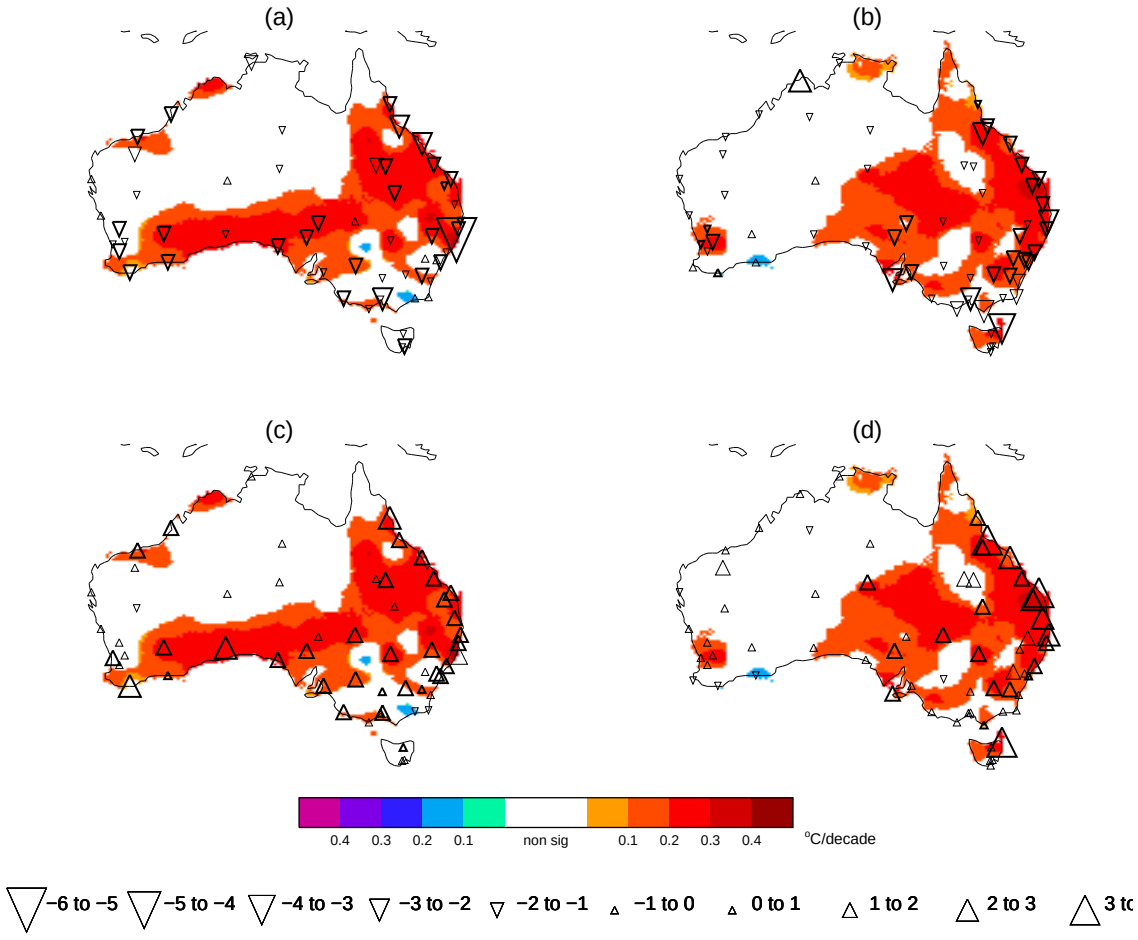

Fig. 2.1: Annual trends (°C/decade) in mean minimum temperature and mean maximum temperature for 1957-2005. Only statistically significant trends are shown in colour. Maps are overlaid with annual trends (%/decade) at each station location with sufficient high quality data represented by upward (downward) triangles for increasing (decreasing) trends for (a) cold nights (TN10p), (b) cold days (TX10p), (c) warm nights (TN90p) and (d) warm days (TX90p) (**Table 2.1**). The size of the triangle reflects the magnitude of the trend. Bold indicates statistically significant change.

Annual results can mask significant seasonal changes so mean minimum (**Fig. 2.2a, 2.2c, 2.2e** and **2.2g**) and mean maximum (**Fig. 2.2b, 2.2d, 2.2f** and **2.2h**) temperatures were analysed for summer (Dec-Feb), autumn (Mar-May), winter (Jun-Aug) and spring (Sep-

Nov) respectively. Corresponding seasonal results are also shown in **Fig. 2.3** with trends in warm nights and warm days. **Fig. 2.2** shows that decreases in annual mean maximum temperature in northwest Australia and the southern coast of south west Australia are mostly a result of a significant decrease in daytime temperature in summer. Cold days are increasing in this region (**Fig. 2.2b**) and warm days are decreasing (**Fig. 2.3b**). Mean minimum temperatures are also decreasing although not statistically significantly in parts of the northwest in all seasons except spring, generally with an associated decrease in warm nights (**Fig. 2.3a, 2.3c, 2.3e** and **2.3g**).

2.4.2 Maps – precipitation

Fig. 2.4 shows seasonal trends in mean precipitation for two periods, 1910-2005 and 1951-2005, overlaid with seasonal trends in maximum 1-day precipitation. The trends vary throughout the seasons, highlighting the importance of examining each season rather than just the annual average. The spatial variability in precipitation is much greater than for temperature and it is clear that there is much less statistical significance in the precipitation trends. Where long term trends in mean precipitation are significant, they tend to be positive outside southwest Western Australia for the September to March period (**Figs. 2.4g, 2.4a, 2.4c**) and mixed for winter (**Fig. 2.4e**). However, in recent decades, a pattern of statistically significant decreases in both the means and extremes has emerged in the eastern half of the country for the December to August period (**Figs. 2.4b, 2.4d** and **2.4f**). In the west the most striking feature of recent trends in mean precipitation is the statistically significant moistening in the northwest in summer (**Fig. 2.4b**). There are no high-quality daily stations in this region to indicate how the extremes are behaving. As suggested in *Nicholls et al.* (1997) and *Power et al.* (1998), this increase is associated with a decrease in maximum temperature (**Fig. 2.2b**). The driver behind this feature is not clear, and is the topic of on-going studies which will be discussed in more detail in **Section D**. One suggestion is that the continental warming further south is driving an enhancement of the Australian monsoon (*Wardle and Smith* 2004).

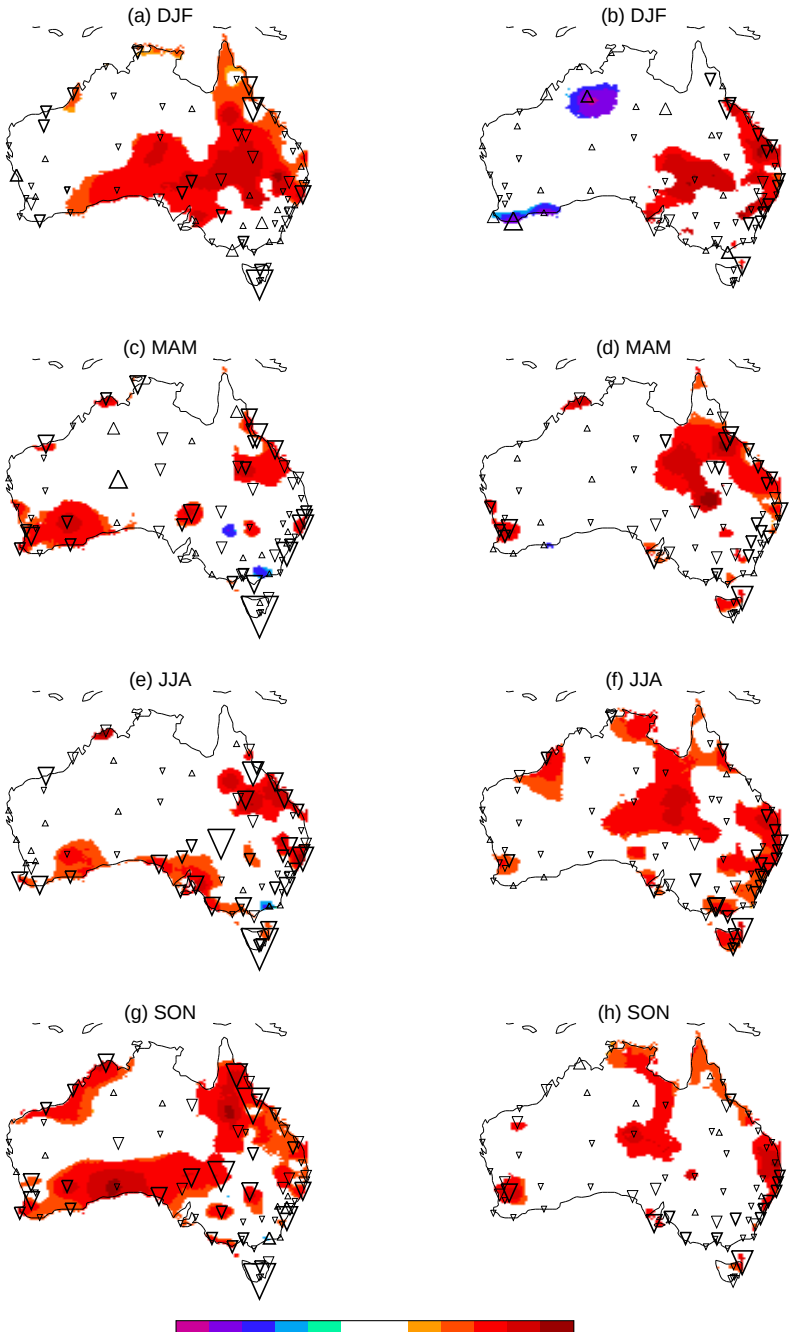

Fig. 2.2: Seasonal trends (°C/decade) in mean minimum temperature (LHS) and mean maximum temperature (RHS) for 1957-2005. Only statistically significant trends are shown in colour. Maps are overlaid with annual trends (%/decade) at each station location with sufficient high quality data represented by upward (downward) triangles for increasing (decreasing) trends for (a), (c), (e) and (f) cold nights (TN10p) and (b), (d), (f) and (h) cold days (TX10p). The size of the triangle reflects the magnitude of the trend. Bold indicates statistically significant change.

For trends in precipitation extremes there is a mixed pattern throughout the seasons but more recent decades generally show larger absolute trends. In general, the directions of the trends in the extremes follow the mean trends but there are a few occasions when a significant decrease in the mean is associated with a significant increase in the extremes or vice versa *e.g.* southwestern Western Australia in spring (**Fig. 2.4g**). One day maximal precipitation trends in summer are increasing at most sampled locations over the period 1910-2005 (**Fig. 2.4a**). The more recent trend (**Fig. 2.4b**) shows a very mixed signal but with larger increases in the southwest and general decreases along the east coast compared to the longer term period. While the long term trend in autumn shows small and mostly non-significant trends in extreme precipitation (**Fig. 2.4c**), probably the most striking feature in recent decades is the decrease in both the means and extremes across Tasmania and the southern coastline of South Australia and Victoria (**Fig 2.4d**). This feature can also be seen in maximum five-day precipitation totals (not shown). In winter the decline in mean rainfall in the southwest is evident, and the most extreme daily totals are also declining over the last 100 years (**Fig. 2.4e**); however there is a mixed response more recently (**Fig. 2.4f**). In the last 50 years mean rainfall decreases are evident along the east coast, and the extremes show some associated significant declines (**Fig. 2.4f**). In spring there is generally little change in the mean across Australia from 1910-2005, except for some small areas of increase and decreases in the southwest (**Fig. 2.4g**). The trends in maximal one-day precipitation are positive at most sampled locations, even in the southwest, indicating that the intensity of the rainfall is increasing. This signature appears to be present in the most recent 50 years (**Fig. 2.4h**) but in general the trends are larger.

2.4.3 Spatial correlations

To determine how well the trends in extremes were correlated with trends in the mean across Australia we calculated linear trends for all the stations in our study. These trends were then correlated (with the individual stations as cases) to represent the spatial rather than temporal relationship between the mean and extremes. The correlations are listed in **Tables 2.3** and **2.4**.

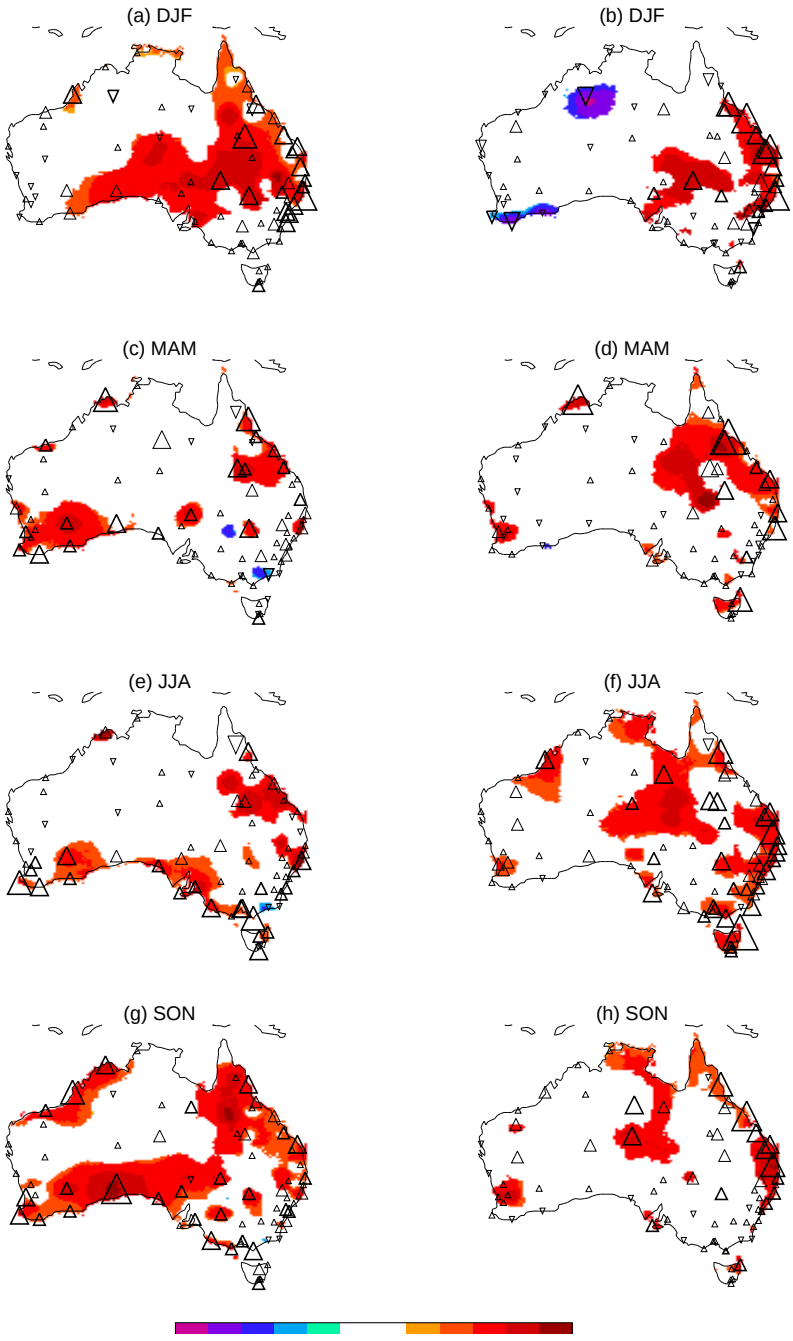

Fig. 2.3: Seasonal trends (°C/decade) in mean minimum temperature (LHS) and mean maximum temperature (RHS) for 1957-2005. Only statistically significant trends are shown in colour. Maps are overlaid with annual trends (%/decade) at each station location with sufficient high quality data represented by upward (downward) triangles for increasing (decreasing) trends for (a), (c), (e) and (f) warm nights (TN90p) and (b), (d), (f) and (h) warm days (TX90p). The size of the triangle reflects the magnitude of the trend. Bold indicates statistically significant change.

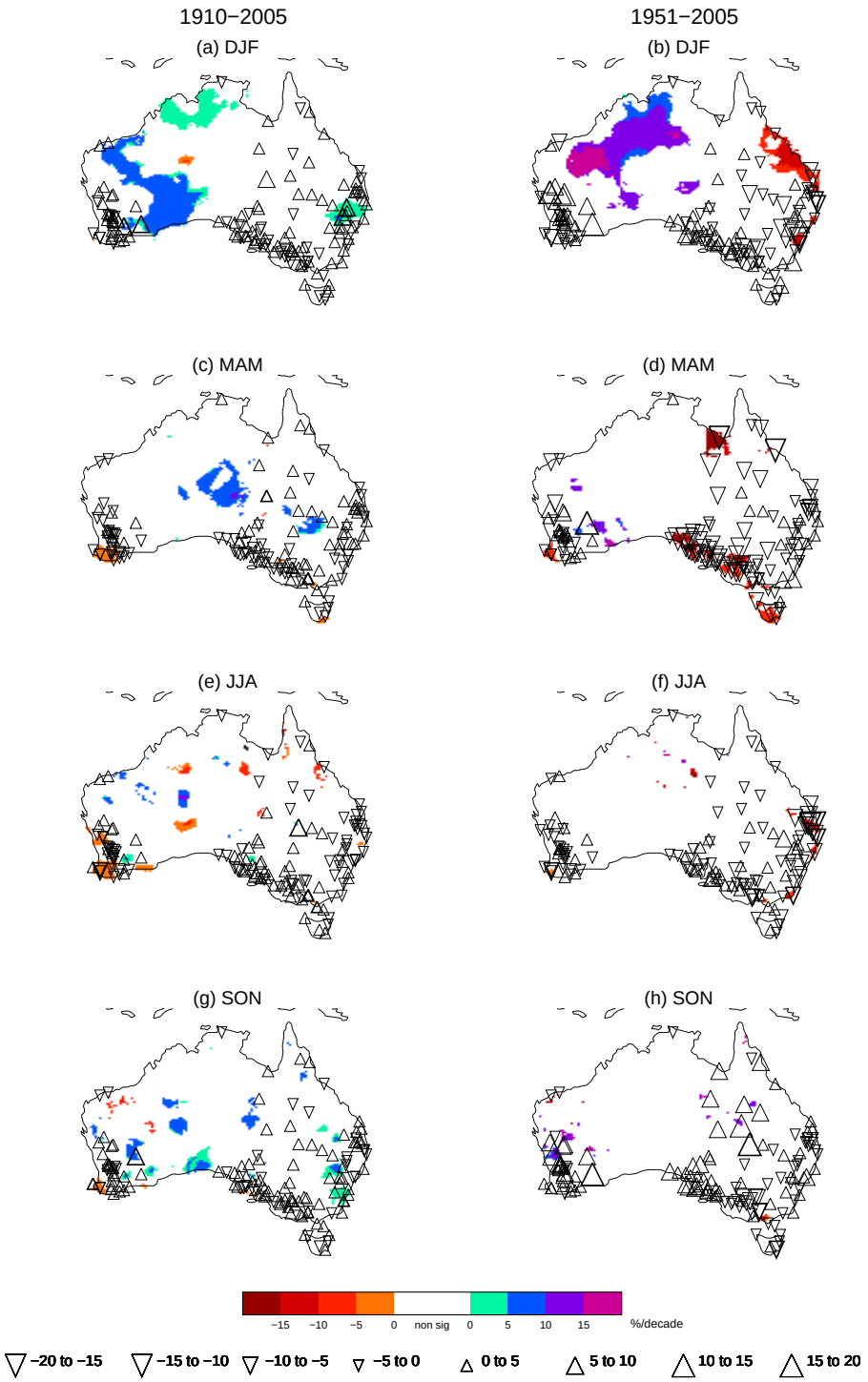

Fig. 2.4: Seasonal trends (%/decade) in mean rainfall for 1910-2005 (LHS) and 1951-2005 (RHS). Only statistically significant trends are shown in colour. Maps are overlaid with annual trends (%/decade) at each station location with sufficient high quality data represented by upward (downward) triangles for increasing (decreasing) trends for (a)-(h) seasonal maximum 1-day precipitation totals (RX1day). The size of the triangle reflects the magnitude of the trend. Bold indicates statistically significant change.

Table 2.3: Spatial correlations, using high quality temperature data at stations across Australia (*Trewin* 2001), between annual and seasonal trends in temperature indices (**Table 2.1**) and trends in either mean minimum or mean maximum temperature, 1957-2005 (1957/58-2004/05 for DJF). Correlations significant at the 5% level are marked in bold.

Minimum temperature					
Index	**Annual**	**DJF**	**MAM**	**JJA**	**SON**
TNx	**0.49**	**0.53**	**0.41**	**0.53**	**0.42**
TNn	**0.64**	**0.33**	**0.65**	**0.83**	**0.48**
TN10p	**-0.82**	**-0.61**	**-0.72**	**-0.83**	**-0.69**
TN90p	**0.79**	**0.74**	**0.67**	**0.70**	**0.60**
DTR	**-0.65**	**-0.34**	**-0.73**	**-0.85**	**-0.75**
FD0	-0.25				
TR20	**0.52**				
CSDI	**-0.52**				

Maximum temperature					
Index	**Annual**	**DJF**	**MAM**	**JJA**	**SON**
TXx	**0.66**	**0.72**	**0.53**	**0.48**	**0.33**
TXn	**0.40**	**0.46**	**0.35**	**0.42**	0.16
TX10p	**-0.80**	**-0.84**	**-0.71**	**-0.67**	**-0.57**
TX90p	**0.77**	**0.76**	**0.71**	**0.78**	**0.61**
DTR	**0.61**	**0.79**	**0.55**	**0.47**	**0.60**

2.4.4 Temperature

Table 2.3 indicates that there is a high correlation between most temperature extremes indices and trends in mean minimum or maximum temperature in all seasons (*i.e*. a station with a strong trend in the mean will generally exhibit a strong trend of the same sign in the extremes). Trends in maximum temperature means and extremes are generally more highly correlated than for the means and extremes of minimum temperatures particularly in summer (DJF). Minimum temperature extremes, however, are much more highly correlated with mean minimum temperatures in winter (JJA). Seasonally the smallest correlations occur in spring (SON) which is also when there is the weakest correlation between the means and extremes of precipitation (see **Table 2.4**). This is in agreement with

the finding of *Alexander et al.* (2006) who showed that global trends in temperature extremes were generally smallest in September-November irrespective of which hemisphere was analysed.

Table 2.4: Spatial correlations, using high quality precipitation data at stations across Australia (*Haylock and Nicholls* 2000), between annual and seasonal trends in precipitation indices (**Table 2.1**) and trends in mean precipitation, 1910-2005 (1910/11-2004/05 for DJF). Correlations significant at the 5% level are marked in bold.

Index	Annual	DJF	MAM	JJA	SON
RX1day	**0.56**	**0.81**	**0.81**	**0.83**	**0.65**
RX5day	**0.60**	**0.88**	**0.87**	**0.85**	**0.79**
SDII	**0.35**				
R10mm	**0.75**				
R20mm	**0.63**				
CDD	-0.36				
CWD	0.12				
R95p	**0.55**				
R99p	**0.44**				
PRCPTOT	**0.92**				

In summer, the majority of stations (71%) have trends greater in magnitude in the warmest daily maximum temperature than mean maximum temperature (**Fig. 2.5a**) and over half (55%) of stations have greater absolute trends in the coldest daily minimum temperature than mean minimum temperature (**Fig. 2.5b**). In winter, 46% of stations have greater absolute trends in extreme high maximum temperature than mean maximum temperature (**Fig. 2.5c**) and 74% of stations (the largest proportion in any season) have greater absolute trends in extreme low minimum temperature than mean minimum temperature (**Fig. 2.5d**). For the remaining absolute-threshold temperature indices *i.e.* TXn and TNx (see **Table 2.1**), well over half of stations show increased trends (whether positive or negative) compared to the mean trend in all seasons and annually. While stations are not equally spaced, they are well distributed across the country although since there is a greater density of stations in the east and south than the north and west, the analysis may be weighted more towards these well sampled areas. Generally the mean and extremes are of the same sign but there are instances where there are increasing means and decreasing extremes and

vice versa. In a few cases the extremes are increasing (decreasing) faster than the mean is decreasing (increasing). In these cases the shape of the temperature distribution could be changing although the high signal-to-noise ratio of these types of extremes makes it difficult to draw definitive conclusions.

Fig. 2.6, like **Figs. 2.2** and **2.3**, shows that both the extremes and mean of maximum and minimum temperature are increasing across much of Australia in all seasons. The cold tails of minimum temperature (**Fig. 2.6a, 2.6e, 2.6i** and **2.6m**) are warming faster than the warm tails of minimum temperature (**Fig. 2.6c, 2.6g, 2.6k** and **2.6o**) in every season. These results are consistent with the results of Trewin (2001). For maximum temperature, this differential warming of the cold (**Fig. 2.6b, 2.6f, 2.6j** and **2.6n**) and warm (**Fig. 2.6d**, **2.6h, 2.6l** and **2.6p**) tails is less evident. However, there appears to be enhanced warming in the warmest maximum temperatures in summer (**Fig. 2.6b** and **2.6d**) with some enhanced warming in the cold tails in winter (**Fig. 2.6j** and **2.6l**). In all cases the proportional warming in the extremes is greater than the proportional warming in the median. This does not necessarily indicate a change in the shape of the frequency distribution: for example, in a normal distribution, an increase in the location parameter with no change in the scale parameter will lead to a greater proportional change in the extreme indices than in the mean index (*Katz and Brown* 1992). Although it is not possible to make a direct comparison because of the different units used, it does appear that in some cases the most extreme events (**Fig. 2.5**) are changing more rapidly than the distribution tails (**Fig. 2.6**). However, this can only be inferred from the results presented here and would require a full analysis of the distribution of daily temperature to answer definitively.

2.4.5 Precipitation

Table 2.4 shows that trends in precipitation extremes are highly correlated with total precipitation trends. This is particularly true of maximum 1-day (RX1day) and 5-day precipitation (RX5day), number of days above 10 mm (R10mm) and 20 mm (R20mm) and very wet days (R95p) and extremely wet days (R99p). Consecutive dry days (CDD), consecutive wet days (CWD) and daily intensity (SDII) show weaker correlations. The correlations are also strong in every season for the two indices that can be defined seasonally although the correlations are slightly smaller in spring when the relationship between the means and extremes of maximum and minimum temperature is also weakest.

The seasonal correlations are stronger than the annual correlations because as the sample size reduces (*e.g.* from annual to seasonal), the influence of these extremes on the total precipitation is much greater.

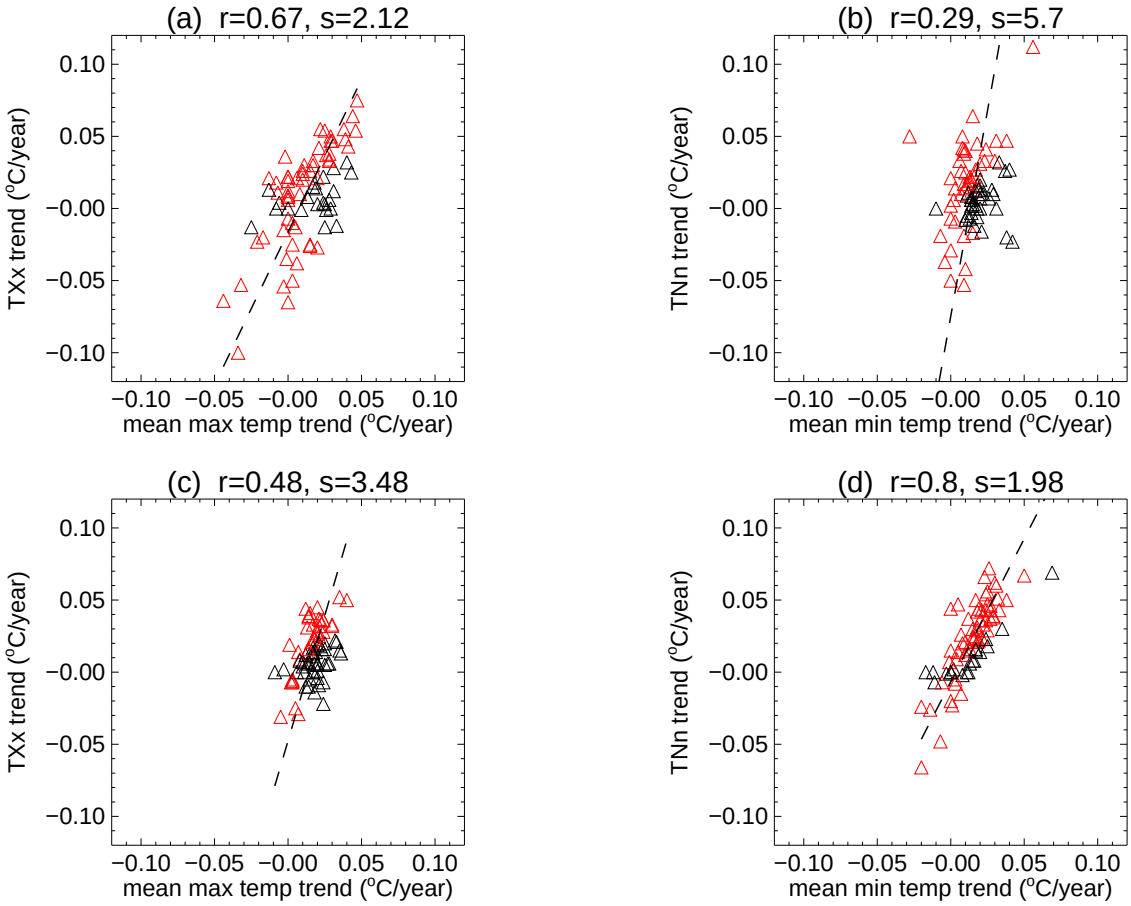

Fig. 2.5: Triangles represent annual trends (°C/year) in mean maximum (minimum) temperature at high-quality Australian station locations (*Trewin* 2001) plotted against trends in the hottest (coldest) maximum (minimum) daily temperature (°C/year) at those stations for (a) and (b) summer and (c) and (d) winter between 1957 and 2005. Red triangles indicate where the absolute seasonal trend in the warmest ((a) and (c)) or coldest ((b) and (d)) day at a station is greater than the absolute seasonal trend in mean maximum ((a) and (c)) or minimum temperature ((b) and (d)) at that station *i.e.* where the magnitude of the trend in the extremes is greater than the magnitude of the mean trend. The line of best fit calculated using total least squares regression is shown in red, s is the slope of the line and r is the spatial correlation.

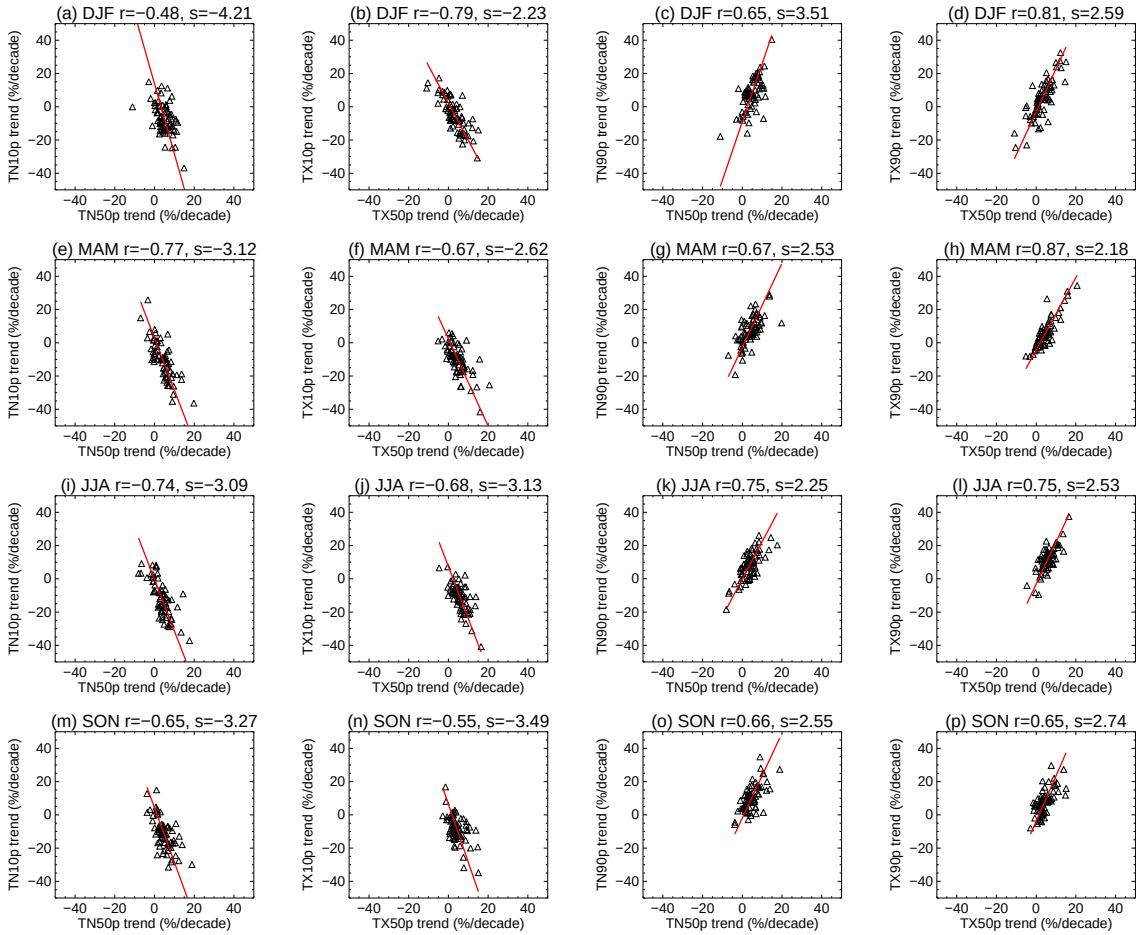

Fig. 2.6: Seasonal trends (%/decade) in 10th and 90th percentile indices (**Table 2.1**) with respect to seasonal trends (%/decade) in the median (denoted on the x-axes by TN50p for minimum temperature and TX50p for maximum temperature) for (a)-(d) Dec-Feb, (e)-(h) Mar-May, (i)-(l) Jun-Aug and (m)-(p) Sep-Nov. Each symbol represents a station. The line of best fit calculated using total least squares regression is shown in red, s is the slope of the line and r is the spatial correlation.

Percentage trends in each precipitation index between 1910 and 2005 were plotted and compared. Except for daily intensity (SDII), the slope of the line of best fit is greater than 1.0, indicating enhanced variability in the trends of precipitation extremes compared to the mean trends. **Fig. 2.7** shows the results for very wet and extremely wet days. Although the correlations between the mean and R99p are smaller than R95p (**Table 2.4**), the steeper slope of the line of best fit in **Fig. 2.7b** compared to **Fig. 2.7a** indicates that the most extreme events may be changing at a faster absolute rate in relation to the mean than more moderate events. This result is expected under climate change simulations with enhanced greenhouse gas forcing (*IPCC* 2001) and also agrees with statistical theory that

precipitation extremes are more sensitive to changes in the scale parameter of the precipitation distribution (*e.g.* *Katz* 1999).

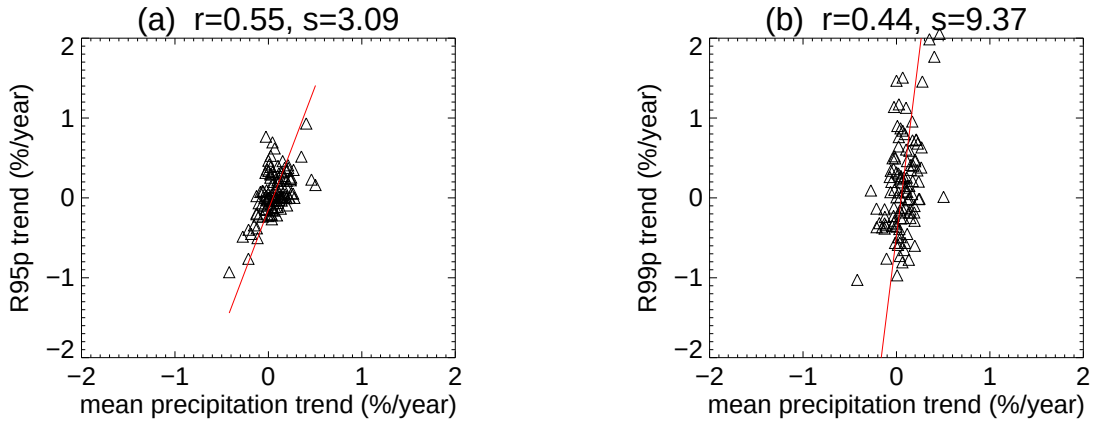

Fig. 2.7: Annual trends (%/year) at Australian stations for (a) R95p and (b) R99p plotted against annual trends (%/year) in mean precipitation between 1910 and 2005. The line of best fit calculated using total least squares regression is shown in red, s is the slope of the line and r is the spatial correlation.

2.5 Comparison between Australia and other parts of the world

Table 2.5 shows the correlations between 1951 and 2003 for PRCPTOT and the precipitation indices from **Table 2.1** for the globe and five regions defined by non-overlapping latitude bands. The correlations between the means and extremes of rainfall in Australia are similar to the correlations for the globe and all of the regions studied.

Plotting the percentage trends shows just how similar the relationships between the means and extremes of precipitation are for Australia and the globe (**Fig. 2.8**). For the majority of indices the correlation between the means and extremes of rainfall is above 0.5 except for CDD (r=-0.36) and CWD (r=0.48). **Table 2.5** and **Fig. 2.8a** show that the annual number of days above 10 mm (R10mm) is the most strongly correlated extreme index globally. Also shown are the relationships between percentage trends in PRCPTOT and percentage trends in R95p (**Fig. 2.8b**), R99p (**Fig. 2.8c**) and RX5day (**Fig. 2.8d**). Unlike R10mm, these indices were all originally measured in the same units (mm) so it is easier to undertake a like-by-like comparison. The relationship between the trends in means and extremes is remarkably coherent across the globe for all indices studied. Although the

correlations are statistically significant (**Table 2.5**) in all cases, it is clear from **Fig. 2.8** that the slope of the line of best fit is significantly above 1.0 *i.e*. extreme precipitation events are changing at a disproportional rate to mean changes when averaged across the globe. In addition, as with the results for Australia, the most extreme precipitation events (**Fig. 2.8c**) are more extended in scale than more moderate events (**Fig. 2.8b**) indicating enhanced trends in the more extreme tails of the precipitation distribution. This is the first time using high quality, long-term datasets, that global changes in extremes have been compared directly with changes in average precipitation.

While in this study we have been unable to do the same comparison between global mean temperature and temperature extremes, other studies (*e.g*. *Caesar et al*. 2006) have analysed trends in various percentiles for maximum and minimum temperatures for Australia and other parts of the globe. *Caesar et al*. (2006) analysed nine percentiles (*i.e*. 10^{th}, 20^{th},…, 90th) for maximum and minimum temperature over a large scale from a newly created daily temperature dataset. They showed that Australia had a much more uniform significant warming across the whole percentile range unlike other regions studied *e.g*. USA, Europe, China and Russia. This would seem to confirm that it is the whole temperature distribution which is shifting towards increases in temperature in Australia. However that study excluded the analysis of the most extreme events compared with mean trends. Therefore, it is impossible to say whether the most extreme events are behaving differently from more moderate extreme events which would seem to be the suggestion given the results from the Australian temperature stations studied here.

Table 2.5: Spatial correlations, using high quality precipitation data (*Alexander et al.* 2006), between trends in PRCPTOT (which is being used as a proxy for annual precipitation) and trends in precipitation indices (**Table 2.1**) between 1951 and 2003 for the globe and 5 non-overlapping latitude bands. Correlations significant at the 5% level are marked in bold.

	R10mm	**R20mm**	**R95p**	**R99p**	**SDII**	**RX1d**	**RX5d**	**CDD**	**CWD**
Global	**0.86**	**0.76**	**0.76**	**0.52**	**0.58**	**0.50**	**0.61**	**-0.36**	**0.48**
90°S-30°S	**0.94**	**0.89**	**0.86**	**0.67**	**0.64**	**0.69**	**0.78**	**-0.36**	**0.57**
30°S-0°S	**0.88**	**0.90**	**0.88**	**0.66**	**0.47**	**0.76**	**0.78**	**-0.43**	**0.55**
0°N-30°N	**0.86**	**0.88**	**0.77**	**0.54**	**0.60**	**0.53**	**0.63**	**-0.29**	**0.42**
30°N-60°N	**0.86**	**0.75**	**0.74**	**0.51**	**0.56**	**0.48**	**0.58**	**-0.36**	**0.46**
60°N-90°N	**0.80**	**0.57**	**0.76**	**0.51**	**0.71**	**0.45**	**0.63**	**-0.51**	**0.61**

2.6 Discussion

This chapter has determined relationships between means and extremes in Australia using a set of standard climate extremes indices which in turn have been compared with global results. It has been shown that the relationships between the trends in means and extremes are consistent throughout Australia and the globe. Globally, the enhanced warming of minimum temperatures compared to maximum temperature extremes is the expected response (*e.g.* *Hegerl et al.* 2004) to increasing levels of atmospheric greenhouse gases (*IPCC* 2001). However recent studies show that the regional responses of observed trends in means and extremes of temperature and precipitation can also largely be driven by large scale 'natural' climate variability (*Scaife et al.* 2008) although this variability may not be completely unaffected by anthropogenic forcings.

Southwest Western Australia is a region of Australia where a number of studies have attempted to attribute the observed climate changes. The region has seen a significant decrease in rainfall over recent decades associated with a decrease in troughs and increase in high pressure systems (*Hope et al.* 2006). Although the rainfall decrease can be captured by long climate simulations (*Cai et al.* 2005), the timing of the response appears to be anthropogenic in origin (*Timbal et al.* 2006). As trends in other regions become increasingly large (*e.g.* recent trends in northwest and southeast Australia), studies to separate the natural climate responses from anthropogenic influences will become increasingly important. These will require careful consideration and the appropriate experimental set up, but might be able to begin to answer the question of whether current trends will persist into the future. One indicator that there is an anthropogenic influence on the trends observed in Australia is the fact that there is a strong link between the Australian and global pattern for changes in means versus extremes, which suggests an over-arching influence on the whole globe.

Irrespective of the cause, given the enhanced variability of trends in extremes compared to mean trends it is likely that these extreme changes will have severe impacts on vulnerable regions (*e.g.* *Green et al.* 2009). Factors such as changes in land use, water storage/usage practices or population density will change how certain regions are able to adapt to the extreme changes in climate which have been highlighted by this and many other studies. In

some regions, increases in rainfall would come as welcome relief, in others unseasonable rainfall will potentially bring with it certain weed species which can kill crops and cattle (Ian Foster personal communication). Changing temperatures may have beneficial affects for some animal or plant species while pushing other ecosystems towards extinction. For this reason changes in extremes need to be assessed not as a threat in isolation from other forms of social and environmental change but within a framework analysing the cumulative and interacting threats and vulnerabilities of these changes. However, the relationships between means and extremes described here cannot be a substitute for a full analysis of changes in the distribution of daily temperature and precipitation which should be the basis of any further study.

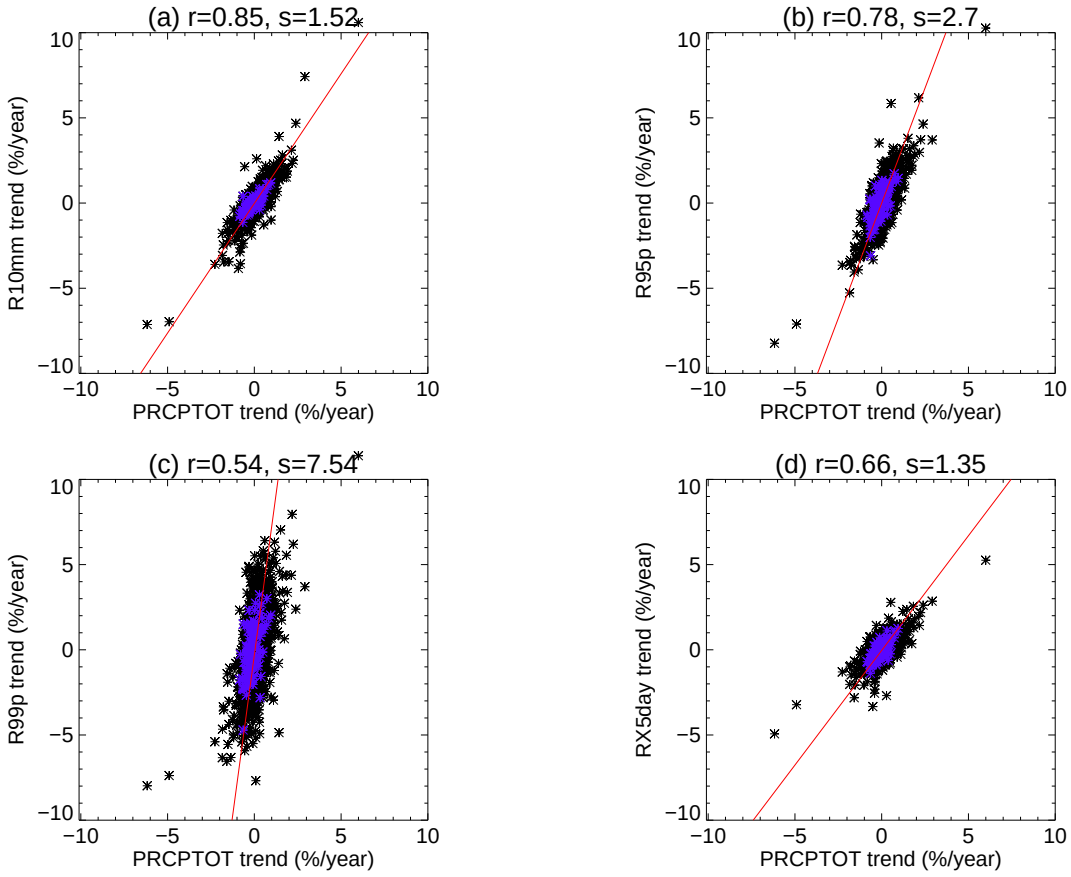

Fig. 2.8: Trends (%/year) in (a) R10mm, (b) R95p, (c) R99p and (d) RX5day on the y-axis plotted against trends (%/year) in annual total precipitation > 1mm for global stations from *Alexander et al. (2006)* with at least 40 years of non-missing data. Each symbol represents a station. The line of best fit calculated using total least squares regression is shown in red, s is the slope of the line and r is the spatial correlation using the percentage trends. Australian stations are represented by blue asterisks.

2.7 Conclusions

In this chapter we have updated previous analyses of long-term observed trends in temperature and precipitation extremes for Australia, analysed how these relate to trends in means and, for the first time, have compared these relationships with those for other parts of the world.

Trends in extremes are highly correlated with trends in means for both temperature and precipitation in Australia, suggesting that the mechanisms driving mean change are also driving changes in extremes. However the results also suggest that absolute trends in extremes across the country as a whole are larger relative to trends in means.

In Australia, the most extreme minimum and maximum daily temperature trends are greater than corresponding trends in the mean. Cold minimum temperature extremes are warming faster than warm minimum temperature extremes in every season. The warm and cold tails of the maximum temperature distribution appear to be warming at approximately the same rate except in summer, when warm maximum temperatures appear to be increasing faster than cold maximum temperatures. Whilst the warm and cool tails are showing greater proportional changes than the mean, it has not been determined whether these changes are significantly different to those which could be explained by a simple increase in the mean of the frequency distribution without any other changes (*e.g.* variance and skewness) in the distribution.

For precipitation, if the mean is increasing then the extremes tend to increase at a faster rate and vice versa for decreasing mean precipitation. The results also tentatively suggest that the most extreme events also appear to be changing at a faster rate than more moderate extreme events.

Trends in annual mean precipitation were available for the globe permitting an analysis of the relationships between these trends and those in precipitation extremes. The relationships for Australia were found to be consistent with those for the globe.

The results are consistent with climate model simulations of the 20th Century that incorporate anthropogenic forcings (*e.g.* *Folland et al.* 2001) and suggest that extremes of temperature and precipitation are changing at a faster rate than are the means.

However, temperature and precipitation extremes are not the only types of extremes that can have significant impacts for Australia. The next chapter investigates how 'storminess' has changed in Australia over century and longer timescales.

C. Stormy weather?

On 3rd June 2007, after a two year search, the Southern Ocean Exploration Team discovered the wreck of the cargo ship SS Alert in Bass Strait off the coast of Cape Schanck, Victoria. The ship was wrecked in severe weather on 28th December 1893. According to the National Shipwrecks Database of Australia (NSD; http://www.environment.gov.au/cgi-bin/heritage/nsd/nsd_list.pl), over 700 ships have been wrecked along the Victorian coastline over the past 200 years. The NSD states that "*the weather off the coast of Victoria at the time of the* (SS Alert) *sinking was the worst for many months*" although the subsequent investigation of the wreck suggests that the Scottish-built ship was never designed for Southern Ocean sailing (The Age, June 13th 2007).

Despite the risks, Bass Strait was a major shipping route of significant economic importance during the 19th and early 20th centuries. Ship after ship carried supplies, convicts and immigrants past Victoria's coastline on the way to Melbourne, Sydney and other large and growing settlements. Many lives were lost, often after being ship-wrecked by fierce storms rolling in from the Southern Ocean. The sailor and explorer Matthew Flinders had "*seldom seen a more fearful section of coastline*" so it is little wonder that the Victorian coast is sometimes called the "*Shipwreck Coast*".

Fortunately, weather-related shipwrecks have declined over the past century. While this is undoubtedly due to improvements in ship building techniques, technology and forecasting, was it also stormier along the Victorian coastline during the late 19th century than it is today? Given that the climate is changing due of global warming, has this produced a trend in the frequency or intensity of storms over the past 150 years?

A new data set from the Bureau of Meteorology (BoM) is helping us address such questions. The data set consists of in-situ sub-daily air pressure data for about 50 observation stations around Australia. Rapid changes in pressure enable us to pin-point when storms and gales occurred, how often they occurred, and can even shed light on how intense the storms might have been.

Most studies using sub-daily to daily in-situ data have been limited to the Northern Hemisphere and particularly Northern Europe where century and longer timescale observations are available (*WASA Group* 1998; *Alexandersson et al.* 2000; *Barring and von Storch* 2004). *Alexander et al.* (2005) and *Allan et al*. (2008) used an absolute change of 10 hPa over a 3-hour period as a measure of severe storm events over the British Isles and Iceland while other studies have focussed on analysis of storminess using wind gust characteristics (*e.g. Smits et al*. 2005), daily pressure tendencies (*e.g. Alexandersson et al*. 2000) and geostrophic winds deduced from station triangles of pressure observations (*e.g. Schmidt and von Storch* 1993; *Matulla et al.* 2008). Studies have shown that measures of storminess calculated from pressure observations generally provide a much more homogeneous record for analysis than wind speeds for example, which are very sensitive to site moves and changing instrumentation (*WASA Group* 1998). In the Southern Hemisphere, while the structure, location, density and number of storms and extra-tropical cyclones have been studied (*e.g. Simmonds and Keay* 2000; *Lynch et al*. 2006; *Frederiksen and Frederiksen* 2007; *Lim and Simmonds* 2007; *Pezza et al.* 2007), attention has been largely limited to the period covered by reanalysis data *i.e*. the last 50 years. So while the study of in-situ pressure observations limits the space scale of the analysis of storms, it does allow us - for the first time - to study the variations in storms over a much longer period of approximately 150 years.

One of the stations included in the new data set is Cape Otway, situated near the eastern end of the "Shipwreck Coast". There has been a lighthouse at Cape Otway since 1849 and meteorological observations have been taken since 1861, making it one of the longest-running continuous observational records in Australia. While there are other stations in the BoM data set on the coast of Tasmania and South Australia, the data are incomplete and do not provide the length of record that can be obtained from the Cape Otway site. The Cape Otway record therefore provides a unique and complete insight into climate variability and changes across the region since the 1860s. We will use data from this station to illustrate how severe storms can be diagnosed and the quality control procedures needed to ensure that the data are interpreted correctly.

C.1 Severe Storm Index

Cape Otway has an almost complete record of 09:00 and 15:00 (local time) pressure observations since 1865 (held at the National Archives of Australia). However, when the observations were digitized they were generally not quality controlled or homogenised to remove inconsistencies that may be introduced through changes in instrumentation, for example. By considering pressure tendencies (*i.e.* the difference in pressure between two observing times) as a proxy for "storminess" rather than actual pressure values, we can eliminate some of the bias that may have been introduced over time as instrumentation and observing practice changed (*Alexander et al.* 2005). For this reason, pressure tendencies between 09:00 to 15:00 (6-hour tendency) and 15:00 to 09:00 (18-hour tendency) have been calculated for each day between 1865 and 2006. Sub-daily tendencies should detect more of the faster moving, intense storms that would be missed if only one daily tendency were considered (*Alexander et al.* 2005). To identify the most severe storms, the 1st and 99th percentiles of all 6-hour and 18-hour pressure tendencies for each month were calculated using a simple rank percentile method. Station level rather than mean sea level pressure measurements were used so that possible changes in the method in which corrections were made to convert to mean sea level did not adversely influence the result. Every occasion where a pressure tendency was below (above) the 1st (99th) percentile was classified as a "severe storm". The percentile threshold values for each month are shown in **Table C.1** and suggest that while the thresholds are generally larger in winter, the severe storm thresholds at Cape Otway vary little throughout the year. This indicates that storms can be as fierce in summer as in winter. One example of such an event in summer occurred on 3rd February 2005 (identified by the severe storm index since there was an 18-hour tendency decrease of 12 hPa). **Fig. C.1** shows the striking satellite image of the event. In total, 951 severe storm events were identified between 1865 and 2006.

Unfortunately additional problems can arise whereby not all very large tendencies correspond to a severe weather event. For example, if a pressure observation was recorded or digitised incorrectly, *e.g.* by incorrectly transposing digits, this will very likely produce and error in our severe storms index. To counter this, each of the 951 possible events identified in the raw index was hand-checked against the original weather logs for Cape Otway to determine whether a storm had actually occurred. Being historical documents, the weather logs are both valuable and fragile and need to be handled carefully making the

process of hand checking very time consuming. However, they do provide much more information than can be obtained from the pressure tendencies alone. Barometer readings were generally available for many more time periods during the day than had been digitised and temperature, rainfall, wind speed and direction and other meteorological variables were also available. The observer notes (where available) also proved to be a valuable and interesting source of additional information about each event (see **Fig. C.2**). Of the 951 events that we identified using the method described here, 115 (12 %) were identified as erroneous. This was mostly due to digits being transposed when keyed electronically or in some cases when observers have incorrectly recorded the observation in the original handwritten archive (see **Fig. C.3** for an example).

Table C.1: Thresholds (in hPa) for the 1st and 99th percentile of 6-hour and 18-hour pressure tendencies at Cape Otway, 1865-2006.

	6-hour tendency (hPa)		**18-hour tendency (hPa)**	
	1%ile	99%ile	1%ile	99%ile
Jan	-7.1	6.7	-13.2	14.4
Feb	-6.9	6.7	-11.3	14.0
Mar	-6.7	6.7	-10.5	13.9
Apr	-6.9	7.1	-12.6	14.4
May	-7.2	7.1	-12.5	13.7
Jun	-7.4	6.9	-14.0	15.9
Jul	-7.9	6.8	-13.5	16.6
Aug	-8.0	8.3	-14.5	15.5
Sep	-8.6	7.7	-14.8	16.9
Oct	-8.4	8.7	-14.3	15.7
Nov	-7.8	6.8	-14.6	14.5
Dec	-7.0	7.0	-13.7	13.7

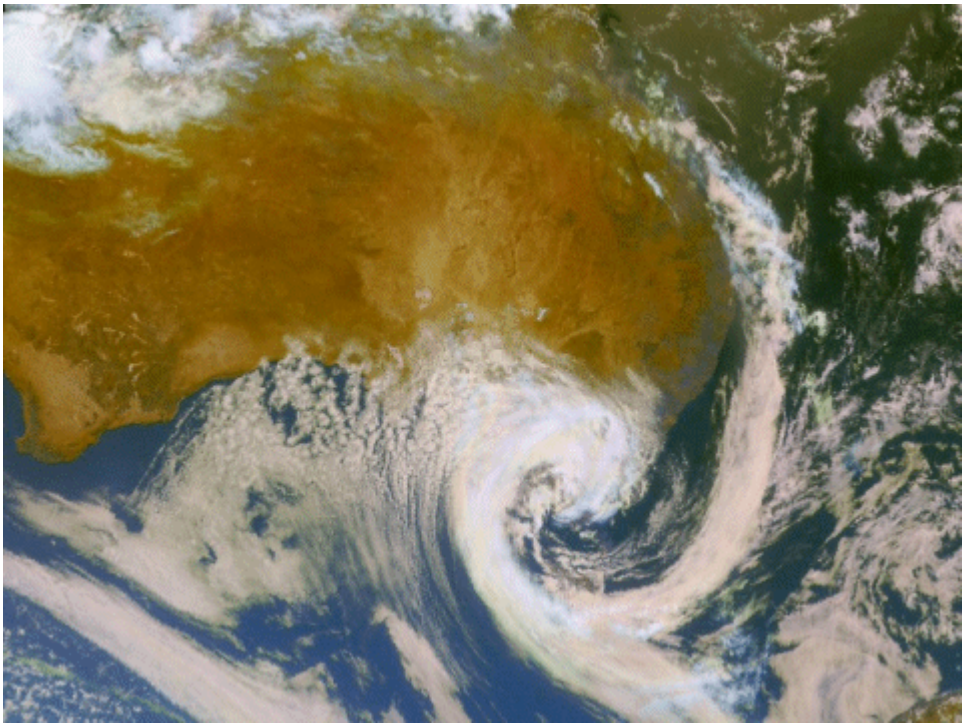

Fig. C.1: Satellite image over Victoria at 0225 UTC (1325 EDST) on 3rd February 2005 corresponding to the severe storm index at Cape Otway. Satellite image originally processed by the Bureau of Meteorology from the geostationary satellite GOES-9 operated by the National Oceanographic and Atmospheric Administration for the Japan Meteorological Agency. Image obtained from http://www.bom.gov.au/announcements/sevwx/vic/2005feb/index.shtml.

The method described here does not necessarily pick up all the severe storms that occurred along the "Shipwreck Coast", particularly some of the events that occur between 15:00 and 09:00, since the 18-hour tendency can miss some of the fast moving events which develop over shorter timescales *e.g.* a gale on 25th April 1880 with maximum wind speed of 78 mph (126 km/h) does not show up in the severe storm index. However, the method used provides a consistent and objective technique for identifying severe storm events over a period of about 150 years.

C.2 Shipwrecks

The dates when the storms mentioned above were identified were also compared with data from the National Shipwrecks Database (NSD). **Table C.2** lists occasions where the severe storms index coincides with shipwrecks along the Victorian coastline between 1865 and 1900. The NSD does not always contain full details about the shipwrecks *e.g.* the reason

for the wreck might be registered as "*unknown*" or the exact date of the wreck is not known. Not all shipwrecks in the database were weather related and a lot of ships were deliberately "*scuttled*" or sank through human error such as in the case of one paddle steamer which burnt and sank while at anchor when "*crew away fishing*" or in another case simply "*ran ashore due to careless navigation*". Conversely, some of the shipwrecks noted in the NSD as weather-related do not show up in the severe storms index. This is the case with perhaps one of the most famous shipwrecks, The Loch Ard, which was wrecked on 1st June 1878 with only 2 survivors out of the 54 people on board. Between 15:00 on 31st May and 09:00 on 1st June 1878 there was a large increase in pressure of 9.3 hPa in the 18-hour tendency at Cape Otway. However this is several hPa less than the 99th percentile threshold value of 13.7 hPa for this time of year (**Table C.1**) so the event is not classified as a severe storm by our definition.

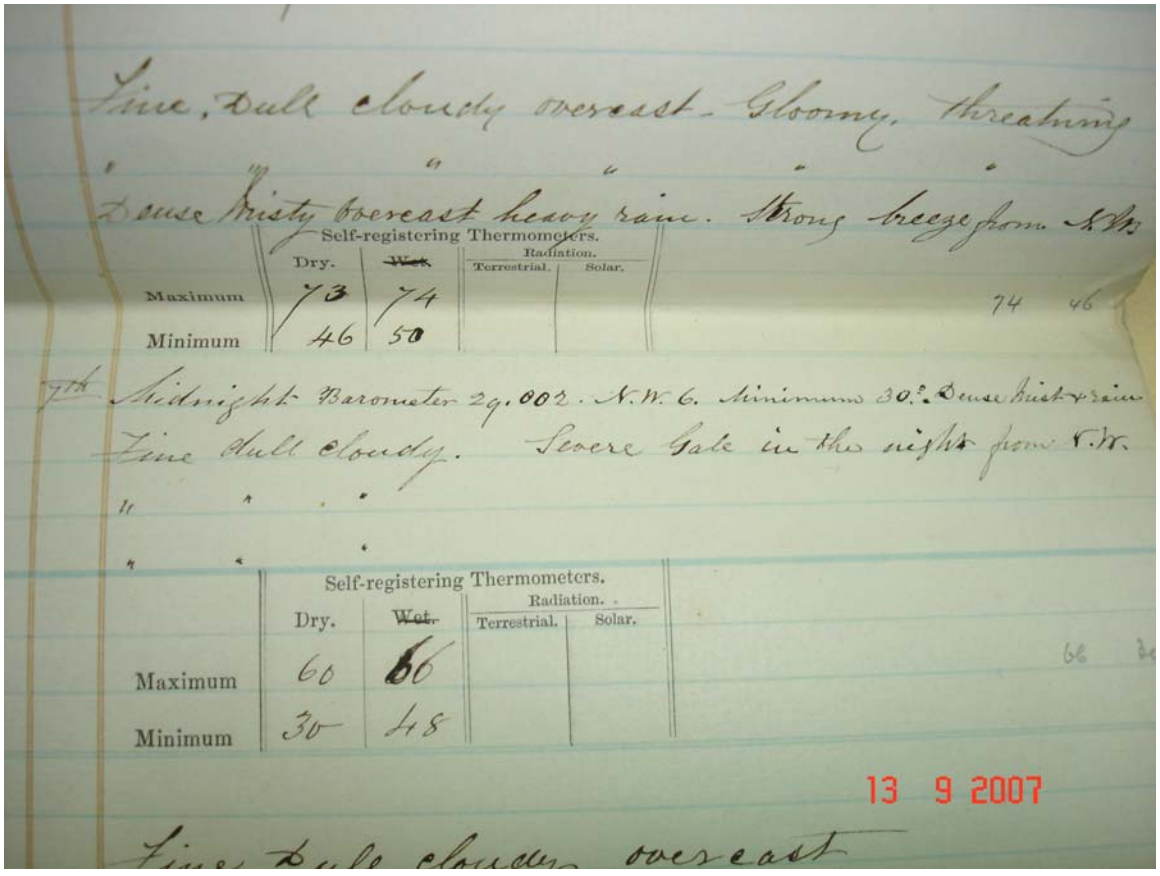

Fig. C.2: Weather log from 7th March 1866 which reads "Midnight barometer 29.002. N.W.6. Minimum 30°. Dense mist and rain. Fine dull cloudy. Severe gale in the night from N.W.". The ships Bitter Beer (schooner) and Pomona (ketch) were likely wrecked when caught in this gale, described in the NSD as "one of the fiercest gales ever experienced on the Victorian Coast".

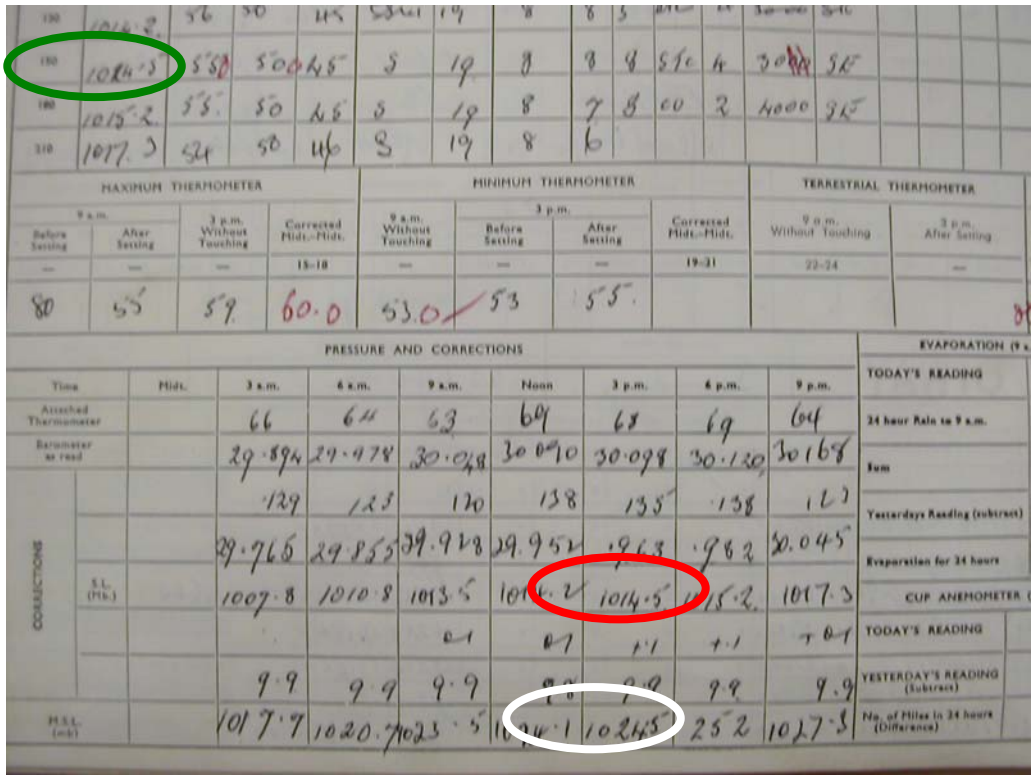

Fig. C.3: An example of an incorrectly recorded value in the original handwritten archive (and hence wrongly digitised). The 3pm mean sea level pressure reading of 1024.5 hPa (white circle) has been incorrectly recorded in the observation column (green circle) rather than the station level pressure reading of 1014.5 hPa (red circle). This produced an 11 hPa increase in the storm index in a 6 hour period rather than the correct 1 hPa increase.

Some of the shipwrecks from **Table C.2** are noted in the NSD as "*disappeared without a trace"*. This is the case with the Dunkeld which is noted as "*last seen near Wilsons Promontory, and became one of the many vessels that disappeared without trace along the Victorian coast*". Our analysis sheds light on this long-standing mystery. The Dunkeld was last seen 40 nautical miles east of Wilsons Promontory on its voyage south from Newcastle on the 27th June 1870 (http://oceans1.customer.netspace.net.au/vic-wrecks.html). On that very same day, there was a sharp pressure drop at Cape Otway of 10.2 hPa over a 6 hour period. **Fig. C.4** shows the pressure tendencies just before and after the event. A drop like this is consistent with severe weather. The mysterious disappearance of the Dunkeld, it seems, is a little less mysterious now. This connection was probably realised at the time, but it does not seem to have been recorded in existing historical documents. Thus the Cape Otway pressure records have enabled us to make an interesting "re-discovery".

Table C.2: Dates between 1865 and 1900 identified as "severe storms" when ships were also wrecked along the Victorian Coastline according to the NSD. Where "unkn" appears in the last column, the number of fatalities is unknown. *According to NSD these wrecks were not weather-related.

Date of severe storm	Name of ship wrecked (from NSD)	Wreck found	Number of fatalities
8/2/1866	Pryde	N	0
7/3/1866-8/3/1866	Bitter Beer	N	unkn
	Pomona	N	unkn
11/8/1866	Nith	N	unkn
15/4/1867	Black Watch	N	0
18/4/1867-19/4/1867	Admiral	N	0
	Emily	N	0
11/10/1868	Lucy Lee	N	1
25/11/1869	Marie Gabrielle	N	unkn
1/3/1870	Eliza	N	unkn
27/6/1870	Dunkeld	N	unkn
29/3/1876	Eva	N	unkn
31/8/1876	Cygnet	N	unkn
9/5/1881	Caroline	N	unkn
10/7/1887	Dart	N	0
19/7/1887	Magnolia	N	4
15/1/1888	Edinburgh Castle*	Y	0
11/12/1892	Kermandie	N	3
1/10/1897	Omega	Y	0
2/3/1898	SS Perserverence*	N	0
30/7/1898	Emily	N	2
13/7/1899	Excelsiour	N	unkn
25/3/1900	SS Glenelg	N	31
9/5/1900	Magnat	Y	1
	Sierra Nevada	Y	23

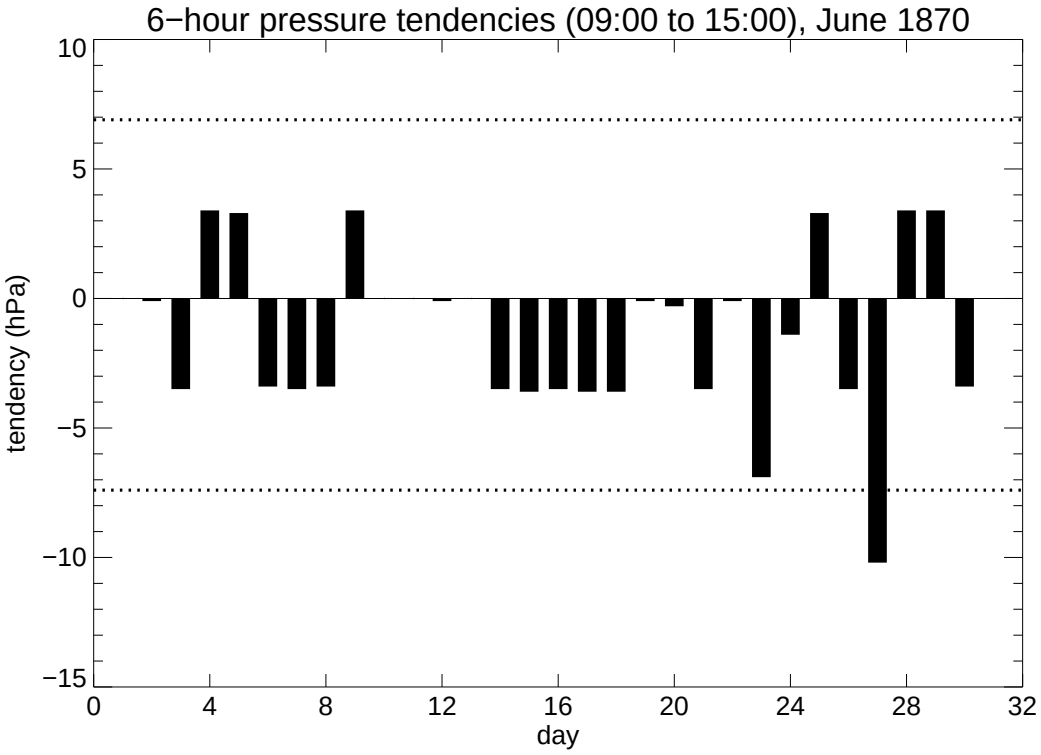

Fig. C.4: Pressure tendencies (09:00 to 15:00) for Cape Otway for each day in June 1870. The dotted lines represent the 1st and 99th percentiles of the 6-hour pressure tendencies (**Table C.1**) described in the text. A severe storm event is defined on 27th June.

C.3 Variations in severe storms at Cape Otway

Following quality control, 836 severe storms were identified at Cape Otway between 1865 and 2006 *i.e.* approximately 6 severe storms/year. The trend in the annual number of severe storms was calculated using ordinary least squares regression and trend significance was calculated at the 5% level using a non-parametric Mann-Kendall test (*Mann* 1945; *Kendall* 1975). Since 1865 there has been a significant decline of 0.22 days/decade in the number of severe storm events at Cape Otway (**Fig. C.5**). This means that in recent times there have been about 3 fewer severe storms per year than at the end of the 19th century *i.e.* this equates to about 40% fewer storms – a sizeable drop. **Fig. C.5** also shows marked decadal variability with peaks in storminess approximately every 25 years. However the past 50 years or so have not seen such strong multi-decadal peaks, perhaps indicating a change in the large scale circulation and/or mechanisms driving these events. The results are certainly consistent with studies over more recent periods, which indicate that there has been a southward shift in storm tracks in the Southern Hemisphere (*e.g.* *Hope et al.* 2006;

IOCI 2005; *Frederiksen and Frederiksen* 2007; *CSIRO-Bureau of Meteorology* 2007). This southward shift has impacted the weather systems affecting south-west Western Australia and this has contributed to the large drying evident there (*IOCI* 2005; *Power et al.* 2005; *Bates et al.* 2008).

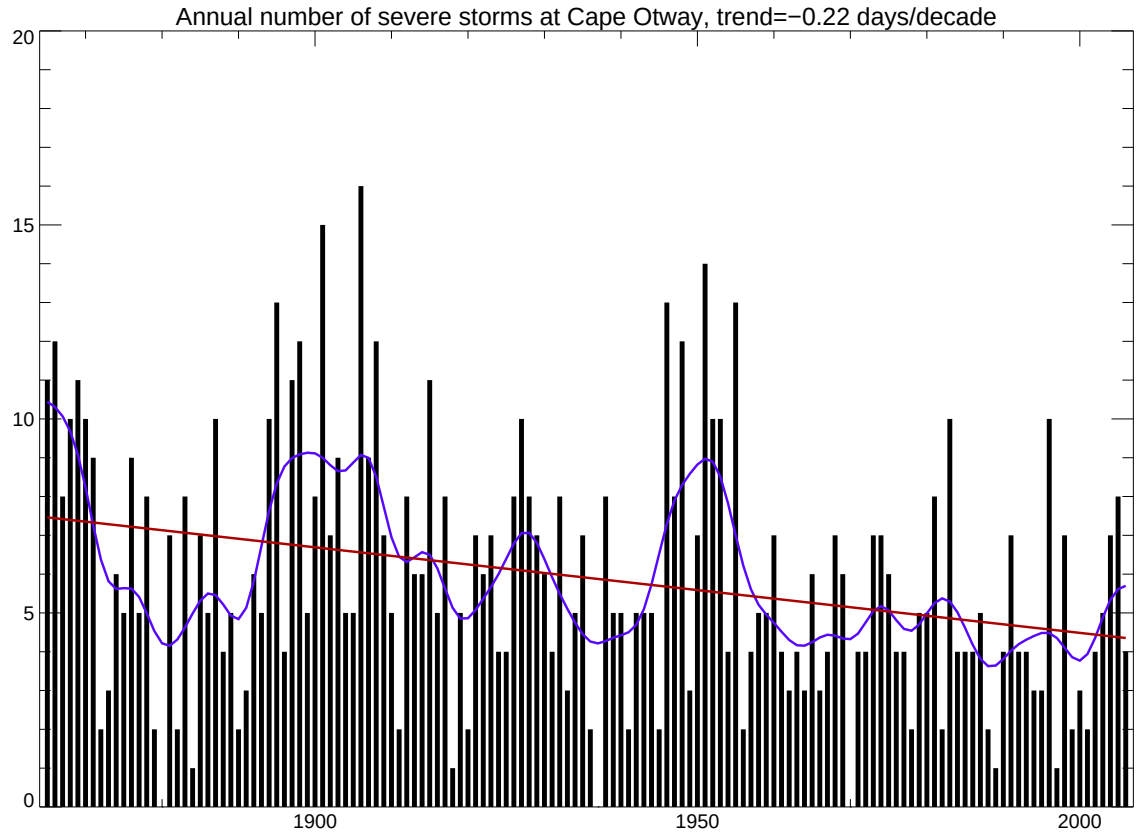

Fig C.5: Bars represent the number of severe storms per year at Cape Otway, 1865-2006, the blue line is a 21-term binomial filter representing decadal fluctuations in the data and the red line is the linear fit to the data. The trend is significant at the 5% level.

The conclusions drawn here are limited since only one station has been analysed but the newly digitized BoM data now grants us the opportunity to study some of the mechanisms that may be driving this reduction in storminess at Cape Otway. This is the first time that extreme storm events in southern Australia have been able to be analysed on the timescales of Northern European studies and thus highlighting the importance of maintaining long-running, continuous meteorological stations for studies of long-term climate variability.

In the next chapter all of the stations in the BoM dataset are used to create daily synoptic patterns for Australia for the past century. These are then used to investigate whether the changing frequency of large scale pressure patterns over Australia has been a factor in driving the observed changes in some of the extremes that we have identified in previous chapters.

3. Diagnosing the synoptic influences driving changes in climate extremes over southern Australia during the last century

Summary

A high quality daily dataset of in-situ mean sea level pressure was collated for Australia for the period 1907 to 2006. Using the method of Self-Organizing Maps (SOMs), daily synoptic pressure patterns were produced for Australia. Twenty patterns derived from the in-situ pressure observations were mapped to patterns derived from ERA-40 reanalysis data to create daily synoptic pressure fields for the past century. Changes in the frequencies of these patterns were analysed and showed that there has been a significant reduction in the rain bearing systems affecting southern Australia since the beginning of the 20th century. Extreme climate indicators derived from daily precipitation and pressure were analysed to investigate some of the changes in the driving mechanisms of extreme events over southern Australia. Results showed a significant decrease in severe storms in south-east Australia linked to the decrease in the frequency of the main synoptic patterns driving these events over the past century. Daily rainfall amounts and intensity were analyzed at four major cities across southern Australia and showed more complex changes related to location.

3.1 Introduction

Climate modelling studies suggest that under anthropogenic climate change storm tracks will shift polewards in the future (*e.g.* *Bengtsson et al.* 2006; *Lynch et al.* 2006), at least partly associated with shifts in the zonal sea surface temperature gradient. Studies using re-analyses data in the southern Hemisphere suggest that this might already be occurring (*Hope et al.* 2006; *Pezza et al.* 2007). A likely impact of this for Australia would be a reduction in rain-bearing systems in southern regions and there is already evidence that this is contributing to the large scale drying in south-west Western Australia (*Hope et al.* 2006; *IOCI* 2005; *Power et al.* 2005; *Frederiksen and Frederiksen* 2007; *Bates et al.* 2008).

The location of storm tracks and the structure, density and number of extra-tropical cyclones in the Southern Hemisphere has been well researched in recent years over the period when re-analysis data have been available *i.e*. approximately the last 50 years (*e.g.* *Simmonds and Keay* 2000; *Lynch et al.* 2006; *Lim and Simmonds* 2007; *Pezza et al.* 2007). As stated in the last section most of the work on centennial and longer timescales has been confined to the Northern Hemisphere and mostly covers the North Atlantic and Northern Europe where there are very long records of in-situ pressure observations (*WASA Group* 1998; *Alexandersson et al.* 2000; *Bärring and von Storch* 2004; *Ansell et al.* 2006; *Matulla et al.* 2008). Studies show that while the period covered by reanalysis has shown marked variation in storm activity, it has not been exceptional when taken in the context of a longer-term climate perspective (*Allan et al.* 2008; *Bärring and Fortuniak* 2008). An interesting question would be whether it would be possible to draw similar conclusions for the Southern Hemisphere *i.e*. would the recent southward shifts detected in the synoptic patterns defined from re-analyses data show up as unusual from a century-long perspective for example? Recently, the Australian Bureau of Meteorology (BoM) digitized historical sub-daily station and mean sea level pressure data for approximately 50 stations across Australia dating back as far as 1859. This long record now provides the opportunity to study synoptic patterns and trends in storminess in Australia for the first time on the timescales of the Northern European studies.

Synoptic patterns are identified as the most typical large-scale systems that affect the weather and climate of a region. There are various well tested “clustering” techniques

which have been used to classify synoptic patterns. *Philipp et al.* (2006) used simulated annealing clustering to identify synoptic patterns over Europe since 1850 while *Rossow et al.* (2005) used K-Means clustering to identify typical tropical cloud regimes from satellite data. Here a technique called Self-Organizing Maps (SOMs) is employed which was first applied to climate by studies such as *Cavazos* (2000), *Malmgren and Winter* (2000) and *Hewitson and Crane* (2002). Subsequently this method has been widely used in Southern Hemisphere studies to look at large scale drivers of climate change *e.g*. *Lynch et al.* (2006), *Hope et al.* (2006), *Vernon-Kidd and Kiem* (2008).

The aim of this study is for the first time to classify synoptic patterns over Australia using quality-controlled daily in-situ pressure observations combined with re-analysis data to determine if, or how, these patterns have changed over the past century. The first section of the paper is concerned with the data quality control and homogeneity which then leads into a description of how the synoptic patterns are created. Finally, long term trends in each of the synoptic patterns are identified and are linked to changes in extreme events over southern Australia.

3.2 Data quality control

Sub-daily pressure data (up to eight observations a day) were digitized for 49 stations across Australia for the period prior to 1950. After 1950, pressure observations were obtained from the Bureau of Meteorology electronic database for these stations for all available observation times. Since some stations had stopped reporting in more recent decades, observations from neighboring stations were also obtained. In total 80 stations were used in the analysis up to 2006. **Fig. 3.1** shows the locations of these stations. The earliest observations date back to 1859 but it is not until 1907 that most of the "four corners" of Australia have data so this is the start year used for this analysis. Not all data have complete records and in addition, in most cases, these data have been keyed 'as read' *i.e*. directly transcribed from original manuscripts without quality control. Gravity and index corrections were not performed and, depending on barometer type, these could be quite large (up to several hPa – B. Trewin, personal communication). For this reason, it was necessary to quality control and homogenize the data. The following sections describe

the techniques used to ensure that as high quality and consistent data as possible are used in our analysis.

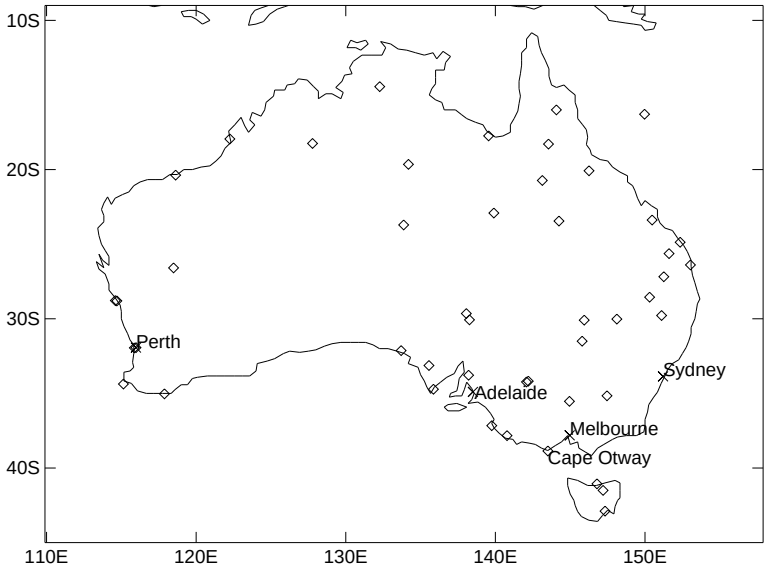

Fig. 3.1: Location of stations (◊) used in this study. Some metropolitan centres (x) are also marked for reference. Macquarie Island (54.5S, 158.94E) and Heard Island (53.02S, 73.39E) were also digitized but are not marked on the map.

3.2.1 Removing erroneous values

Errors in the pressure data described here can be introduced by mistakes made when digitizing values from the original hand written records or indeed when observers incorrectly recorded values in the original field books. In general, the majority of errors occur because digits have been transposed (*Alexander et al.* 2005). It is not always possible to identify this type of error by looking at the actual pressure values because an incorrectly recorded observation could still be a valid observation if it was within the limits of the probability distribution of pressure values. More likely these errors will be highlighted by analysing pressure tendencies *i.e.* the difference between two subsequent pressure readings. Given that all the stations record at local time and have differing numbers of observations during the day, data at each station were averaged to make daily mean sea level pressure (MSLP) observations relative to UTC (accounting for the introduction of daylight saving in some states in the 1970s). This meant that a comparable calculation of

day-to-day pressure tendencies could be produced at all stations. MSLP tendencies were therefore calculated for each station as the difference between subsequent daily observations, and a probability distribution function (PDF) was created using all of these values. From these PDFs, the 1st and 99th percentiles were calculated and used to identify "extreme" events *i.e*. days with values of the tendency below the 1st percentile or above the 99th percentile. These events, while including MSLP tendencies that could correspond to actual severe storm events, should also identify the majority of digitization errors that have been produced through digit transposition. These "extreme" events were examined for each station. In the majority of cases, they highlighted individual observations where digits had been transposed or in several cases where MSLP had been keyed as station level pressure (SLP) or vice versa for individual or sequences of observations. If it was not clear that there was a keying error, data from neighboring stations were checked to help judge whether to amend or remove the observation. One station, Cape Otway, which had almost complete twice-daily observations since 1865, had even further quality-control applied through direct inspection of the original meteorological log books (see **Section C**). However, this type of data quality checking cannot usually identify sudden non-climatic jumps that may be introduced in the data timeseries through, for example, changes in observing practice or instrumentation. Such problems can be identified by either a thorough investigation of station metadata or by using sophisticated statistical techniques that can identify potential inconsistencies in the data. The former method is extremely time-consuming and the type of data required are rarely available (or in a convenient format). However, statistical techniques are available which can be used with or without access to original station metadata, and these techniques are described in the following section.

3.2.2 Homogeneity testing

There are many statistical techniques available to assess the consistency of climate data (*e.g. Wijngaard et al.* 2003; *Wang* 2008; *Menne and Williams* 2005). Here RHTestV2 (*Wang* 2008) is used because the software is well tested and freely available from http://cccma.seos.uvic.ca/ETCCDI/software.shtml. The method is based on the penalized maximal t and F test and can identify, and adjust for, multiple change points in a time series (see *Wang* (2008) and website for more details). To test for potential inhomogeneities in the data, daily quality controlled MSLP data for each station between

1907 and 2006 were fed into RHTestV2. If, for example, there is a non-climatic jump in the data because the barometer is replaced or has changed height, then an inhomogeneity will likely exist in the data as a step change. If no dates are identified as having potential step jumps then the station is determined to be homogeneous. This is also the case for stations with less than 20 years of data in total as the test is less reliable for smaller amounts of data. **Table 3.1** indicates the months and years (if any) where RHTestV2 has identified inconsistencies in the data for each of the 80 stations. In total, 21 of these stations were identified as having one or more step changes throughout the base timeseries. For these stations, the next step of the RHTestV2 software was run to produce an adjusted daily homogeneous series.

In some cases the step changes could indicate real climatic events. One example is the El Niño-Southern Oscillation (ENSO), which has a major influence on the climate of Australia (*McBride and Nicholls* 1983). There is evidence that some of the step changes in **Table 3.1** are in fact related to major El Niño events rather than artificial jumps in the timeseries. For instance, it is possible that the 1941/42 El Niño produced step changes at four of the stations. An inspection of the metadata for these stations did not suggest that there were any reasons (*e.g.* change in instrumentation) to indicate that these changes were anything other than real. For this reason, this time period was not corrected for biases.

The quality-controlled, homogenized daily pressures produce what we believe to be the only century-long high quality timeseries of daily in-situ MSLP for Australia.

3.3 Self-Organizing Maps (SOMs)

The daily MSLP dataset described above enables us to investigate if, and how, large-scale pressure (synoptic) patterns have changed over Australia during the past century and whether any such changes are linked to changes in observed climatic events. The first step is to categorize what are the most usual large-scale pressure patterns dominating the Australian climate. This can be done using a 'cluster' analysis. While there are many clustering techniques that could be used to categorize synoptic patterns from large datasets, here the technique of Self-Organizing Maps (SOMs) was employed. This is now a well

tested method in climate science and has been shown to perform well when compared to other clustering algorithms (*e.g.* *Hewitson and Crane* 2002; *Cassano et al.* 2006).

Table 3.1: Homogeneity information on the stations used in this study. Only stations where break points have been identified and the timeseries adjusted are included.

Station name	Station no.	Lat	Lon	Break points (year/month)
Halls Creek Arpt	002012	-18.23	127.66	1967/12 1998/05
Port Hedland	004032	-20.37	118.63	1970/09 1973/04 1976/03 1998/04 2001/03
Meekatharra	007046	-26.59	118.49	1944/05
Geraldton Arpt	008051	-28.80	114.70	1955/02
Albany	009500	-35.03	117.88	1955/07
Cape Leeuwin	009518	-34.37	115.14	1936/06 1979/05
Tennant Creek	015087	-19.65	124.19	1935/05 1939/08 1942/03 1943/06 1943/10 1955/02 1957/03 1962/03 1965/08
Robe	026026	-37.16	139.76	1944/11
Palmerville	028004	-16.00	144.08	1966/12
Burketown	029004	-17.74	139.55	1954/03
Georgetown	030018	-18.29	143.55	1918/03 1948/05 1948/10 1948/11 1949/02 1957/02
Richmond	030045	-20.73	143.14	1915/06
Charters Towers	034002	-20.08	146.26	1977/05
Boulia	038003	-22.91	139.90	1956/12 1982/04
Gayndah	039039	-25.63	151.61	1942/01
Dalby	041023	-27.18	151.26	1910/08 1910/11
Bourke	048013	-30.09	145.94	1941/09
Cobar	048030	-31.50	145.80	1921/11 1922/03 1929/04
Walgett	052026	-30.02	148.12	1915/06
Mildura	076077	-34.23	142.08	1939/01 1942/04
Willis Island	200283	-16.29	149.97	1991/03

The SOM algorithm (*Kohonen* 2001) applies an unsupervised learning process to map input data onto the elements of a regular one- or two-dimensional array thus providing an efficient means of interpreting and visualizing large data sets. The technique is characterized by a tendency to categorize data by preserving its probability density to produce sets of approximately equi-probable patterns or 'nodes' for each SOM. The preservation of probability density is an important component of the technique since other traditional cluster analyses such as K-Means can tend to group less frequent data points in

larger classes that are not necessarily representative (*Michaelides et al.* 2001), therefore making it difficult to pinpoint the driving mechanisms of extreme events for example. Another advantage of SOMs is that the input data need not be spatially or temporally complete; such incompleteness is usually the case when dealing with observational datasets (*Samad and Harp* 1992). A detailed description of the SOM technique as applied in this study is given in *Cassano et al.* (2006).

Although the SOM technique provides an objective method for grouping large datasets, the choice of the number of nodes to have within the SOM is somewhat subjective. Obviously, the more nodes that are defined, the smaller the aggregated Euclidean distance error from the target dataset but this can come at the cost of having too many nodes to give a useful climate signal. Too few nodes can mean that quite different synoptic patterns may be grouped together. To optimize the SOM algorithm, SOMs using different numbers of nodes (*i.e.* 6, 12, 20, 30 and 42 nodes) were calculated and assessed to find the smallest error whilst still maintaining meaningful synoptic climatologies. In addition, the SOM was trained by varying two parameters: a user-defined radius, r, dependant on the number of nodes within the SOM and a learning rate parameter, α, which was varied with each value of r (in this study α=0.001, 0.002, …, 0.01, 0.02, …, 0.1, 0.15, 0.2, …1 was tested). Each parameter decreases linearly to one (r) or zero (α) during the training of the SOM. In addition to the observed daily MSLP dataset, daily averaged fields of ERA-40 reanalysis data (*Uppala et al.* 2005) were also calculated between 1958 and 2001 to investigate spatially complete synoptic patterns and to compare with the in-situ observations.

Table 3.2 shows the errors produced by varying the number of nodes within the SOM algorithm for both the observed daily MSLP dataset and the ERA-40 reanalysis. The errors in the observed dataset are slightly larger and this is most likely due to the greater variability of the point estimates. In each case the optimum search radius was 2 (except for the ERA-40 6x7 SOM where r=5). From a visual inspection of the resulting patterns, it was determined that SOMs with less than 20 nodes did not fully represent all the synoptic situations that occurred over Australia. SOMs with more than 20 nodes, while having smaller errors, resulted in patterns that occurred infrequently thus making further statistical analysis of the results less robust. The 20-node (4x5) SOM therefore gave the best compromise between minimizing errors and giving enough meaningful classifications of synoptic patterns over Australia to be useful for a climate change study. This is in

agreement with the *Hope et al.* (2006) and *Vernon-Kidd and Kiem* (2008) studies on the synoptic influences on south-west Western Australia and Victoria respectively who also found that a 20-node SOM was most useful for categorizing the synoptic patterns influencing those parts of the country.

Table 3.2: Information on the minimum errors produced (with associated value of the alpha parameter) in the SOM analysis using both the observed daily MSLP dataset created in this study and daily averaged MSLP ERA-40 reanalysis data. Errors are calculated as the sum of all the root mean squared Euclidean distances between the SOM and the target dataset.

Number of SOM nodes	Error (obs) 10^{th} hPa	α (obs)	Error (ERA-40) 10^{th} hPa	α (ERA-40)
6 (2x3)	267.25	0.001	246.58	0.002
12 (3x4)	233.08	0.002	222.85	0.35
20 (4x5)	215.91	0.006	203.60	0.55
30 (5x6)	203.70	0.003	193.72	0.90
42 (6x7)	194.98	0.008	185.76	0.45

Subsequently a single set of twenty synoptic patterns or nodes was derived by applying the SOM algorithm and using all days of daily averaged fields of MSLP between 1907 and 2006. Similarly, a 20-node SOM was produced from the ERA-40 reanalysis using data from 1958 to 2001 (see **Fig. 3.2**).

For convenience, the SOMs will be referred to as SOM_{OBS} for those patterns derived from the in-situ observations and SOM_{ERA} for those patterns derived from the ERA-40 reanalysis. Assuming that synoptic patterns have not changed over the last 100 years (without making any assumptions about whether they have changed in frequency) the SOM_{ERA} patterns can be used to map to the SOM_{OBS} patterns to produce a spatially complete picture of the changes in synoptic patterns over the last century. This was done as follows.

Each station point in SOM_{OBS} is assumed to represent the MSLP value for the nearest 1 degree gridbox on the same grid as the ERA-40 analysis. Where there was more than one

station in a gridbox, the value was calculated as the average of two or more stations. Given the unsupervised nature of the SOM algorithm, equivalent patterns will not necessarily appear in the same order in SOM_{OBS} as they do in SOM_{ERA} *e.g.* in **Fig. 3.2** node 1 in SOM_{OBS} might be most closely related (in terms of giving the smallest root mean squared error (RMSE)) to node 4 in SOM_{ERA}, node 2 in SOM_{OBS} to node 16 in SOM_{ERA} etc. But if the same synoptic patterns have been driving Australian climate over time it would not be unreasonable to assume that each node in SOM_{OBS} appears only once in SOM_{ERA}. However, finding the permutation of the 4x5 SOM_{OBS} that best maps to SOM_{ERA} to produce the smallest total RMSE would require 20! (*i.e.* $2.4\text{x}10^{18}$) calculations. Therefore another method of approximating the smallest total RMSE needs to be implemented which does not involve performing an impossibly large number of computations.

Suppose that *a* represents the SOM_{OBS} node that best maps to SOM_{ERA} node *b* to give the smallest error, then the RMSE, $E_{a,b}$ between the two nodes, *a* and *b*, is given as:

$$E_{a,b} = \sqrt{\frac{1}{G}\sum_{g=1}^{G}\left(SOM_{OBS\,a,g} - SOM_{ERA\,b,g}\right)^2} \qquad \forall\, a,b = 1,2,...n \qquad \textbf{(Eqn. 3.1)}$$

where *n* represents the number of nodes in the SOM and *G* is the total number of gridboxes with corresponding data between SOM_{OBS} and SOM_{ERA}. This is performed as an iterative process such that the values of a_1 and b_1 in the first iteration are defined as:

$$(a_1, b_1) = (a,b) \text{ where } E_{a,b} = \min(E_{a,b}) \qquad \textbf{(Eqn. 3.2)}$$

In the next iteration, **Eqn. 3.1** is substituted with nodes *c* and *d*, where $c \neq a$ and $d \neq b$ such that **Eqn. 3.2** becomes $(c_1, d_1) = (c,d)$ where $\text{E}_{\text{c,d}} = \min(E_{c,d})$. This process is repeated *n* times (*i.e.* for $e \neq a$, *c* and $f \neq b$, *d etc.*) until all the nodes of SOM_{OBS} are mapped to only one of the nodes of SOM_{ERA}. This process gives an RMSE of 50.19 hPa. To test how good this estimate is, the RMSE was calculated for $10.0\text{x}10^4$ random permutations of SOM_{OBS} and SOM_{ERA}. Errors ranged from 64.48 to 144.02 hPa. The global minimum error

(that is the error that would be produced if a one to one mapping of SOM_{OBS} to SOM_{ERA} was not assumed) is 35.1 hPa, strongly suggesting that our estimate is close to the actual minimum RMSE.

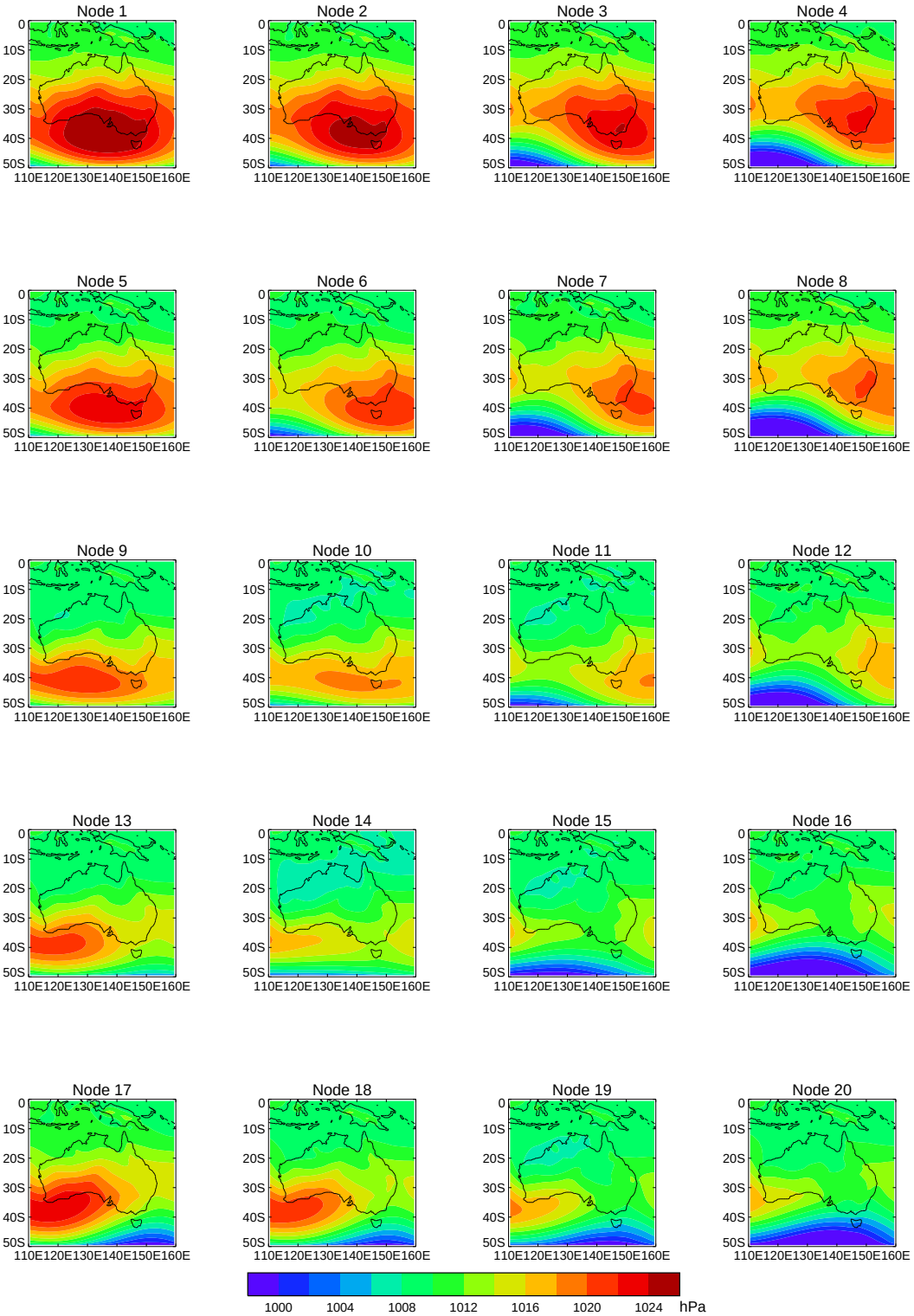

Fig. 3.2: Synoptic patterns for Australia derived using SOMs.

So while the SOM_{OBS} nodes calculated from 1907 to 2006 daily station MSLP are used in the analysis in the next sections, it is now possible to relate these visually to the spatially complete synoptic patterns from SOM_{ERA} (**Fig. 3.2**). In each case the SOM_{OBS} results are presented in the order that they appear in SOM_{ERA} making the results from **Fig. 3.3** onwards more easily comparable with the large-scale patterns in **Fig. 3.2**.

The result is a spatially and temporally complete representation of daily synoptic patterns over Australia over the last century. For convenience, these permuted patterns of SOM_{OBS} will be referred to in the following sections as *SOM*.

3.4 Trends in the frequency of synoptic patterns over Australia and links to changes in observed climate

Each node of the *SOM* can be related to the synoptic pattern on an individual day making it possible to calculate the frequency of each large-scale pattern for all years from 1907 to 2006. It would be expected that in general the patterns on the right hand side (particularly the bottom right hand corner) of **Fig. 3.2** would reflect the weather systems bringing rain to southern Australia while the high pressure patterns on the left hand side (particularly the top left hand corner) of the figure would be more likely to be associated with clear sky conditions over much of southern Australia. **Fig. 3.3** shows the timeseries of frequencies of each *SOM* node from **Fig. 3.2** over the last century. In general, patterns with a marked trough to the south of Australia show a decline in frequency over the last 100 years. Indeed, nodes 4, 12, 16 and 20 all indicate a statistically significant decline. In total, eight nodes show a decline in frequency while 12 nodes show an increase, only one of which is significant (node 15). While node 15 also has a trough to the south of the country it is shifted further southwards of the patterns that show a significant decrease in frequency. This may be indicative of a poleward shift of the Southern Hemisphere storm tracks. If this was the case one might expect to see decreases in rainfall across most of southern Australia. *Hope et al.* (2006) showed that this was the case for south-west Western Australia over the last 50 years although other studies using station data have shown mixed patterns of daily rainfall decline depending on region and season (*e.g.* *Hennessy et al.* 1999; *Haylock and Nicholls* 2000; *Alexander et al.* 2007; *Gallant et al.* 2007). High quality

rainfall measurements are available for station locations across Australia since 1910 (*Haylock and Nicholls* 2000) along with other proxy variables such as a 150-year severe storm record at Cape Otway (see **Section C**) so this theory could be tested.

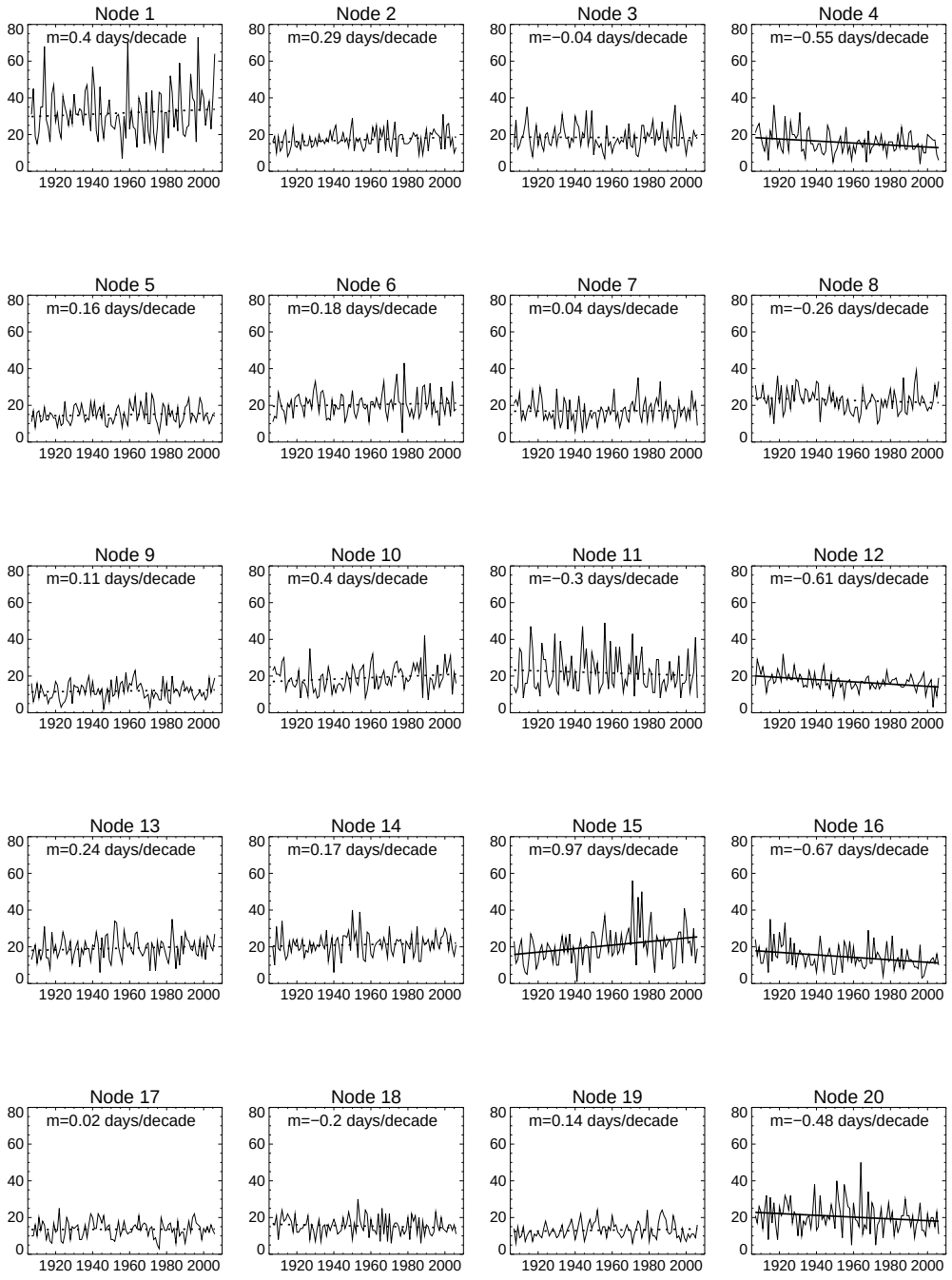

Fig. 3.3: Frequency of each synoptic pattern from **Fig. 3.2** from 1907 to 2006. Decadal trends are shown in the top left hand corner of each graph. Solid and dashed lines represent the line of best fit to the data using ordinary least squares regression. Solid lines indicate that the trend is significant at the 5% level using a Mann-Kendall test.

In the next sections the effect that the changing frequency of synoptic patterns (**Fig. 3.3)** has had on these precipitation and storminess records is assessed. Significance levels are tested at the 5% level throughout.

3.4.1 Severe storm index

In the last chapter the calculation of a severe storm index for Cape Otway on the southern Coast of the state of Victoria was described (see **Fig. 3.1** for the location). That analysis showed that between 1865 and 2006, there has been a significant decline in the number of severe storms at this location. This could suggest that there has been a shift in the storm tracks related to a reduction of the essential rain-bearing weather systems reaching southern Australia. To investigate this, the large-scale pressure patterns on each date between 1907 and 2006 when a severe storm occurred at Cape Otway (a total of 543 events) were analysed to determine if any particular node or nodes were responsible for driving these events. **Fig. 3.4a** shows the percentage of severe storm events that are driven by each *SOM* node along with the node's relative frequency within the *SOM*.

The frequency of the *SOM* nodes is relatively evenly distributed around 5% (with 95% confidence that the random process is in the range [4.78, 5.22%]), the most frequent pattern (node 1) occurring 8.7% of the time and the least frequent pattern (node 9) occurring 3.25% of the time. **Fig. 3.4a** indicates that the nodes which occur during severe storms at Cape Otway are dominated by the nodes that are decreasing in frequency (see **Fig. 3.3**). This is even more apparent in **Fig. 3.4b** which shows the ratio of the percentage of each pattern relative to the frequency of that pattern within the *SOM*. Here, nodes 4, 16 and 20 stand out clearly as dominating the Cape Otway severe storm index and **Fig. 3.3** shows that all these patterns have seen a significant decline in frequency over the past century. These three patterns, combined, occur less than 14% of the time but account for over 40% of the large-scale synoptic situations occurring during severe storm events at Cape Otway. If all eight nodes from **Fig. 3.3** that are decreasing in frequency are combined, then it was found that over 66% of severe storm events were driven by these patterns. The reduction in the frequency of these nodes is certainly a reasonable explanation as to why severe storm events have significantly decreased at Cape Otway over this period.

3.4.2 Daily rainfall intensity

To investigate how changes in the frequency of synoptic patterns may influence the amount and intensity of rainfall, daily rainfall observations from four stations located close to large urban centers in southern Australia (Sydney, Melbourne, Adelaide and Perth[1]) were obtained from the high quality, post-1910 rainfall dataset described in *Haylock and Nicholls* (2000). Each of these cities has over one million inhabitants (over 10 million in total) making up over half of Australia's population therefore making it extremely important to understand if changes in large scale processes are affecting the amount of rainfall reaching these areas. Two measures are examined to document how daily rainfall events may be changing: 1) a measure of the intensity of daily rainfall and 2) the maximum 1-day rainfall amount associated with each *SOM* node. These indices are generally referred to as SDII and RX1day respectively (*Alexander et al.* 2007).

All days with rain (*i.e.* ≥ 1mm) at each of the four locations were assigned a synoptic type as denoted by the *SOM*. Average daily rainfall intensities were calculated as the total rainfall each year divided by the number of rain days for each *SOM* node at each location. **Fig. 3.5** shows a boxplot of the daily average rainfall intensity associated with each synoptic type in **Fig. 3.2**. The boxes represent the inter-quartile range, the line through the boxes represents the median value, and the lower and upper "whiskers" represent the 5th and 95th percentiles respectively of the daily rainfall intensity distribution for each *SOM* node. In addition, timeseries from 1910 to 2005 of the average daily intensities and maximum daily rainfall amounts were analyzed for each location. **Table 3.3** shows the trends and significance calculated for these variables.

Fig. 3.5a shows that the patterns on the right hand side of the *SOM* in **Fig. 3.2** are associated with the least amount of daily rainfall intensity in Sydney both in terms of the average and wet extremes. This may be expected since the areas of high pressure become more centered over Sydney as one moves from the left to the right of the *SOM*. Therefore the decreases seen in these *SOM* nodes in **Fig. 3.3** are likely to have little impact on the overall daily rainfall intensity for this city. Indeed, **Table 3.3** indicates both non-significant increases and declines for both daily intensity and maximum 1-day rainfall totals in these

[1] Stations used were Cataract Dam (Sydney), Yan Yean (Melbourne), Happy Valley Reservoir (Adelaide) and Manjimup (Perth) with co-ordinates, 150.81E, 34.27S; 145.11E, 37.57S; 138.56E, 35.06S; 116.14E, 34.24S respectively.

SOM nodes. Interestingly *SOM* node 15, which is associated with the largest daily rainfall intensities in Sydney, has significantly increased in the last century although with some evidence of a decline since the mid 1970s (**Fig. 3.3**). **Table 3.3** indicates that this has been associated with increases in both maximum daily rainfall and rainfall intensity but neither increase is significant. In fact, there are no significant increases or decreases in either SDII or RX1day associated with any *SOM* node for Sydney.

Table 3.3: Decadal trends in (a) RX1day *i.e.* maximum daily rainfall values (mm/decade) and (b) SDII *i.e.* daily rainfall intensity (mm/day/decade) during each *SOM* node for four locations across southern Australia. Bold signifies that trends are significant at 5% level (using a non-parametric test proposed by Zhang *et al.* (2000)). Where no value is recorded there were insufficient data points to calculate a trend.

Node	Sydney		Melbourne		Adelaide		Perth	
	RX1day	SDII	RX1day	SDII	RX1day	SDII	RX1day	SDII
1	0.34	0.00	0.16	0.00	**0.32**	**0.11**	-0.42	0.05
2	0.32	0.06	-0.14	-0.11	-	**0.13**	-0.68	-0.23
3	-0.46	-0.14	-0.14	-0.03	-0.17	-0.01	-0.64	**-0.25**
4	0.00	-	0.49	**0.21**	0.63	0.30	**-0.93**	**-0.24**
5	0.00	0.05	0.17	0.05	0.22	0.14	0.09	0.09
6	-1.27	-0.26	0.42	0.17	0.31	0.15	**-1.08**	**-0.46**
7	0.72	0.23	0.49	0.18	0.19	-	**-1.31**	**-0.52**
8	-0.24	0.06	-0.32	**-0.11**	0.29	0.08	**-0.80**	-0.09
9	-0.12	-0.07	0.40	0.07	0.00	-0.12	0.20	0.07
10	0.64	-0.04	0.27	0.08	-	-	0.00	-0.09
11	-0.61	-0.09	0.50	0.20	0.00	-0.08	0.05	0.09
12	-0.09	0.02	-0.47	-0.07	0.00	0.03	-0.11	0.03
13	-0.03	-0.12	-0.44	-0.16	0.00	-0.03	-	-0.24
14	-0.59	-0.27	-0.41	-0.09	-	-	-0.01	-0.04
15	0.87	0.17	0.49	0.20	-0.19	-0.26	-	-
16	0.30	0.15	-0.56	-0.16	-0.04	0.16	**-0.72**	-0.15
17	-0.22	-0.12	0.10	-0.01	0.00	-0.04	0.18	0.17
18	-0.26	-0.08	-0.24	-0.12	0.01	-0.06	-0.23	-0.10
19	-0.23	-0.15	-	-	-	-	0.00	-0.03
20	0.00	0.01	0.09	0.00	0.03	-0.01	-0.62	-0.10

Melbourne, however, shows an increase in daily rainfall intensity of 0.21 mm/day/decade associated with *SOM* node 4 which is interesting because this is one of the nodes that has significantly decreased in frequency (**Fig. 3.3**). The intensity of daily rainfall associated with node 8 shows a significant decline of 0.11 mm/day/decade associated with a non-significant decline in the frequency of this node (**Fig. 3.3**). Neither of these nodes however

produces the largest daily rainfall events for Melbourne (**Fig. 3.5b**) so these significant changes may have limited impact. The results indicate that there may be more complex regional processes (*e.g.* convection, orography) driving intense rainfall in Melbourne than can be explained simply by changes in synoptic systems alone.

Adelaide generally indicates increasing trends in SDII and RX1day (**Table 3.3**). *SOM* node 1 produces significant increases in both (0.11 mm/day/decade and 0.32 mm/decade respectively) while nodes 2 and 4 have also seen significant increasing trends in daily rainfall intensity (0.13 mm/day/decade and 0.30 mm/day/decade respectively). Contrary to the situation in Sydney, rainfall intensities in Adelaide are greatest during synoptic patterns which are found on the right hand side of the *SOM* (**Fig. 3.5c**) so the reductions in the frequencies of these patterns (**Fig. 3.3**) do not seem to have affected the rainfall extremes in Adelaide (which have generally increased during these *SOM* nodes). Again this suggests more complex processes than can be explained solely by large scale driving system changes.

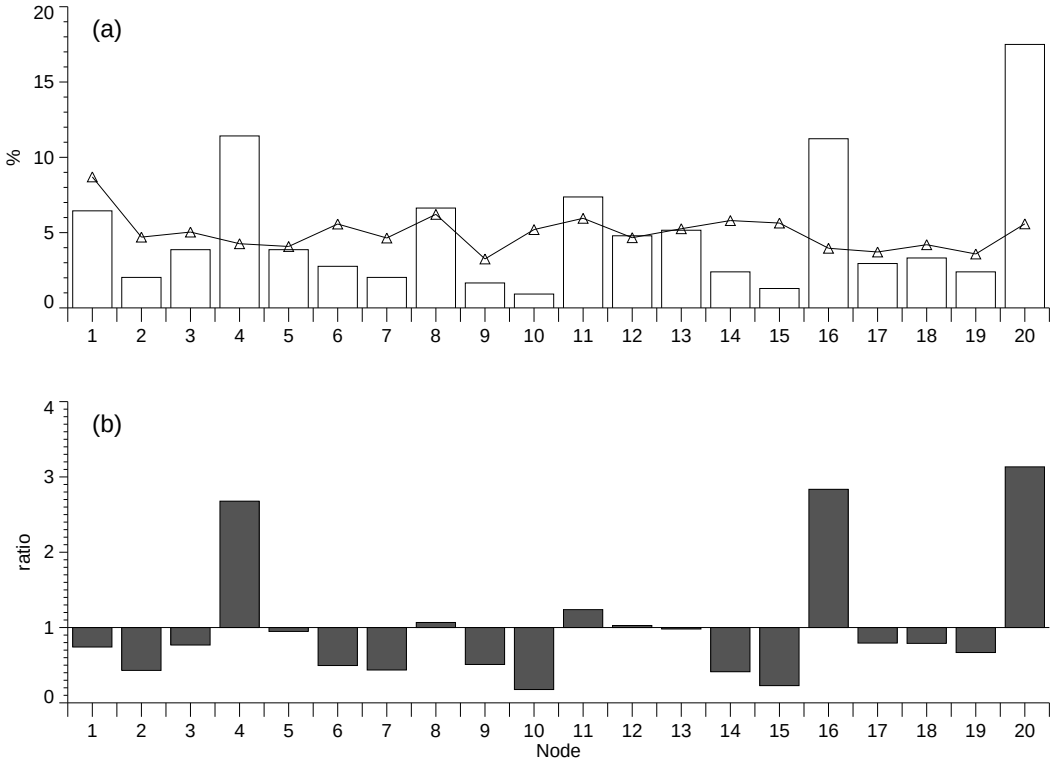

Fig. 3.4: (a) Bars represent the percentage of synoptic patterns occurring during "severe storms" at Cape Otway overlaid with the relative frequency of each node within the *SOM* and (b) represents the ratio of when synoptic patterns are driving severe storms at Cape Otway to the relative frequency of that pattern within the *SOM*. The x-axis represents the *SOM* nodes from **Fig. 3.2**.

Perth shows the most significant changes in rainfall extremes, in the majority of cases exhibiting a decline in both maximum daily amount and intensity (**Table 3.3**). South-west Western Australia has perhaps seen the most sustained decline in average rainfall of any Australian region in the last few decades and *Hope et al.* (2006) suggest that this is related to a decrease in troughs affecting the region, and an increase in high pressure systems. *Li et al.* (2005) who looked at changes in extreme rainfall events in south-west Western Australia suggested that there was evidence for a drying of winter daily rainfall extremes after 1965 related to changes in the Antarctic Oscillation (AAO). The results here show that five of the nodes (4, 6, 7, 8 and 16) are associated with significant decreases in the amount of 1-day maximum rainfall (**Table 3.3**), the largest significant decreases of -1.08 and -1.31 mm/decade from nodes 6 and 7 respectively are from two of the nodes which bring the most intense rainfall to the region (**Fig. 3.5d**). Four nodes (3, 4, 6 and 7) are also associated with significant declines in daily rainfall intensity (**Table 3.3**) in this region.

3.5 Conclusions

In this study, quality-controlled and homogenized daily station MSLP data were used in conjunction with re-analyses data to produce daily synoptic patterns for Australia for the past 100 years using Self-Organizing Maps (SOMs). Twenty patterns or 'nodes' were identified to be the major large-scale systems affecting the climate of Australia. The frequencies of each of the synoptic patterns were analyzed over the past century and indicated that there has been a significant decline in those patterns which have a marked trough to the south of the country. The results here mostly confirm the conclusions from previous studies using a similar technique over shorter timescales, namely *Hope et al.* (2006) over south-west Australia and *Vernon-Kidd and Kiem* (2008) over south-east Australia who showed there had been significant changes to the synoptic systems driving rainfall in those regions. In this paper, however, we have extended these studies to analyze patterns for the whole of southern Australia for a longer time period and have shown that decreases in the frequency of these large scale synoptic systems are likely to be part of a longer-term decline.

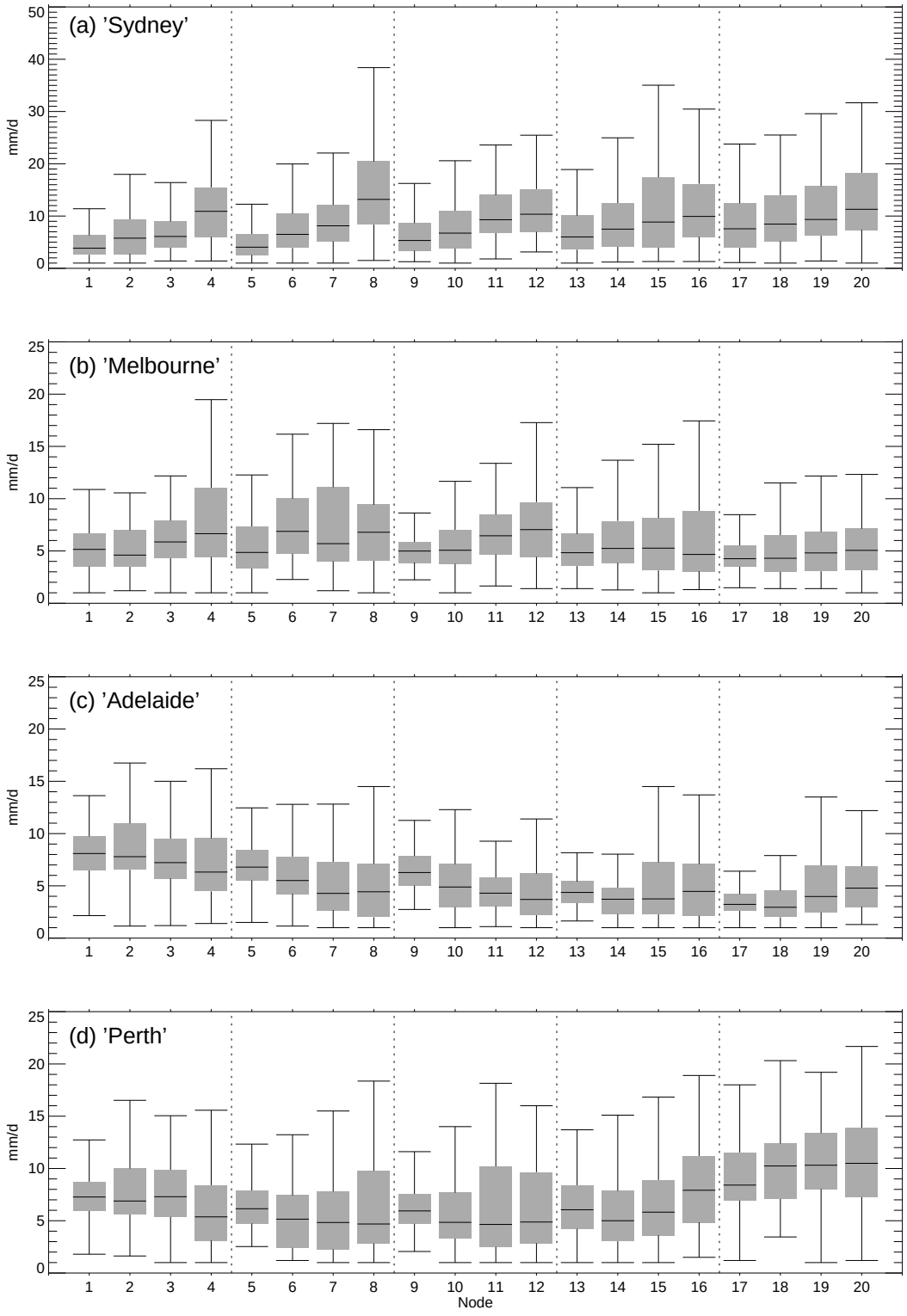

Fig. 3.5: Boxplot of annual daily rainfall intensity from rain days (≥ 1mm) during each *SOM* node for stations from the high-quality dataset (*Haylock and Nicholls* 2000) closest to (a) Sydney, (b) Melbourne, (c) Adelaide and (d) Perth using all daily data from 1910 to 2005. Dotted lines indicate the end of each *SOM* row.

Using a Cape Otway storm index it was shown that observed decreases in severe storm events in south-east Australia over the past century have been associated with decreases in the frequency of the synoptic patterns driving these events. Daily rainfall amount and intensity indicators for Sydney, Melbourne, Adelaide and Perth were also analyzed. The results for the rainfall indices were not as conclusive as those for the storminess indicator. Sydney showed no significant changes in either daily maximum rainfall or average daily intensity for any of the driving *SOM* nodes while Melbourne and Adelaide showed significant increases in daily rainfall intensity associated with a *SOM* node that has actually decreased significantly in frequency over the past century. Perth showed the most consistent and significant changes in daily maximum rainfall amount (daily intensity) with significant declines in five (four) of the 20 *SOM* nodes.

The results from this study provide further independent evidence that the expected southward shift in storm tracks due to anthropogenic climate change is actually taking place. The effect that this has had on severe storm events in southern Australia seems clear *i.e.* a contribution to the significant decline in storminess. However, there is no consistent pattern on the effects of shifting synoptic patterns on rainfall intensity changes across Australia's major urban centers, with only Perth indicating a sustained decline in extreme rainfall. This would indicate that more work is required to understand the complexities of daily rainfall distribution changes across different regions of Australia if we are to adequately understand how this might impact the already strained water resources of the densely populated regions of southern Australia in the future.

D. Driving Forces

The last few chapters have shown that climate extremes have significantly changed in Australia over the observational record. For changes in severe storms it was shown that this is most likely to have been related to a southward shift of storm tracks in the Southern Hemisphere over the past century. But what might be some of the other large-scale drivers of changes in climate extremes? It was suggested in **Chapter 2** that because there were such strong correlations between the trends in mean and extreme temperature and precipitation, that the mechanisms driving the means were likely to be the same as those driving the extremes. Some of the driving mechanisms of regional observed trends in Australia are still under debate. While a number of studies have attributed portions of the drying in the southwest to anthropogenic forcing (*Hope* 2006; *Timbal et al.* 2006; *Cai and Cowan* 2006), the impact of natural variability (*Cai et al.* 2005; *Ummenhofer et al.* 2008) and land cover change (*Pitman and Narisma* 2005; *Timbal and Arblaster* 2006) appear to be reasonably large also. The increase in precipitation and associated cooling in northwest Australia is well known to researchers (*e.g. Nicholls et al.* 1997; *Power et al.* 1998). *Rotstayn et al.* (2007) suggests that it may be the poor simulation of aerosols in global climate models (GCM) which is failing to capture these trends although *Shi et al.* (2008) suggest this may be a model artefact. *Wardle and Smith* (2004) suggest that the continental warming further south is driving an enhancement of the Australian monsoon, leading to increased precipitation in the north-west. As well as mechanisms, there are known biases in the ability of climate models to simulate tropical mean climate and variability including the response of certain cloud feedbacks to CO2 that might be causing the sea surface temperatures (SSTs) to warm unevenly (*Meehl et al.* 2000; *Barsugli et al.* 2005). Recent research at the Bureau of Meteorology finds Australian precipitation trends to be consistent with the decadal variability in tropical Pacific SSTs (personal communication Harry Hendon). Thus if GCMs could capture the zonal gradient of the SST changes, with a minimum in warming in the central Pacific, they would likely capture the increase in northwest Australian mean precipitation and by extension extremes. Although *Santer et al.* (2006) attribute changes in tropical Atlantic and Pacific SSTs to anthropogenic forcing, the extent to which the pattern of observed trends in tropical SSTs is anthropogenic is unknown. Further study would be required to untangle the contributions of unforced and forced variability to recent changes in Australian climate.

Irrespective of the interacting and driving mechanisms, the evidence is clear that the mean climate of Australia is affected by both natural and anthropogenic influences. Changes in synoptic patterns and their effect on decreases in storms in southern Australia were discussed in the last chapter so the next two chapters will focus on answering questions about the influences and interactions of (a) cloud regimes; (b) SST variability and (c) anthropogenic forcing on Australian climate extremes.

The answer to (c) is discussed in detail in **Chapter 5** and also in *Alexander and Arblaster* 2008. Globally there is certainly evidence that anthropogenic forcing of the climate system through increased greenhouse gas emissions, in addition to natural variations in climate can account for the changes that have been observed in (minimum) temperature extremes since the 1950s (*Trenberth et al.* 2007). A regional anthropogenic signal, however, is much harder to detect and particularly over a country like Australia where the climate is strongly modulated by ENSO variability which GCMs have been shown to be unable to adequately simulate (*Leloup et al.* 2007b). Until the study of *Alexander and Arblaster* 2008 there had been no attempt to do this for Australian temperature and precipitation extremes.

In the next sections changes in cloud regimes along with their interaction with large scale pressure patterns and links to changes in precipitation extremes across southern Australia are discussed. This is followed by a discussion of the effect of sea surface temperatures on both global and Australian climate extremes.

D.1 Regime change

Results from **Chapter 2** indicated that in the northwest of Australia there has been a statistically significant moistening in the northwest in summer (**Fig. 2.4b**). *Nicholls et al.* (1997) and *Power et al*. (1998), suggest that this increase is associated with a decrease in maximum temperature and **Fig. 2.2b** indicates that this is also the case for maximum temperature extremes in summer. This is consistent with the hypothesis that an increase in cloud cover may be enhancing wetting and cooling in the region. In other parts of Australia, however, there have been significant decreases in precipitation (*e.g.* **Fig. 2.4**) and significant increases in both maximum and minimum temperatures (*e.g.* **Fig. 2.2** and **Fig. 2.3**). This may indicate either a decrease in cloud cover and/or changes in cloud types

or that there are other driving forces in these regions affecting extremes. **Chapter 3** showed that there have been significant shifts in synoptic systems over Australia in the past century. Although there might not be a direct relationship between pressure and cloud type it is unlikely that the changes observed in large scale pressure systems would be entirely independent of changes in cloudiness given the interacting dynamics of the atmosphere.

Changes in cloud cover and type can now be identified using International Satellite Cloud Climatology Project (ISCCP; *Rossow and Schiffer* 1991) data, available at 250km resolution, 3–hourly timescale from July 1983 to December 2004 (*Jakob and Tseliodis* 2003; *Rossow et al.* 2005). These data contain optical thickness (τ) and cloud top pressure measurements at various levels in the atmosphere so it was possible to classify different types of cloud regimes *e.g.* "most convectively active" to "least convectively active". Tropical cloud regimes or "weather states" using ISCCP data have already been identified by *Rossow et al.* (2005) for a region covering 15°S to 15°N. However this region excludes most of Australia. Therefore cloud regimes were reclassified for the continent. Different dynamical regimes exist between tropical and extratropical regions so two regions were chosen: 110E to 160E, 0S to 25S and 110E to 160E, 25S to 50S, although most of the focus on this section will be on the extratropical region where the majority of the population live. The same technique used by *Rossow et al.* (2005) was implemented to identify different cloud regimes *i.e.* a K-Means clustering algorithm (*Anderberg* 1973). This technique iteratively searches for a predefined number (k) of clusters by a) assigning one member clusters to each of the k elements of the dataset of size N, b) assigning each of the remaining N-k elements to the cluster with the nearest (Euclidian distance) centroid whereby after each assignment the centroid of the gaining cluster is recalculated and c) after all elements have been assigned the centroids found in step b) they are used as new seed points and the algorithm is iterated. *Rossow et al.* (2005) showed that for tropical cloud regimes, when $k < 6$ (*i.e.* the number of clusters was less than six), the results were unstable and that for $k > 6$ there were members that were too highly correlated with each other. For this reason, six clusters were chosen for this study to represent tropical and extratropical cloud patterns over Australia although it is possible that this number may not be sufficient for the southern region. In addition, since optical thickness can only be calculated with the visible channel, two daytime periods were investigated (morning to early afternoon and mid afternoon to early evening) to allow for the differences in convective situations that occur during the day.

Fig. D.1 shows the frequency distribution of cloud top pressure versus optical thickness (τ) for extratropical Australia for morning and afternoon. The figure reflects the typical amount and type of cloud in each 250km gridbox within the ISCCP dataset in southern Australia as calculated by the K-Means algorithm for six regimes. Each regime is defined over seven atmospheric levels and six optical thickness ranges (defined within the ISCCP dataset) ranging from "optically-thin" cumulus at the bottom left of the histogram to the "optically-thick" deep convection at the top right of the histogram. Data for the 20-year period 1985 to 2004 were used in the calculation since this period contains continuous data. To our knowledge, this is the first time that cloud regimes have been defined for extratropical Australia. It is clear that there are strong similarities between the morning (**Fig. D1a**) and afternoon (**Fig. D1b**) situations. The same technique was used to identify cloud regimes for tropical Australia which agree well with the tropical weather states defined by *Rossow et al.* 2005 (not shown). Although 20 years may not be long enough to perform robust trend analysis of the frequency of each regime, there are indications that over the past two decades there have been increases in some of the cloud regimes and decreases in others. **Fig. D.2** shows timeseries of the extratropical cloud regimes from **Fig. D1a**. Two of the regimes indicate significant trends at the 5 % level over the 20 year period of study. **Fig. D.2** shows that there has been a significant increase of 22 days/decade in cloud regime four from **Fig. D1a**. This regime is marked by low clouds most of which are in the low to medium optical thickness range and therefore would not usually be associated with rain. Regime six on the other hand shows a significant decrease in frequency of 23 days/decade. This regime is more convectively active than regime four, marked by higher clouds and clouds of greater optical thickness. So based on the last 20 years of data, results indicate that there has been a significant decrease in one of the cloud regimes that brings rainfall to southern Australia. However these broad trends may not reflect the frequency of cloud regimes in different regions of Australia. To account for this, the frequency of each cloud regime was analysed for the four Australian cities from **Chapter 3** (Sydney, Melbourne, Adelaide and Perth). This was done by analysing the regimes within the closest 250km grid box to each city. Trends in the cloud patterns at each city are given in **Table D.1**. From this, it is clear that trends in each cloud regime are indeed dependant on location. Sydney and Melbourne show significant increases of 10.44 and 12.92 days/decade respectively in cloud regime three (which is one of the less convectively active regimes) while Adelaide shows a significant decline in this regime of 10.21 days/decade.

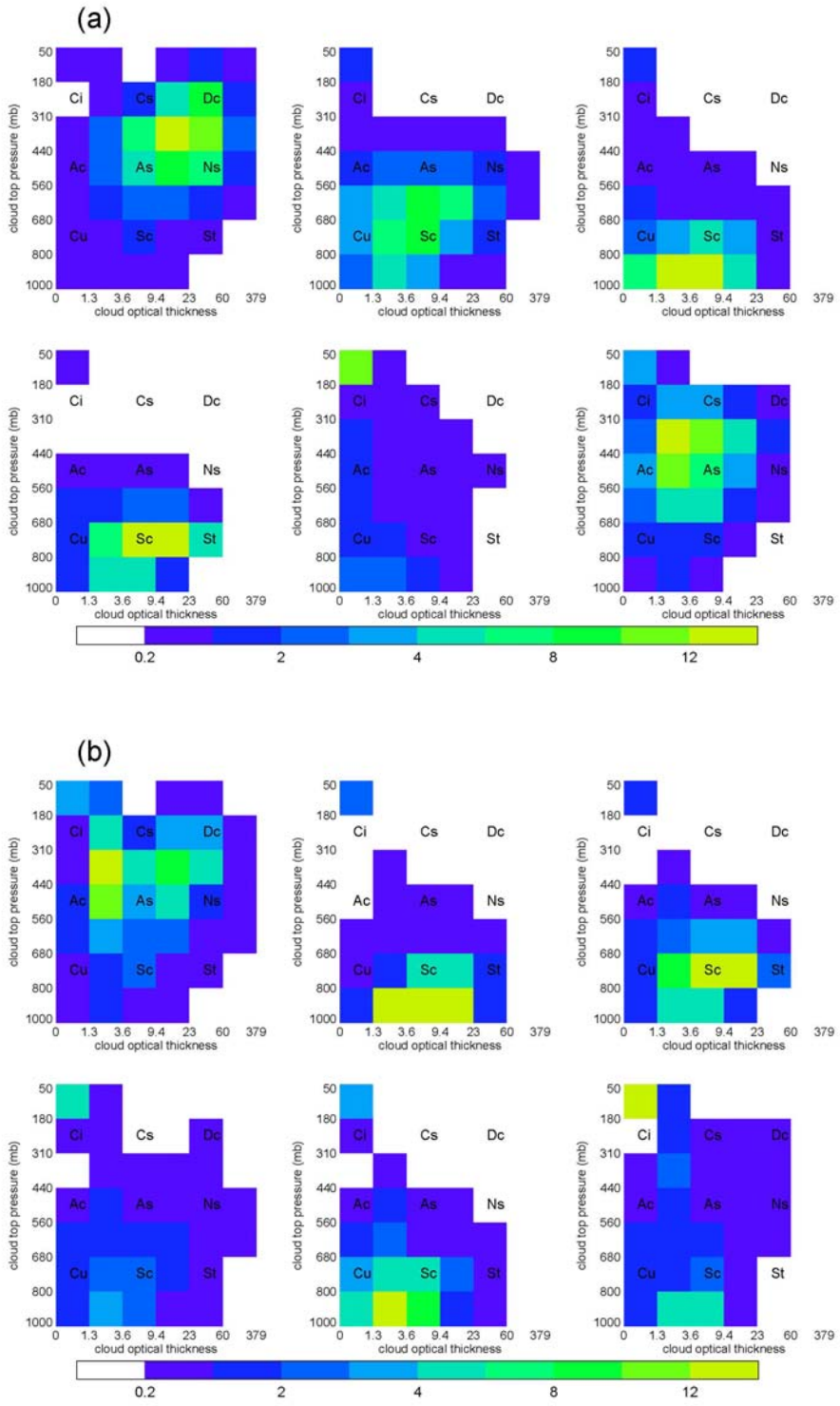

Fig. D.1: Six cloud top pressure - optical thickness frequency histograms (cloud regimes) that best describe the 3-hourly variations of cloud properties across extratropical Australia for (a) morning and (b) afternoon. The types of clouds represented by the histogram from top left to bottom right are Cirrus (Ci), Cirrostratus (Cs), Deep convection (Dc), Altocumulus (Ac), Altostratus(As), Nimbostratus (Ns), Cumulus (Cu), Stratocumulus (Sc) and Stratus (St). Throughout the text regimes are referred to as numbers one to six from top left histogram to bottom right histogram.

Adelaide is interesting because it shows both significant increases and decreases in two of the cloud regimes that are most likely associated with rainfall (an increase in regime one of 5.21 days/decade and a decrease in regime six of 3.04 days/decade). Indeed Adelaide is the only city analysed that shows a statistically significant decrease in regime six agreeing with the sign and significance of the trend in this regime over southern Australia as a whole (**Fig. D.2**) although with a trend of much smaller magnitude. Perth is different again with a significant increase in regime two, a regime characterised predominantly by cumulus and stratocumulus and few high clouds.

Table D.1: Trends (days/decade) in the frequency of cloud regimes from **Fig. D1a** at four Australian cities. Bold signifies that trends are significant at the 5% level.

Cloud regime	Sydney	Melbourne	Adelaide	Perth
1	4.53	2.49	**5.21**	0.12
2	-0.95	4.72	8.20	**10.08**
3	**10.44**	**12.92**	**-10.21**	-2.35
4	1.74	-0.71	5.08	1.70
5	-3.32	-14.68	3.54	4.11
6	-2.66	4.41	**-3.04**	1.57

So it appears that the significant trends in cloud regimes four and six over southern Australia as a whole (**Fig. D.2**), are not reflected at individual sites across the region which generally indicate significant trends in other cloud regimes (**Table D.1**). However it should be noted that the results from the trend analysis presented here should be treated with caution because of the short period of study and because of potential inhomogeneities which may exist within the ISCCP dataset (*Kato et al.* 2006). However since this is the first time that these dynamical cloud regimes have been characterised for extratropical Australia it was possible to make direct links between these regimes and synoptic pressure patterns. In addition it was also possible to determine how these were associated with changes in some of the climate extremes described in the previous sections.

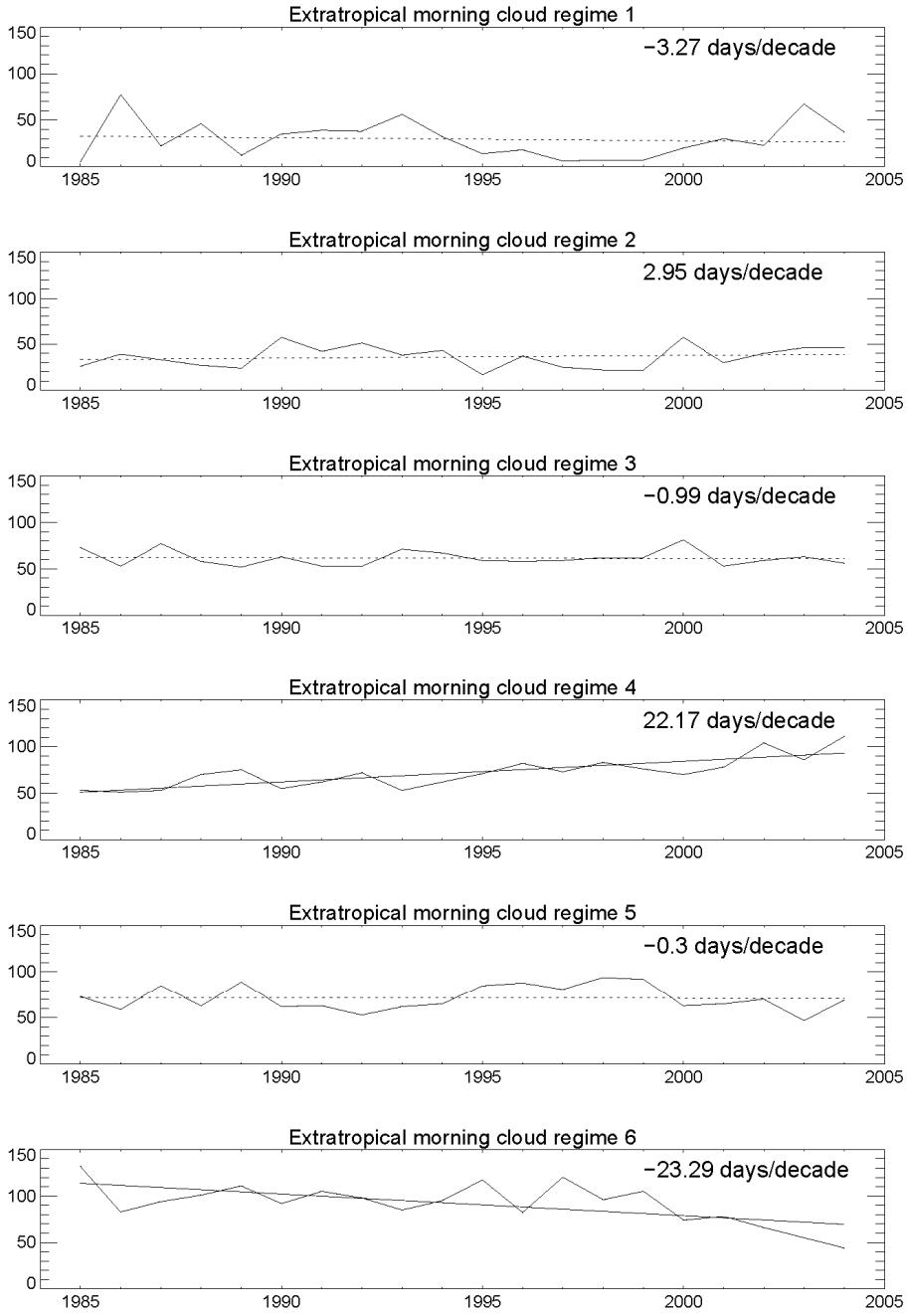

Fig. D.2: Timeseries of frequency of the morning cloud regimes over extratropical Australia. Linear regression lines are shown along with the decadal trends. Solid lines indicate that trends are significant at the 5% level. Trends and significance calculated as in **Chapter 3**.

D.1.1 Interactions with synoptic pressure systems

Using the synoptic systems defined by the SOM algorithm in **Chapter 3**, it was possible to determine the links that exist between large-scale weather systems and the corresponding cloud regimes for the four cities described in the last section. Since the types of regimes

that exist across southern Australia are similar between the morning (**Fig. D.1a**) and afternoon (**Fig. D.1b**), the morning cloud regimes were chosen and compared with the daily synoptic pattern that occurred on that day. This was possible to do for days between 1st January 1985 and 31st December 2004 when full years of ISCCP data were available. **Fig. D.3** shows contour plots of the frequency of each cloud regime from **Fig. D.1a** for Sydney, Melbourne, Adelaide and Perth during the associated large scale pressure patterns from **Fig. 3.2**. The total from left to right for each synoptic pattern equals 100 %. For each city, cloud regime five is the most dominant pattern irrespective of the driving synoptic pattern. In particular this is true for Sydney and Melbourne where cloud regime five occurs between 40 % and 52 % of the time during any given synoptic pattern. This regime is one of the least convectively active, indicating the dominance of clear skies over much of Australia. Over Perth this regime occurs between 24 % and 48 % of the time. Interestingly, regime five peaks in Perth during SOM nodes 4, 8, 12 and 16 (**Fig. 3.2**) *i.e.* the patterns in the right hand column of the SOM all of which have declined in frequency over the last century (**Fig. 3.3**). However the frequency of this regime has increased in Perth between 1985 and 2004 (**Table D.1**) although not significantly. In Adelaide cloud regime five occurs between 24 % and 36% of the time, only slightly more frequently than cloud regime three. **Table D.1** shows that cloud regime three has significantly declined in frequency over the past two decades in Adelaide.

The results indicate that there appear to be links between cloud regimes and the over-arching synoptic patterns over Australia. In **Chapter 3** the links between synoptic patterns over Australia and rainfall intensity at Sydney, Melbourne, Adelaide and Perth were investigated. In the next section we will perform a similar analysis only this assessing the effect of cloud regimes on daily rainfall intensity at the four cities.

D.1.2 Link between cloud regimes and precipitation extremes

Daily rainfall measurements were extracted for stations from the Bureau of Meteorology's high quality dataset (*Haylock and Nicholls* 2000) which were closest to Sydney, Melbourne, Adelaide and Perth (see **Chapter 3**). The period 1985 to 2005 was chosen as this is the same 20-year time period that is spanned by the ISCCP data used in this study. The cloud regimes from **Fig. D.1a** from the closest 250km gridbox to each city were compared with the daily rainfall at each site. The average daily rainfall intensity associated

with each cloud regime was calculated and is shown in **Fig. D.4** along with the relative frequency of the cloud regimes at each city.

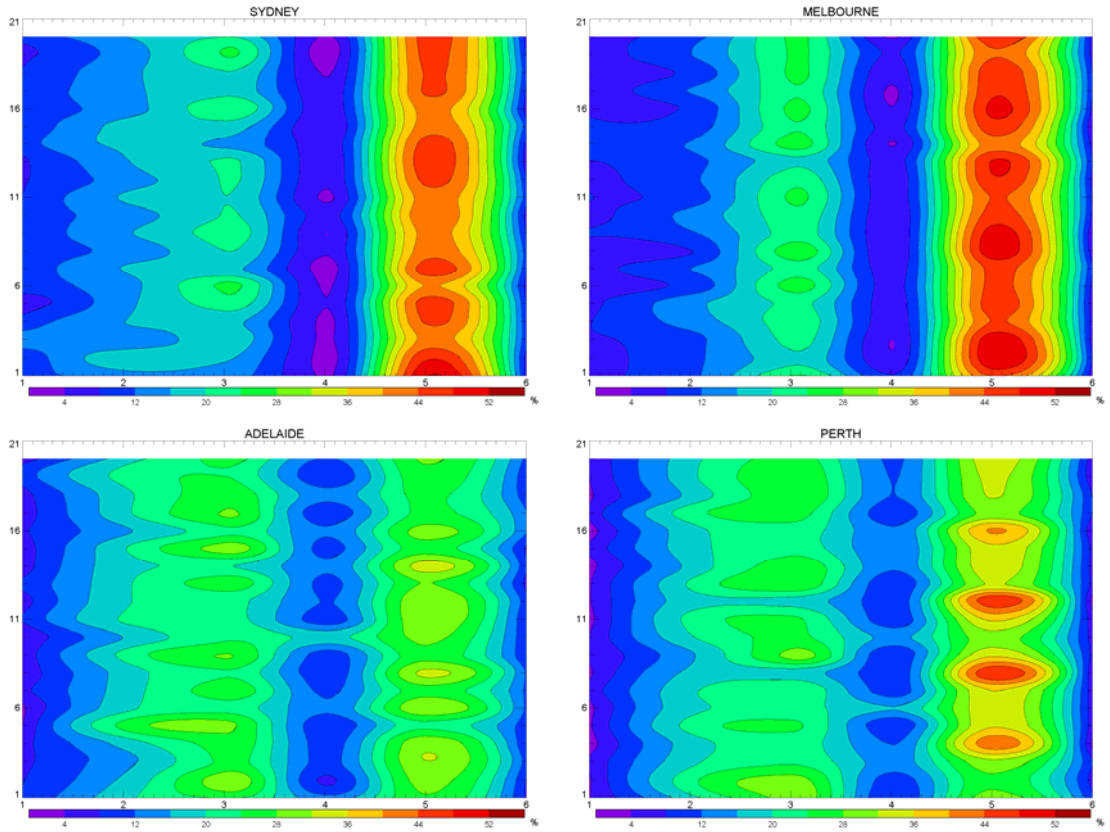

Fig. D.3: Contour plots of the percentage of time during which each cloud regime from **Fig. D.1a** occurs during the synoptic patterns ("nodes") defined in **Fig. 3.2.**

Like **Fig. D.3**, this figure shows that cloud regime five occurs most frequently at each site. However, now it is clear that this regime is associated with the smallest rainfall intensity at each city. In Sydney (which is the wettest of the four cities), the heaviest daily rainfall intensity of about 11 mm/day is brought by cloud regime one. This is perhaps not surprising as this is the most convectively active regime from **Fig. D.1a**. This regime only occurs 9.1 % of the time at Sydney and indeed is one of the least frequent regimes at the other three cities. However, in Melbourne and Adelaide it is cloud regimes four and three respectively which deliver the most intense rainfall. These are curious results as these regimes are not very convectively active so should not be associated with large amounts of rainfall. This perhaps indicates that the number of regimes chosen is inadequate to account for the number of weather types that occur in extratropical Australia. **Table D.1** shows that cloud regime four has significantly declined by 10.21 days/decade in Adelaide. This could

indicate a move towards other regimes such as cloud regime one, for example, which has significantly increased in frequency over Adelaide by 5.21 days/decade over the past 20 years. Although there has not been a statistically significant increase in daily rainfall intensity in Adelaide when averaged over the year (not shown), **Table 3.3** indicates that there have been significant increases in daily rainfall intensity during certain synoptic patterns at this South Australian city.

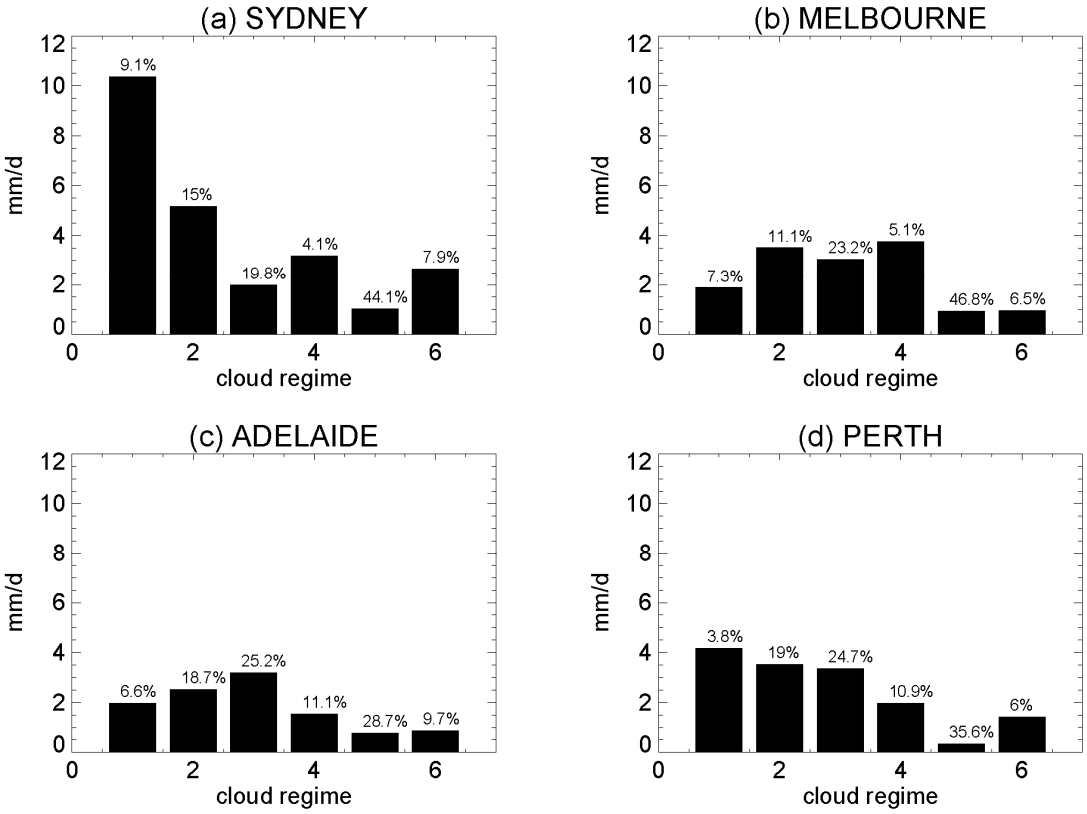

Fig. D.4: Rainfall intensity (mm/day) associated with dynamical cloud regimes from **Fig. D.1a** for (a) Sydney, (b) Melbourne, (c) Adelaide and (d) Perth.

Like Sydney, cloud regime one brings the most intense daily rainfall to Perth although this regime only occurs 3.8% of the time. In Perth, regimes two and three also bring rainfall of similar intensity but combined they occur 44 % of the time and are therefore much more important to the local rainfall regime. Cloud regime two has also significantly increased in frequency in the last two decades (**Table D.1**) so this may indicate that while there has been a significant decline in average rainfall in the region (*Hope et al.* 2006) there is a possibility that extreme rainfall events have increased. However, **Table 3.3** indicates if trends over the last century are considered, it is more likely that extreme rainfall events

have decreased in Perth. Also, as suggested in **Chapter 3**, other studies (*e.g. Li et al.* 2005) have shown evidence for a drying of winter daily rainfall extremes after 1965 related to changes in the Antarctic Oscillation (AAO). So in conclusion, this suggests that depending on the timescale, season and index under consideration, there are many interacting mechanisms which produce a very complex relationship between synoptic patterns, cloud regimes and extreme rainfall across southern Australia.

D.2 El Niño-Southern Oscillation (ENSO)

Another potential driver of Australian climate extremes is changes in sea surface temperatures. It is clear that SSTs have an effect on changes in mean climate across Australia and a large portion of this variability is due to changes in the El Niño-Southern Oscillation (ENSO) (*McBride and Nicholls* 1983; *Nicholls et al.* 1996b). Across south-west Western Australian, *Ummenhofer et al.* (2008) showed that the observed rainfall decline is being forced by differences in sea surface temperatures between the west and east of the Indian Ocean although there is some debate as to whether this is merely a reflection of warming oceans to the north of Australia (personal communication Neville Nicholls). *Kenyon and Hegerl* (2008) found that major modes of climate variability have had a significant influence on changes in climate extremes globally and that minimum temperature extremes are affected differently than maximum temperature extremes. **Fig. D.5** shows the correlations between SSTs and timeseries of various observed climate extreme indices averaged across Australia. Long-term linear trends present in the SSTs and the climate indices were removed before the correlations were calculated. Hence the correlations reflect the response of Australian extremes to short-term variability in SSTs. Significant correlations are seen in many parts of the tropical oceans. These include the tropical Pacific, suggesting that ENSO variability does in fact significantly affect the variability of changes in rainfall, extratropical cyclones and maximum temperature extremes across Australia. However, **Fig. D.6** shows that ENSO variability does not have a significant influence on minimum temperature extreme variability in Australia which is much more highly correlated with local SSTs and Indian and Atlantic Ocean tropical SSTs. In the next section we will look at some of these driving forces and discuss their influence on some of the extremes that have been discussed in previous chapters.

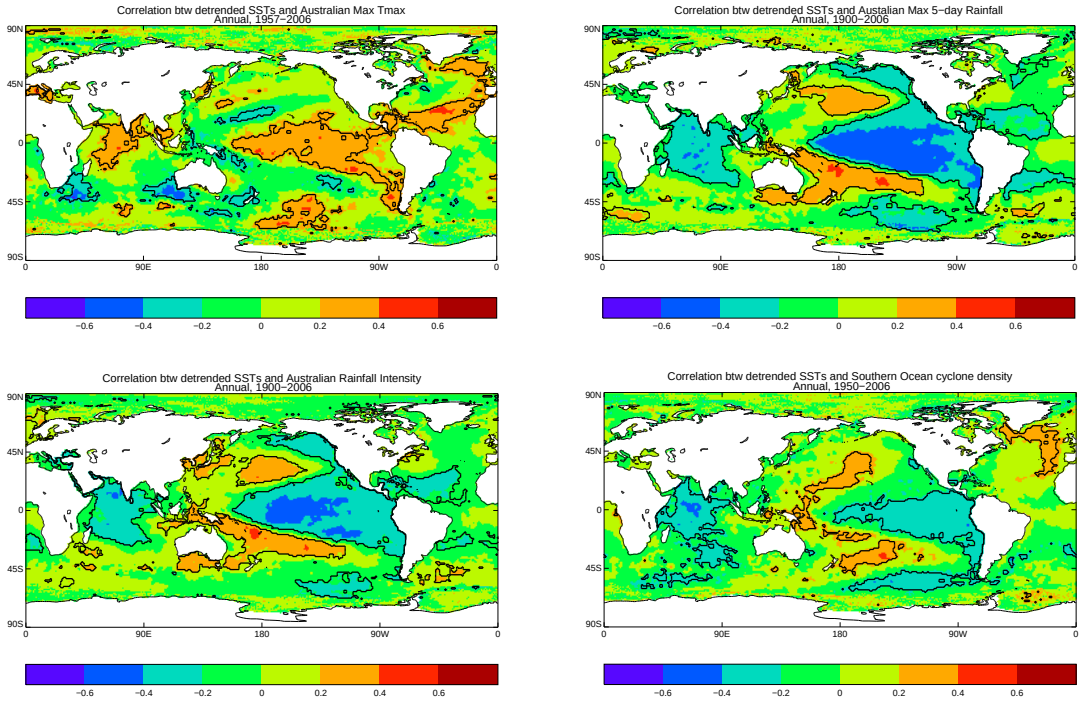

Fig. D.5: Correlations of detrended timeseries averaged across Australia of (a) annual maximum daily maximum temperature, (b) Daily rainfall intensity, (c) annual maximum 5-day rainfall and (d) Southern Ocean cyclone density with detrended timeseries of annual sea surface temperatures from HadISST (*Rayner et al.* 2003). Black lines enclose regions where correlations are significant at 5% level.

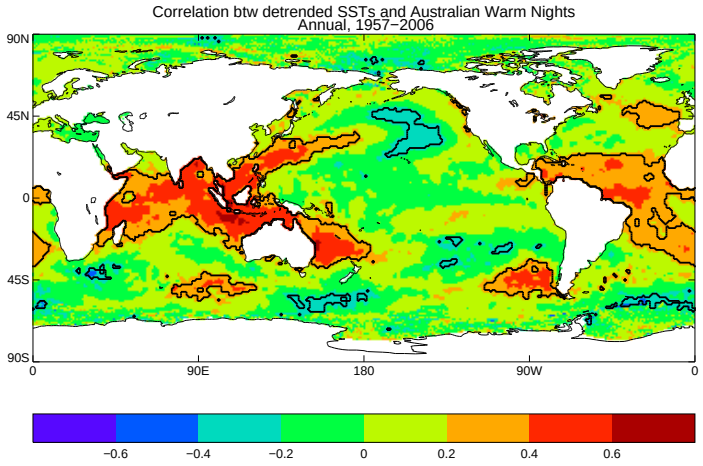

Fig. D.6: As **Fig D.5** but for warm nights across Australia for the period 1957-2006.

4. The influence of sea surface temperature variability on global temperature and precipitation extremes

Summary

The HadISST1 dataset was used to categorise patterns of observed global sea surface temperature (SST) variability using the method of Self Organising Maps (SOM). SST anomalies were calculated seasonally between 1870 and 2006 and were categorized into eight patterns using a SOM algorithm to represent the majority of global SST variability modulated by the El Niño-Southern Oscillation (ENSO). Time series were analysed and showed that there have been periods of "preferred" SST states since the late 19th century. In the latter half of the 20th century the preferred states have moved from La Niña like patterns to more neutral global SST conditions, while weak El Niño patterns have moved preferentially to stronger El Niño states. The eight patterns were used to investigate the global response of extreme temperature and precipitation indices from the HadEX dataset to different nodes of SST variability. Results showed very strong statistically significant opposite responses from the first pattern (strong La Niña) to the last pattern (strong El Niño). Extreme maximum temperatures were significantly cooler during strong La Niña events than strong El Niño events over Australia, southern Africa, India and Canada while the converse was true for USA and north-eastern Siberia. Even interim patterns representing a move from weak El Niño to a weak La Niña phase also produce statistically significant increases in warm nights and warm days particularly across Scandinavia and north-west Russia. While the response of precipitation extremes to global SST patterns was less spatially coherent there were large areas across North America and central Europe which showed statistically significant differences in the response to opposite phases of ENSO. The results indicate that the variability of global SST anomalies is important for the modulation of extreme temperature and precipitation globally. Even weak phases of ENSO can have significant impacts on extreme events across large regions and this is particularly evident in high latitudes. An atmosphere-only global climate model (CAM3) forced with observed SSTs was used to investigate whether state of the art models could reproduce some of the significant responses that have been observed over Australia. Results showed that the model obtained the opposite response to that which was observed. This may indicate that some important atmospheric processes are not well captured by the model.

4.1 Introduction

Sea surface temperature (SST) variability has a significant influence on the global mean climate (*Ropelewski and Halpert* 1987; *Halpert and Ropelewski* 1992). For instance, the El-Niño Southern Oscillation (ENSO) brings drier/warmer conditions to much of Australia, south-east Asia, India, north-west USA and Canada during positive phases (El Niño) and wetter/cooler conditions in most of these regions during its negative phase (La Niña) *e.g. McBride and Nicholls* 1983; *Power et al.* 1998; *Kiladis and Diaz* 1987; *Rasmusson and Carpenter* 1982; *Deser and Wallace* 1987; *Deser and Wallace* 1990; *Ropelewski and Halpert* 1986. While it is important to understand how large scale variability affects mean climate, much more understanding is required on how this variability influences climate extremes since these have a much more significant impact on communities and ecosystems (*Easterling et al.* 2000; *Nicholls and Alexander* 2007). For instance, the unprecedented mortality of the 2003 European heatwave (*Foullet et al.* 2007) has been a catalyst for more urgent understanding of the driving mechanisms of these types of events.

Previous studies have shown that natural modes of climate variability have a significant influence on the regional response of climate extremes on multi-decadal timescales *e.g. Scaife et al.* 2008; *Cai et al.* 2005. *Kenyon and Hegerl* (2008) was perhaps the first study which looked at the affect of a number of large scale climate variability measures on global temperature extremes. Using indices of large scale climate variation, they showed that different phases of ENSO could be seen to influence temperature extremes globally often affecting cold and warm extremes differently although with areas of much stronger response around the Pacific Rim and throughout all of North America. They conclude that modes of variability need to be taken in to account if we are to provide for reliable attribution of changes in extremes as well as prediction of future changes. *Kenyon and Hegerl* (2008) investigated the influence of large scale climate "indices", such as the ENSO Cold Tongue Index (CTI) and the North Pacific Index (NPI), on global temperature extremes. However the aim here is to look at the influence of global "patterns" of SST variability on temperature extremes and for the first time to look at the global response of these patterns on precipitation extremes. This could determine whether patterns other than those defined by positive or negative phases of indices such as NINO3.4, NINO4 etc. had

any impact on global extremes. The method of Self-Organising Maps (SOM) described in **Section 3** was used to categorize observed SST anomalies between 1870 and 2006 from the HadISST1 dataset into common patterns using a similar technique to *Leloup et al.* (2007a). The results were used to show how modes of SST variability influence global temperature and precipitation extremes. Experiments from the CAM3 atmosphere-only global climate model (*Collins et al.* 2006a) were also analysed to test the simulated response of temperature extremes over Australia to SST variability and to compare with the observed response.

4.2 Data and methods (observations)

Two observational datasets were used in this analysis: HadISST1 (*Rayner et al.* 2003) and HadEX (*Alexander et al.* 2006). HadISST1 is a one-degree latitude by one-degree longitude grid of globally complete monthly SST and sea ice concentration measurements from 1870 onwards. For this study HadISST1 data were obtained from 1870 to 2006. Because our interest is in sea surface temperature patterns, areas of 100% sea ice cover were considered to be land. HadEX is a 2.5-degree latitude by 3.75-degree longitude gridded dataset containing indices derived from daily *in-situ* temperature and precipitation observations over much of the global land area from 1951 to 2003. To investigate how temperature and precipitation extremes are affected by SST variability, we focus on six of these indices (four temperature and two precipitation) that were introduced in **Chapter 2** (see **Table 2.1**). These indices are:

1. Percent of days below the 10^{th} percentile (of the 1961-1990 climatological reference period) of seasonal minimum temperature (TN10p);
2. Percent of days above the 90^{th} percentile of seasonal minimum temperature (TN90p);
3. Percent of days below the 10^{th} percentile of seasonal maximum temperature (TX10p);
4. Percent of days above the 90^{th} percentile of seasonal maximum temperature (TX90p);
5. Maximum 1-day seasonal rainfall event (RX1day);
6. Maximum consecutive 5-day seasonal rainfall event (RX5day).

These indices were chosen because they were available seasonally and in addition the temperature indices represent the warm and cold extremes of both maximum and minimum temperature. In addition, the monthly NINO4 index was also obtained from NOAA's National Weather Service Climate Prediction Center. This index is calculated from SST anomalies in the tropical Pacific averaged in the box 6N-6S, 160E-150W and was available from 1950 to provide an independent measure for comparison with the results presented here.

Firstly, seasonal SST anomalies (SSTA) were created from HadISST1 for December to February (DJF), March to May (MAM), June to August (JJA) and September to November (SON) between 1870 and 2006 using 1961-1990 as the climatological reference period. Next, these seasonal SSTA were detrended by fitting an ordinary least squares regression to each grid box with data and calculating the residuals. The reason for removing trends from the data is so that changes observed from one state to another reflect the actual variability of the SSTA patterns rather than changes towards warming oceans. The detrended SSTA were then categorised into most common patterns of variability using a clustering technique called Self-Organising Maps (SOM; *Kohonen* 2001). The SOM technique has been found to be useful in reducing the dimensions of large datasets to enable the visualisation and interpretation of the data characteristics. Details of the approach which is closely followed here are given in *Cassano et al.* 2006 and **Chapter 3**. The SOM approach produces a two-dimensional set of patterns or "nodes" of global SSTA. In this case it was found that eight nodes provided enough patterns to cover most aspects of global seasonal SST variability while ensuring that each node is frequent enough to provide robust statistics for the comparison with the global climate extremes. The SOM algorithm determines which node of the SOM best matches the observed SSTA for that season (that is the SOM node that gives the smallest Eucleidian distance error when compared to the seasonal SSTA pattern). Seasonal values were also calculated for global temperature and precipitation extremes between 1951 and 2003 when data are available from the HadEX dataset. *Alexander et al.* 2006 showed that there has been a significant warming of both maximum and minimum temperature extremes globally during the second half of the 20th century. In order that the results here are not simply a reflection of this warming climate, each of the extremes indices was detrended in a similar way to the SSTA. In addition, because of the varying distribution globally of the rainfall indices, RX1day and RX5day were normalised (*i.e.* each value of the detrended index was

calculated by subtracting the mean and dividing by the standard deviation) so that changes can be compared consistently between different regions. Thus for each season between 1951 and 2003 it was possible to relate the temperature and precipitation extremes to a node of the SOM.

4.3 Observational results

The SSTA patterns produced by the SOM algorithm are shown in **Fig. 4.1**. Clearly the SOM is able to distinguish the modulating influence of ENSO moving from a strong La Niña phase through to a strong El Niño phase with weaker or neutral phases in between. The first node (strong La Niña) appears most frequently within the SOM although all nodes are approximately equally distributed. As we move through the nodes of the SOM, the phases of ENSO weaken with the middle nodes (4 and 5) indicating more neutral global SST conditions. The nodes were compared to the NINO4 index during the time period when this index is available (**Fig. 4.1**). For each occurrence of a node, the average seasonal value of the NINO4 index was obtained. It is clear from **Fig. 4.1** that the probability distribution functions (PDFs) of these values that the strong La Niña pattern (node 1) has almost always a negative NINO4 index and conversely the strong El Niño pattern (node 8) has almost always positive NINO4 index values. For the nodes in between, the PDFs move from negative to positive values and interestingly nodes 3 and 4 have a distinctive bi-modal distribution. Each seasonal SSTA pattern was compared visually with the node assigned to it by the SOM algorithm. In all cases, it was found that the key features of the SSTA pattern, for example the presence or absence of an ENSO signal, were adequately reflected by the assigned SOM node.

Fig. 4.2 shows how the occurrence of each SOM node has changed through time. Each SSTA pattern has occurred throughout most of the 137 year period analysed although some patterns are much more "bunched" than others. In the latter part of the 19th century the "preferred" SST state reflected weak La Niña conditions but with also quite a few episodes of strong El Niño events. Interestingly there is at least a 35-year period in the early 1900s when nodes 3 and 4 did not occur at all in HadISST1 but these have been the predominant SSTA variability modes in the last decade or so. The first half of the 20th century was

classified by weaker El Niño regimes which switched to a predominance of either neutral SSTA or strong La Niña regimes between about 1950 and 1975.

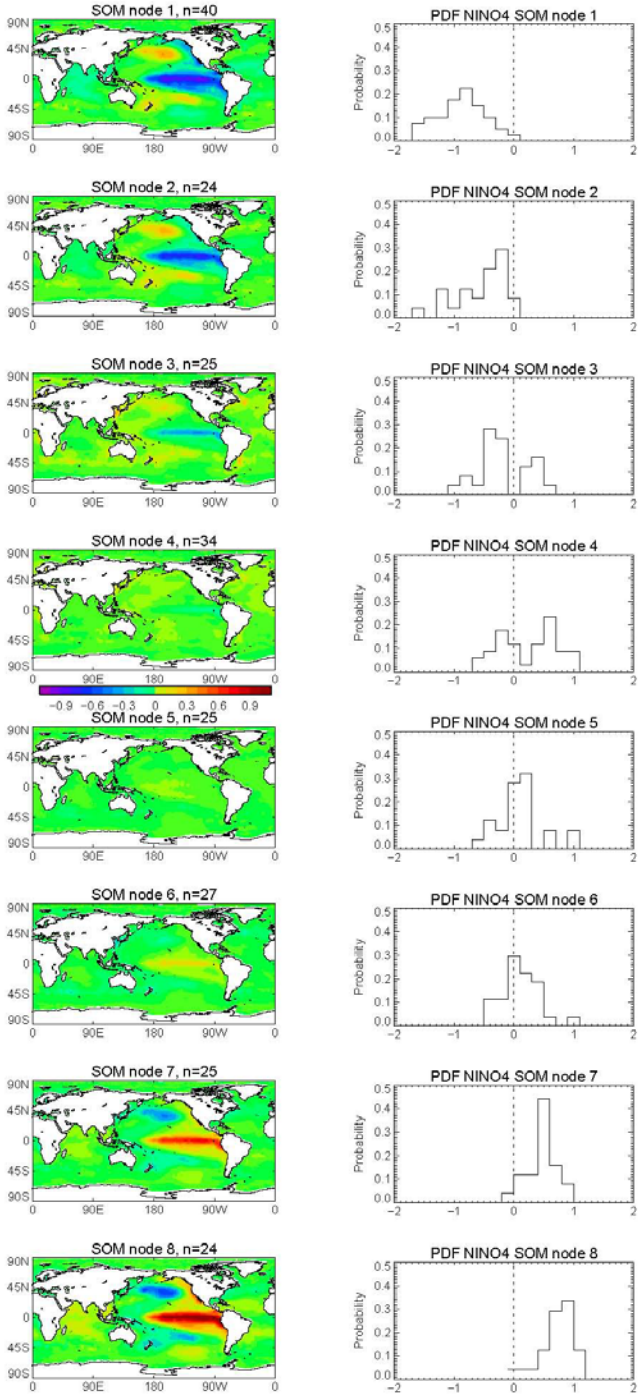

Fig. 4.1: Seasonal SSTA patterns ('nodes') from HadISST1.1 derived using Self-Organising Maps (SOM). Each node is shown alongside the probability distribution function of the associated NINO4 index value for the seasons where this node occurs. The number of times, n, that each node appears within the SOM between 1950 and 2006 when the NINO4 index is also available is shown above each map.

Now that the dominant patterns of global SSTA variability have been classified this information can be used to determine how each of these various nodes influences global patterns of extreme temperature and precipitation.

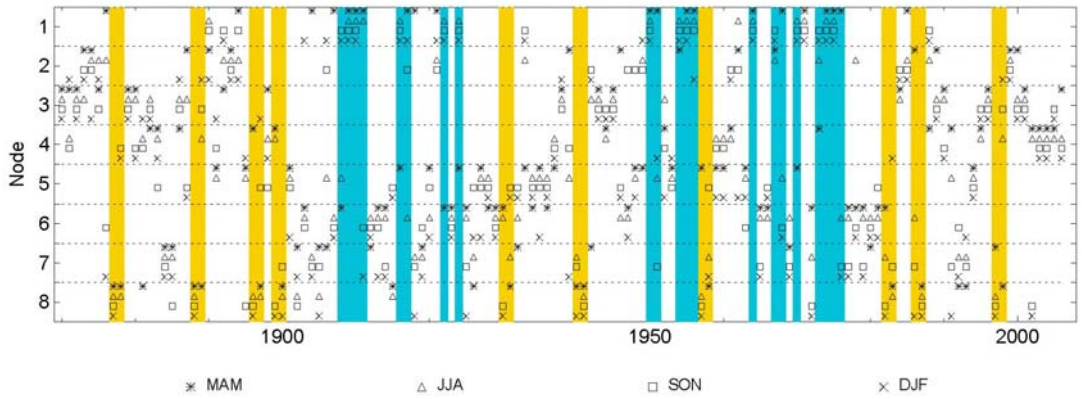

Fig. 4.2: Timeseries of seasonal SSTA from HadISST1 as categorized by the 8 SOM nodes defined in **Fig. 4.1**. Each symbol represents a different season. Lines are shaded blue where at least 3 consecutive seasons most closely resembled node 1 (strong La Niña) and orange where they most closely resembled node 8 (strong El Niño).

Table 4.1 shows globally averaged deviations from the expected values of the various indices used in this study during each of the SOM nodes. Because the expected value of the globally averaged temperature indices is 10 % (approximately 9 days per season), a value of 1 in the table represents an increase of approximately 1 day per season. From **Table 4.1** we can see that there is an increase (decrease) of warm nights (TN90p) during strong El Niño (La Niña) events represented by node 8 (node 1) of around 1 day per season. A similar increase in this index is also seen in node 4, a node that also produces a 1 day per season increase in warm days (TX90p) and a decrease in cool nights (TN10p). These three nodes, associated with the largest deviations in the minimum temperature indices (TN10p and TN90p), are associated with smaller deviations in the maximum temperature indices (TX10p and TX90p). The warm nights index (TN90p) is more sensitive to differences between nodes than cool nights (TN10p), as evidenced by the relative magnitudes of the deviations for the two indices. Similarly, in nearly all cases warm days (TX90p) are more sensitive than cool days (TX10p). No nodes produce large global deviations in the precipitation indices (RX1day and RX5day) although results show more wet extremes during La Niña (node 1) and more dry extremes during El Niño (node 8), which is similar to the effect of ENSO on average rainfall.

Table 4.1: Globally averaged deviations from expected value of each extreme index for each SSTA SOM node from **Fig. 4.1**. Values for temperature indices (TN10p, TN90p, TX10p and TX90p) are deviations from expected value (*i.e*. 10 %). Values for precipitation extremes are numbers of standard deviations from expected value (*i.e.* average value of index from 1951 to 2003).

Node	*TN10p*	*TN90p*	*TX10p*	*TX90p*	*Rx1day*	*Rx5day*
1	0.78	-0.89	0.46	-0.66	-0.03	-0.01
2	0.05	-0.28	0.03	-0.14	-0.003	0.01
3	-0.13	0.38	-0.31	0.54	-0.003	0.02
4	-1.01	1.10	-0.77	0.90	0.03	0.02
5	-0.36	0.46	-0.57	0.54	-0.03	-0.03
6	0.37	-0.83	0.39	-0.59	-0.01	-0.01
7	0.17	-0.45	0.46	-0.60	0.02	-0.01
8	-0.42	1.23	-0.07	0.59	0.04	0.02

However, global averages mask some of the strong differing regional influences of each of the nodes. **Fig. 4.3** presents maps of how the regional response of TN10p (cool nights), TN90p (warm nights) and RX1day (maximum 1-day rainfall) varies during each of the eight SOM nodes. The response of cool nights and warm nights are similar in most regions (note that the colour bar has been reversed between the two indices so that yellow/red indicates warming and green/blue indicates cooling). For both TN10p and TN90p, which represent cool and warm nighttime temperatures respectively, there are clear regional effects of SSTA variability. Much of the globe shows a cooling of temperature extremes during strong La Niña phases (node 1) except for the eastern United States and north east Russia predominantly. Interestingly, south-eastern Australia also shows a slight warming during this phase. Australian temperature and rainfall are significantly correlated with ENSO and each other but there are complex interactions and regional differences (*e.g*. *Jones and Trewin* 2000; *Nicholls* 2003; *Nicholls et al.* 1996b; *Power et al.* 1998) which indicate a non-linear relationship. Similarly the strong El Niño phase (node 8) indicates warmer than usual extreme minimum temperatures and almost the opposite pattern of warming and cooling to node 1. The remaining patterns also have large coherent regions of warming and cooling although generally not as large as the most extreme ENSO phases.

However perhaps what is most striking is that neutral or weak ENSO phases have about as strong an influence on global climate extremes as very strong positive or negative phases of ENSO. For instance, a very weak El Niño-like pattern (node 4) produces warming in most of the global land areas and globally averaged produces about the same global extreme minimum temperature warming as the strong El Niño node (**Table 4.1**). The regional variations between node 4 and node 8 are quite different however; the above average extreme warming across much of Russia in node 4 is countered by quite strong below average extreme cooling across the same region in node 8. In general node 4 does not produce as strong a warming or cooling as node 8 but parts of south-east Asia, India, north-west Australia and southern Africa represent the equivalent of over 3 days increase in the number of warm nights in these regions during this neutral/weak La Niña pattern. Similarly nodes 1 and 6 represent a general global cooling of warm night time temperatures. Particularly, node 6 which relates to a weak El Niño pattern produces substantial nighttime cooling across Europe and north-west Russia. While the patterns of warming and cooling are similar between cool nights and warm nights, in general the upper end of the minimum temperature distribution (TN90p) appears to have a slightly stronger response to SST variability than the lower end of the minimum temperature (TN10p) distribution.

For the precipitation index, RX1day, the patterns are not as coherent as the temperature indices during each of the SSTA phases but there are still some large regions where the SSTA pattern has a clear affect. Increases in RX1day, which represents the wettest day in a season, are likely to indicate increased chances of flooding. The strongest increases are mostly seen during nodes 6 to 8 (representing weak to strong El Niño events), particularly over Europe during nodes 6 and 7, countries adjacent to the Caspian sea during nodes 7 and 8 and western USA, southern Brazil and south-east China during node 8 (strong El Niño). The response of RX1day is generally opposite in these regions during La Niña-like patterns.

The results for the other precipitation index, RX5day, which represents the five wettest consecutive days in a season (see **Fig. 4.4**) are very similar to RX1day indicating the strong relationship between these two indices. It is also clear from **Fig. 4.4** that maximum temperature extremes show similar patterns of regional response as minimum temperature extremes (**Fig. 4.3**) for each of the SOM nodes. However, in the Southern Hemisphere for

instance maximum temperature extremes seem to be more sensitive to SST variability than minimum temperature extremes.

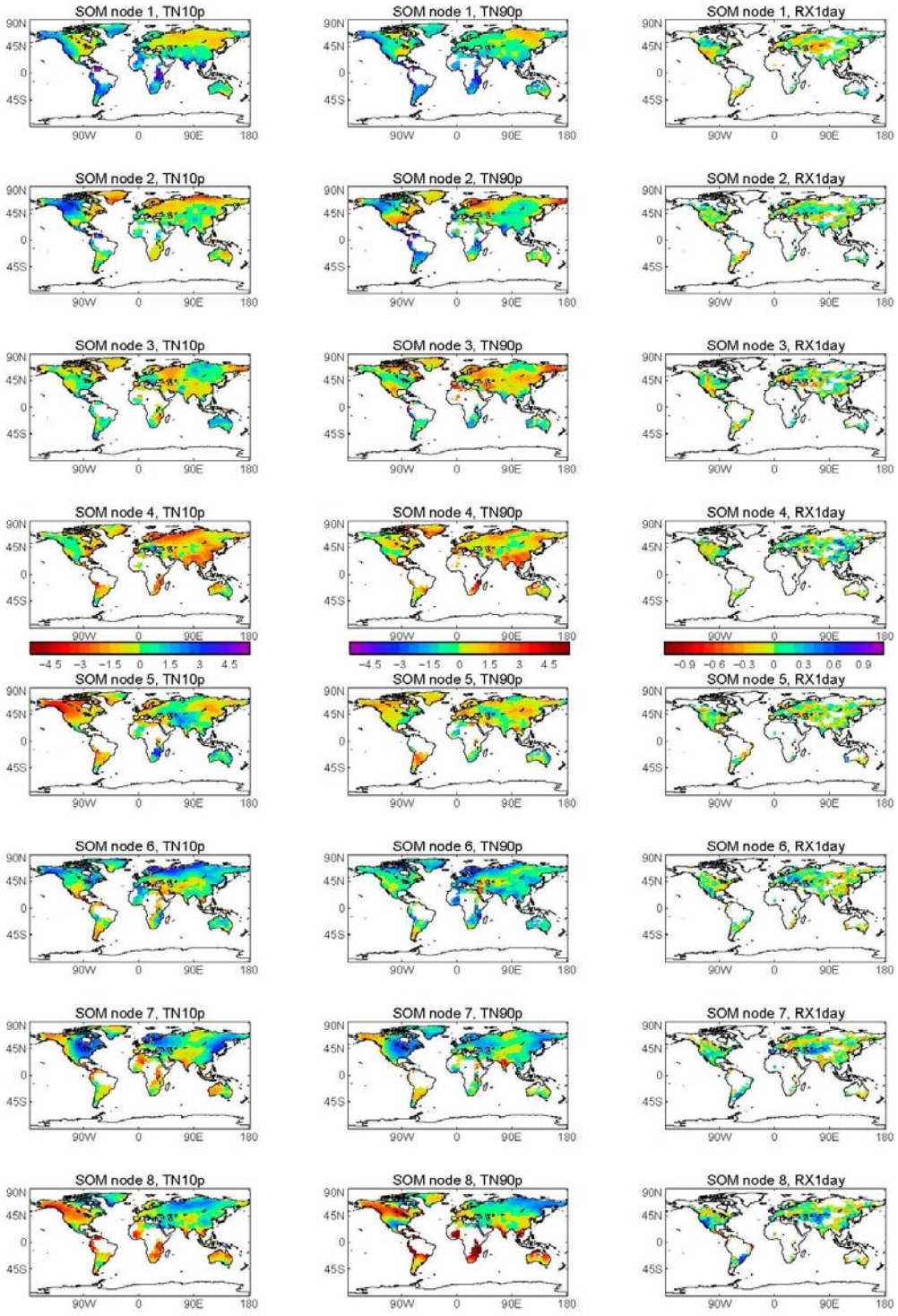

Fig. 4.3: Anomalies are shown for cool nights (TN10p), warm nights (TN90p) and maximum 1-day precipitation totals (RX1day) during each SOM node. Units for temperature indices are percentage deviations from expected value *i.e.* 10% and precipitation extremes are shown as the normalized deviations (by removing the mean and dividing by the standard deviation) from average. Colours are shown such that green/blues (yellow/red) reflect a cooler/wetter (warmer/drier) climate.

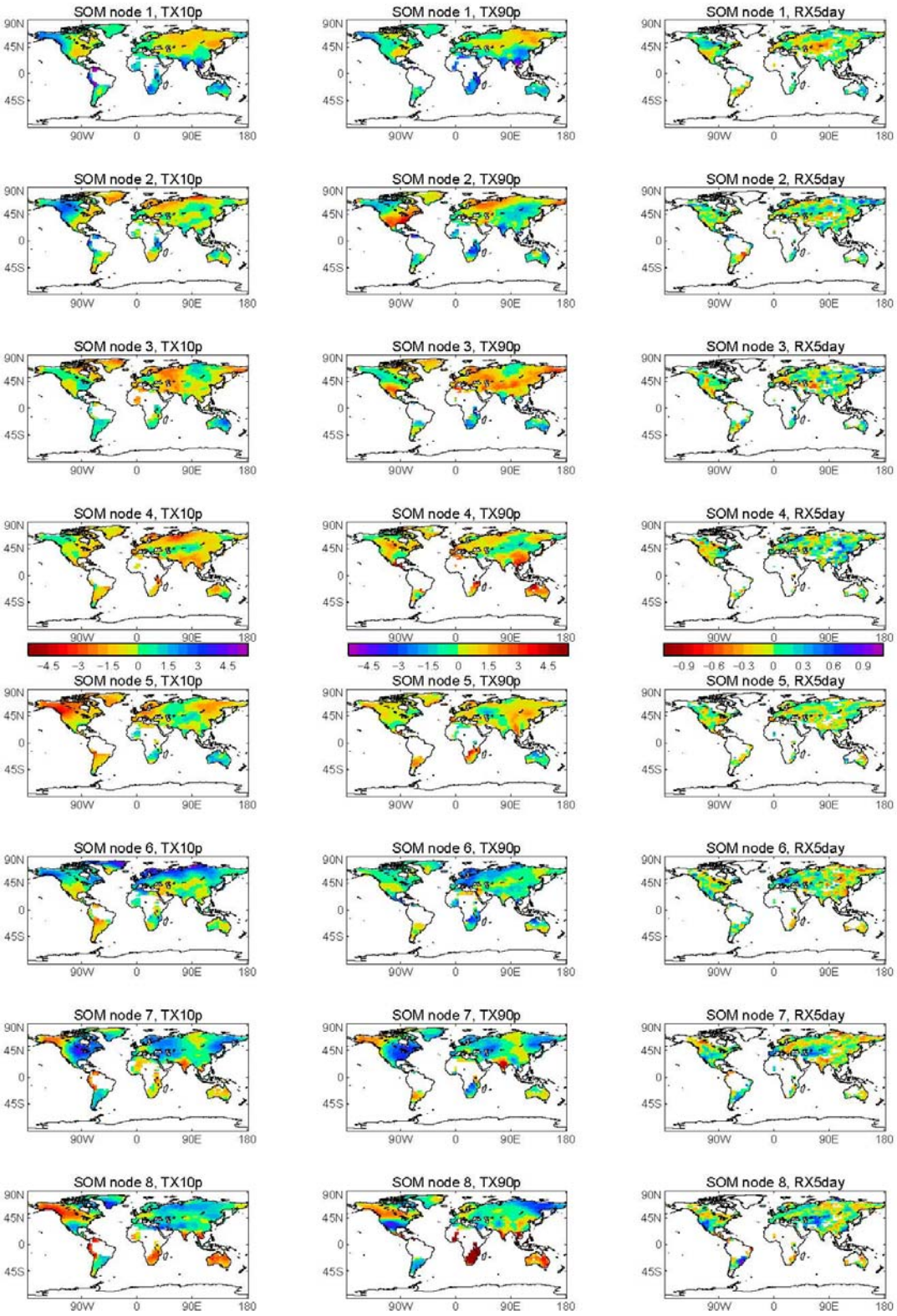

Fig. 4.4: As **Fig. 4.3** but for cool days (TX10p), warm days (TX90p) and maximum consecutive 5-day precipitation totals (RX5day).

A question would be whether any of these differences seen between the nodes are statistically significant. To answer this, the data from every node were compared with the data from every other node. Because each node occurs somewhere between 24 and 40 times (see **Fig. 4.1**) this gives reasonable sample sizes for comparison. Values at each grid box of a given node were compared with the values of the same gridbox from every other node using a Kolmogorov-Smirnoff (K-S) test. This can determine whether two samples are likely to come from the same overall distribution. The null hypothesis that the two samples come from the same distribution was tested at the 5% level. The results indicate that there are large areas where different nodes give statistically significantly different results. **Fig. 4.5** shows the results when comparing node 1 with node 8 and node 3 with node 6. Statistically significant differences are apparent in how maximum and minimum temperature and precipitation extremes respond to node 1 (strong La Niña) compared to node 8 (strong El Niño). For minimum temperature extremes the most significant differences are seen in North America, northern Russia, India, southern South America, southern Africa and Australia (for warm nighttime temperatures). These regions also show a similar response for maximum temperature extremes apart from South America where the differences between node 1 and node 8 are not significant. Most of the USA and Mexico and parts of Russia have significantly warmer maximum temperature extremes during strong La Niña events than strong El Niño events but the opposite is true for most of Canada, Australia, south-east Asia, India and southern Africa. In addition, the warmest minimum and maximum temperatures in Siberia and Australia appear to have a stronger response to varying SSTs than the coldest minimum and maximum temperatures. These results agree well with the results of *Kenyon and Hegerl* (2008). For precipitation, results show significantly wetter 5-day precipitation events during strong El Niño events compared to strong La Niña events in southern Brazil, south-western United States, central Asia and eastern China with an opposite signature in southern Canada and north-eastern Russia (**Fig. 4.5**). Maximum 1-day rainfall (RX1day) shows almost exactly the same response (not shown).

Fig. 4.5 also shows that it is not just the opposite phases of ENSO that produce significantly different results. The most marked results indicate that both the warm and cold tails of maximum and minimum temperature are significantly warmer during node 3 than node 6 in Scandinavia and north-western Russia. For the warmest maximum temperatures this signature is also seen in southern USA and Central America. South-

eastern Australia shows the opposite signature *i.e*. warm maximum temperature extremes are significantly cooler during node 3 than node 6. **Fig. 4.2** indicates that node 3 has been much more prevalent in the last few decades than node 6 and given that much of the differing response between these nodes has been seen in high-latitude regions this could indicate that other external influences in addition to SST variability are dominating in these regions. There are few regions where precipitation extremes indicate significant opposite responses between these two nodes.

It is clear from the results so far that maximum and minimum temperature and precipitation extremes can have significant opposite responses in certain regions to the modulation of global SSTs. A test of global climate models would be whether they could adequately simulate the significantly different responses of climate extremes to SST variability. Because Australia is the main region of interest for this thesis and because maximum temperature extremes particularly in this region are sensitive to differing SST SOM nodes (**Fig. 4.5**), the next section details several experiments using the CAM3 global climate model (*Collins et al*. 2006a) aimed at determining how well climate model simulations can reproduce this observed temperature extreme response.

4.4 Data and methods (model)

To test whether a state of the art climate model can adequately reproduce the maximum temperature extreme response across Australia to varying SSTA, output from the CAM3 model (*Collins et al.* 2006a) was analysed. CAM3 is the atmosphere-only version of the NCAR Community Climate System Model version 3 (CCSM3; *Collins et al.* 2006b). The resolution of the version of CAM3 used was 128 by 64 horizontal grids cells (approximately 2.8 degree resolution) and 26 levels in the vertical. The land surface (*e.g.* vegetation, lakes, glaciers etc.) is represented by the NCAR Community Land Model (*Bonan et al.* 2002; *Oleson et al.* 2004) and a thermodynamic sea ice model is also incorporated. Convection is parameterized following *Zhang and McFarlane* (1995) (for deep convection) and *Hack* (1994) (for shallow convection). The data sets used for specifying monthly SST and sea-ice concentration are described in *Hurrell et al.* (2008). Several studies have already assessed the model's performance and suitability for

applications in climate research relevant to this study and these are discussed in more detail in **Section 4.6**.

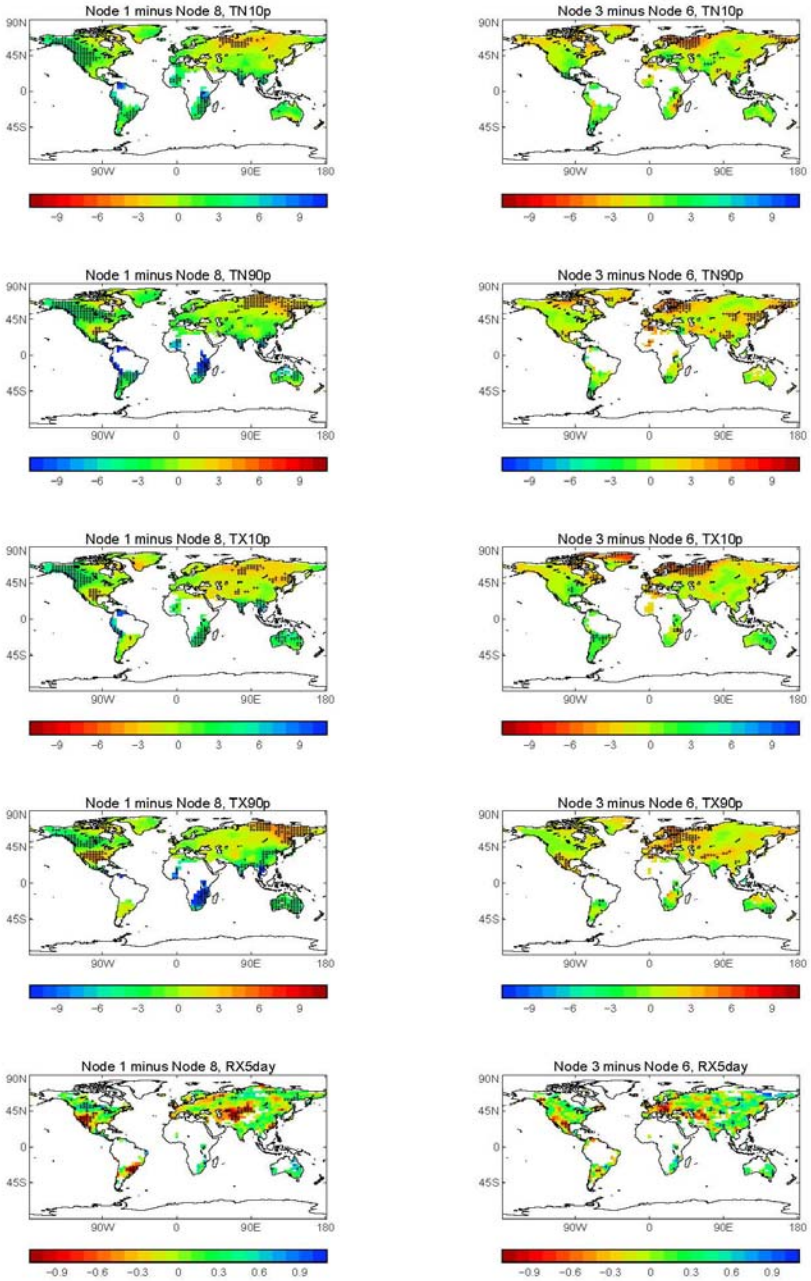

Fig. 4.5: Differences in the value of each index from this study (except RX1day) between SOM node 1 and node 8 (left hand side) and node 3 and node 6 (right hand side). Colour bars are presented such that green/blue (yellow/red) indicate that the node named first in the title is cooler/wetter (warmer/drier) than the node named second. Crosses indicate gridboxes where the difference between the nodes shown is significant at the 5% level using a Kolmogorov-Smirnoff (K-S) test.

Two experiments were analysed which used the CCSM3 model in atmosphere-only mode forced with observed SSTs. Each experiment differed only in initial conditions. The first experiment was a five member ensemble forced by global observed time-varying SSTs from 1950 to 2000. The second experiment used had the same model set-up except it also included volcanic, greenhouse gas, aerosol and solar forcings. Using model runs forced with observed SSTs acts as a test of the model's atmospheric processes. A direct comparison can also be made between the model and observations as the model should be able to reproduce observed SST nodes (**Fig. 4.1**) quite well. However, the model is forced with a different observed dataset (*Hurrell et al.* 2008) so there were some slight differences in the resulting SSTA patterns which were again categorized using SOMs for each model run. Anomalies were calculated with respect to the model climatology from each run.

4.5 Model results

Fig. 4.6 shows the SOM nodes produced from one run of each of the two experiments between 1951 and 1999. The SST data used to force the model are of a lower resolution than the HadISST1 observations but even so they represent the main modulation of ENSO that is seen in **Fig. 4.1**. However there are some unusual features particularly in the southern oceans indicating strong gradients of above average warming or cooling depending on the node (**Fig. 4.6**) and interestingly these features are not exactly the same between the model runs even though the same input SST data were used. The resulting SOM patterns using identical input data should not necessarily be expected to be identical as the SOM algorithm initially makes a first-guess map using the user-defined number of nodes before the SOM is "trained" by the input data. Thus there are likely to be some small random differences between patterns even when the same input data are used.

Because of the significantly different response of maximum temperature extremes in Australia to opposite phases of ENSO (**Fig. 4.5**), the two different model experiments described above were tested for their response to these different phases to determine whether (a) the model could adequately simulate the observed response and (b) whether the response was different/improved with the inclusion of the climate of the 20th century forcing. To do this, observations of maximum seasonal daily maximum temperature (TXx from **Chapter 2**) across Australia were compared with the output from both model

experiments. **Fig 4.7a** shows that the hottest day in a season across Australia is about 1°C warmer during a strong El Niño event than during a strong La Niña event and this difference is statistically significant at the 5% level across most regions of the country. However, neither of the model experiments (see **Fig. 4.7b** and **Fig. 4.7c**) is able to capture this response even when the "climate of the 20th century" atmospheric forcing is included (**Fig. 4.7c**). In fact, in central Australia (and in northern Australia for the all-forcings run) the model gets a significantly different response to the opposite phases of ENSO which is completely the opposite of the observed response *i.e.* there is a significant warming of TXx of about 0.3°C to 0.6°C during strong La Niña events compared to strong El Niño events. So it appears that neither experiment is able to adequately capture this observed response over Australia. This would imply that one or more atmospheric processes and/or interactions within the model are not properly simulated. Indeed, *Collins et al.* (2006a) suggest that there are several systematic biases which may reduce the fidelity of the simulations including underestimation of tropical variability, errors in tropical oceanic surface fluxes and underestimation of implied ocean heat transport in the Southern Hemisphere. Obviously some of these biases only relate to the fully coupled version of the model. However, this may have serious implications for the use of climate models for impacts assessments and is discussed in more detail in the next section.

4.6 Discussion and conclusions

It is important to note that the results shown here have been calculated on detrended datasets. This is important as the results only reflect the response of temperature and precipitation extremes to natural SST variability. The response is generally larger in the temperature extremes when the observed warming globally is retained (not shown). This is particularly true of minimum temperature extremes and particularly true for the response between the interim nodes. This would imply that minimum temperature extremes are driven more by external forces (*e.g.* greenhouse gas forcing) than natural climate variability. Several studies have already shown that minimum temperatures respond more to anthropogenic forcing than maximum temperatures *e.g.* *Kiktev et al.* (2007), *Hegerl et al.* (2004).

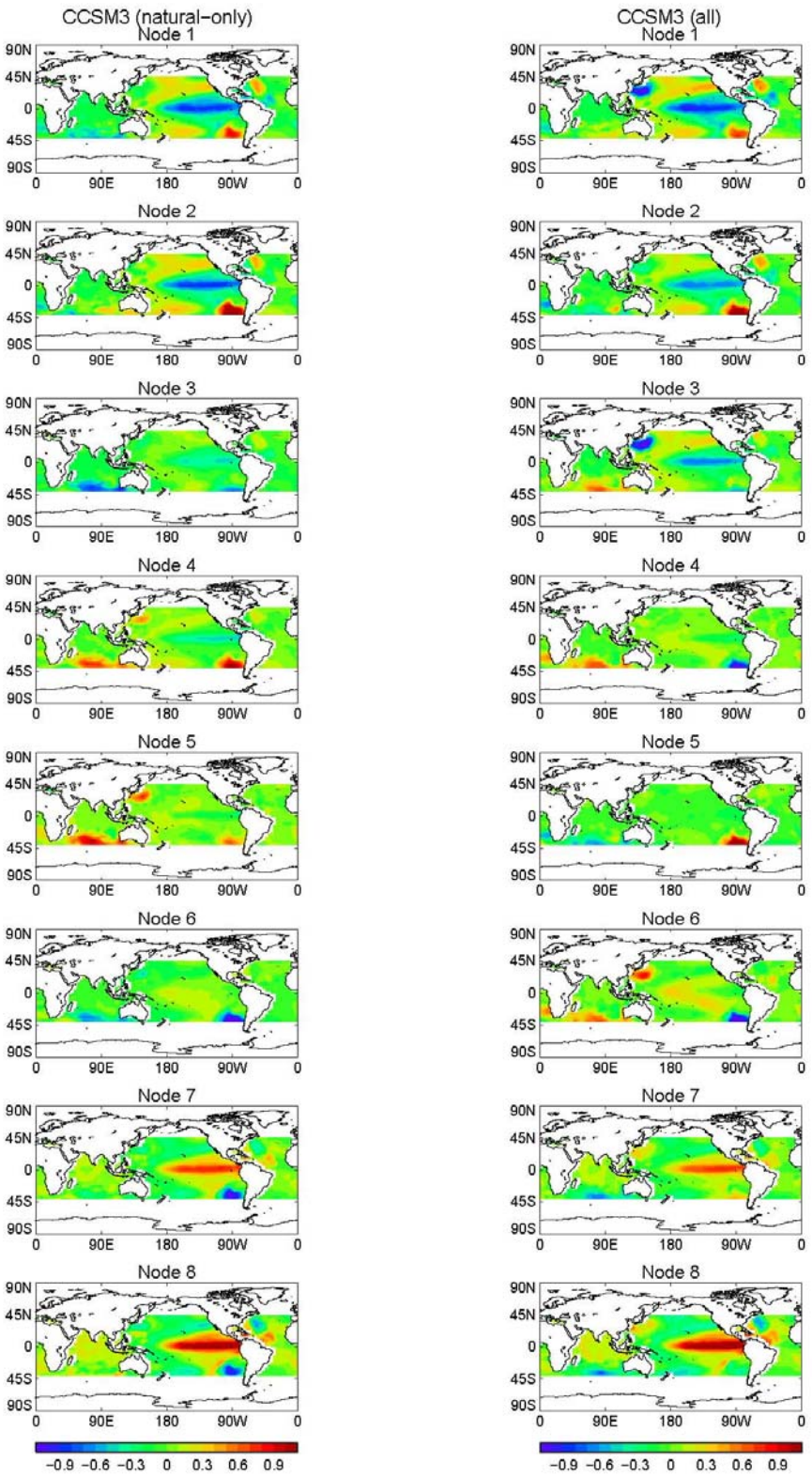

Fig. 4.6: Seasonal SSTA patterns ('nodes') derived using SOMs from (LHS) observed SST-forced CAM3 runs and (RHS) observed SST-forced CAM3 run including "climate of the 20th century" atmospheric forcing.

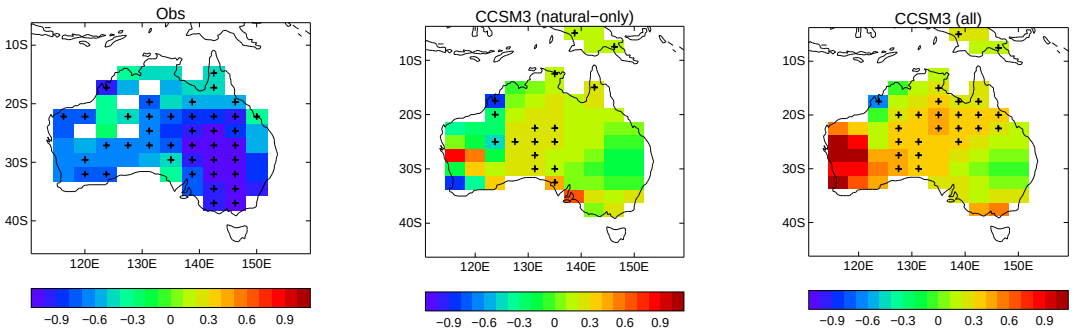

Fig. 4.7: The difference (°C) between the response of TXx to strong La Niña (node 1) minus strong El Niño (node 8) for (a) observations, (b) SST-forced CAM3 run and (c) SST-forced CAM3 run including "climate of the 20th century" atmospheric forcing. Greens/blues (yellows/reds) indicate that the response is cooler (warmer) during La Niña. Crosses indicate where the response is statistically significantly different (at the 5% level using a K-S test).

However, precipitation extremes in this study show a stronger response when observed trends are removed. Results show very significantly wetter 1 and 5-day precipitation events during strong El Niño events compared to strong La Niña events in southern Brazil, south-western United States and to the east of the Caspian Sea. *Leloup et al.* (2007b) recently showed that none of the global climate models in the IPCC-AR4/CMIP3 database were sufficiently good at capturing all aspects of the extent, location and timing of ENSO events. This would be a concern for our confidence in the future projections of global temperature and precipitation extremes given their dependence on the modulation of SSTA (**Fig. 4.3** and **Fig. 4.4**). Perhaps then, one might assume that an improved response could be gained by using global climate model simulations driven by observed sea surface temperatures. However, in this study, two experiments from a global climate model, CAM3, forced with observed SSTs showed that the model was unable to reproduce the significantly different response of maximum temperature extremes in Australia to different phases of global SST variability and indeed showed almost completely the opposite response to that which has been observed. This would certainly imply a problem with the atmospheric processes in the model and many previous studies have outlined potential problems and biases in CAM3 (*e.g.* *Collins et al.* 2006a; *Zhang* 2004; *Boville et al.* 2006; *Hurrell et al.* 2006; *Hack et al.* 2006; *Zhang and Wang* 2006) in relation to the simulation of the hydrological cycle, clouds and dynamics. Over Australia, *Marshall et al.* (2009) summarised some of these biases in regard to the Australian summer monsoon showing

that CAM3 had a much too early onset date to the monsoon season and so had excessive precipitation to that which has been observed between September and December. Indeed, we compared total column integrated precipitable water measurements over Australia using the experiments described here with a comparable measure from the ISCCP dataset described in **Section D**. Using the period, 1985 to 1999 (when both the model output and observations were available), it was found that the model was much too "wet" over most of the country (not shown). In addition, while the response in the model to strong El Niño versus strong La Niña events appeared to have the right sign *i.e.* it was wetter during La Niña than El Niño, the magnitude of the differences were much larger in the model compared to the observations and there was a very different spatial pattern between the two (see **Fig. 4.8**). **Fig. 4.8a** shows the difference in the precipitation response over Australia between node 1 (strong La Niña) and node 8 (strong El Niño) from **Fig. 4.6** using the SST-forced climate of the 20th century experiment from CAM3. **Fig. 4.8b** shows the equivalent response between these two nodes in the observations using the patterns from **Fig. 4.1** and corresponding observations from the ISCCP dataset. The differences are likely to reflect the poor simulation of convective processes and clouds in the atmospheric physics of the model and this might have serious implications for the conclusions reached by more recent studies of the Australian climate using CAM3 which showed that significant changes in rainfall over the south-west of the country were forced by changes in sea surface temperatures (*Ummenhofer et al.* 2008). Studies have shown that CAM3 severely underestimates the response of shortwave cloud radiative forcing to El Niño (*e.g. Li and Zhang* 2008). *Zhang and Bretherton* (2008) show that the physical mechanism of low cloud feedback in CAM3 is through the interaction of a suite of parameterized processes rather than from any single process caused by the larger amount of in-cloud liquid water in stratus clouds from convective sources, and longer lifetimes of these clouds in a warmer climate through their interaction with boundary layer turbulence. Cloud–climate feedback plays a significant role in determining the sensitivity of global climate models (*e.g. Zhang* 2004). The Fourth Assessment Report of the Intergovernmental Panel on Climate Change (*IPCC* 2007) concluded that cloud feedbacks remain the largest source of uncertainty in determining the sensitivity of current climate models. Even when a cloud resolving model is embedded within CAM3 (*Marchand et al.* 2009), a number of shortfalls in the model are revealed including excessive cloud coverage at all altitudes over many convectively active regions and a lack of low-level cloud over all subtropical oceanic basins. Since maximum temperatures are highly correlated with rainfall over Australia (*Nicholls et al*. 1997; *Power*

et al. 1998; **Chapter 2**), it is likely that this poor simulation of convection will be reflected in the poor simulation of maximum temperature responses to large scale climate variability as shown in **Fig. 4.7**.

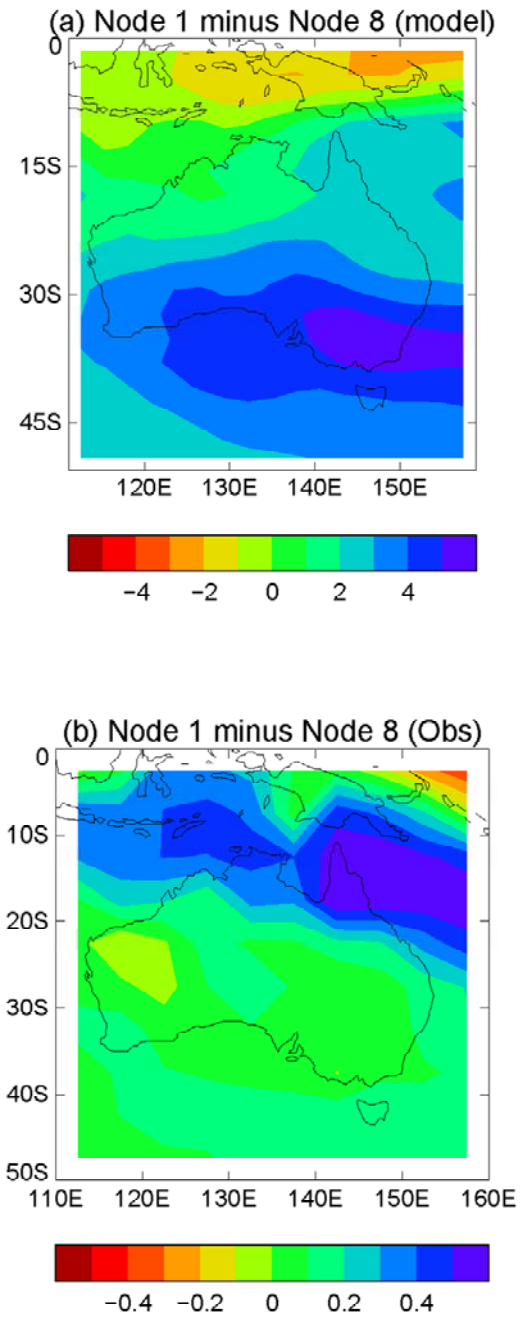

Fig. 4.8: Differences in precipitable water measurements during strong La Niña events (node 1) and strong El Niño events (node 8) for (a) the SST-forced CAM3 run including "climate of the 20th century" atmospheric forcing and (b) observations from the ISCCP dataset (described in **Section D**).

The inability of the model to reproduce this observed response may have serious implications for the use of global climate models for impacts assessments. However in this case only the output from one climate model was used. Other studies indicate that analysing multiple climate model simulations may improve the representativeness of modelled extremes as it could reduce systematic biases that may be present in any one model (*e.g.* *Kiktev et al.* 2007). For this reason, in the next section we determine whether the use of multiple runs from multiple climate models can improve the simulation of observed trends in temperature and precipitation extremes over Australia.

E. Top models

The previous chapters have dealt with how climate extremes have changed in Australia over the observational period and discussed some of the processes which are driving these changes. While it is necessary to understand how the climate has changed in the past to have confidence in what may happen in the future, projections of future climate change generally require access to the output of state of the art regional and/or global climate models.

Climate models have been shown to adequately reproduce changes in mean climate over Australia (*e.g.* *Alexander and Arblaster* 2008; see **Fig. E.1**) but little work has been done on assessing how well climate models are able to reproduce observed changes in climate extremes. Globally, it has been shown that state of the art global models can reproduce the trends in temperature extremes with some skill but the models are less skillful at representing trends in precipitation extremes (*e.g.* *Kiktev et al.* 2003; *Kiktev et al.* 2007; *Kharin et al.* 2007). In addition, recently there has been debate about how best to compare model output (which represents an area mean) with observations of extremes (which are point estimates) (*e.g.* *Chen and Knutson* 2008). Over Australia, *Perkins et al.* (2007) ranked multiple global models by their ability to reproduce the probability distribution functions of observed daily temperature. In doing so, they were able to assign weights associated with the skill of each climate model in reproducing observed temperature. Other work at CSIRO, is also attempting to weight models according to their ability to reproduce past climate. The idea is that we should have more confidence in models that are able to reproduce current climate and therefore should apply more weight to the output of those models in the future.

However, in the last chapter it was shown that at least one GCM was unable to reproduce some important responses of observed extreme temperatures over Australia to varying SSTs. But could the representation of climate extremes be improved if multiple simulations from multiple climate models were used? This might remove some biases that are present in individual models or model runs. In the next chapter we test whether this is the case in addition to determining whether there is an anthropogenic component to observed trends in extremes over Australia.

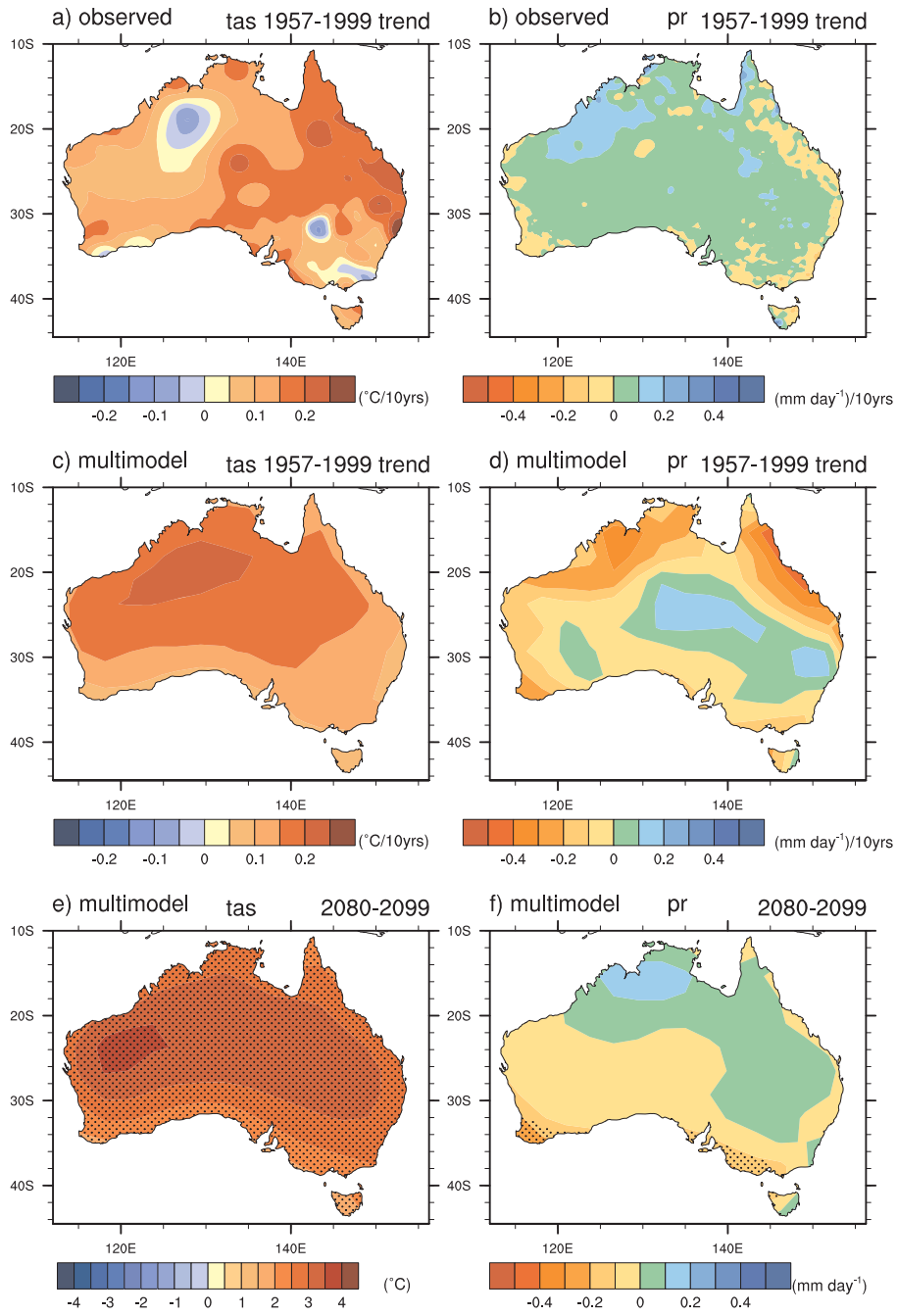

Fig. E.1: Changes in mean temperature (left column) and precipitation (right column) for observations (a, b), 20thC simulations (c, d) and 21stC SRES A1B simulations (e, f). Twentieth Century changes are represented as trends from 1957-1999, while future changes are differences of 2080-2099 minus 1980-1999. Stippling in e) and f) indicates regions where the multimodel mean change divided by the intermodel standard deviation of the change is greater than one, a measure of the consistency of the multimodel response. The same nine models for which extremes indices were analysed are used to form the multimodel means here. Figure produced by Julie Arblaster and presented in *Alexander and Arblaster* (2008).

5. Validating state of the art climate models with observations of climate extremes over Australia

Summary

Multiple simulations from nine global coupled climate models were assessed for their ability to reproduce observed trends in a set of indices representing temperature and precipitation extremes over Australia. Observed trends over the 1957 to 1999 period were compared with individual and multi-modelled trends calculated over the same period. When averaged across Australia the magnitude of trends and interannual variability of temperature extremes were well simulated by most models particularly for the warm nights index. The majority of models also reproduced the correct sign of trend for precipitation extremes although there was much more variation between the individual model runs. A bootstrapping technique was used to calculate uncertainty estimates and also to verify that most model runs produce plausible trends when averaged over Australia. Although very few showed significant skill at reproducing the observed spatial pattern of trends, a pattern correlation measure showed that spatial noise could not be ruled out as dominating these patterns. Two of the models with output from different forcings showed that the observed trends over Australia for one of the temperature indices was consistent with an anthropogenic response but was inconsistent with natural-only forcings.

5.1 Introduction

Extremes research is particularly important for Australia given the vulnerability of its unique flora, fauna and ecosystems to even slight variations in climate (*Fitzharris et al.* 2007). A previous body of work concluded that significant changes in temperature and precipitation extremes have already occurred across the country during the 20th century (*e.g. Hennessy et al.* 1999; *Plummer et al.* 1999; *Collins et al.* 2000; *Haylock and Nicholls* 2000; *Trewin* 2001; *Alexander et al.* 2007; *Gallant et al.* 2007). Regional studies across the Asia-Pacific area (*e.g. Manton et al.* 2001; *Griffiths et al.* 2005; *Salinger and Griffiths* 2001) have shown statistically significant increases in occurrences of warm nights and/or hot days and decreases in occurrences of cool days and cold nights over the past few decades. Over the past century there has been a significant decrease in the frequency and intensity of extreme precipitation events in southwest Western Australia and a significant increase in the proportion of total precipitation from extreme events in eastern Australia (*Haylock and Nicholls* 2000; *Li et al.* 2005). While these studies have been thorough, they have focused on the analysis of extremes at station locations. This makes it difficult to compare observations objectively with simulations from climate models that output data on spatial grids. Some work has suggested increases in hot days and hot spells and decreases in cold days and cold spells in the future (*CSIRO* 2001) and an increase in extreme precipitation (*Groisman et al.* 2005) but relatively little has been published about how extremes might change in the future over Australia or indeed if climate models are able to adequately reproduce the observed trends in extremes (thus increasing our confidence in future projections).

Global studies comparing observed and modelled trends in climate extremes have shown reasonably good agreement with temperature trends but poor agreement (or multi-model disagreement) with observed precipitation patterns or trends (*e.g. Kiktev et al.* 2007; *Kharin et al.* 2007). *Kiktev et al.* (2007) also comment that a 'super ensemble' from multiple climate models appears to perform better than any individual ensemble member or model particularly when there is some skill in the contributing ensemble members. *Kiktev et al.* (2003) found that only the inclusion of human-induced forcings in a climate model could account for observed changes in global temperature extremes. Robust anthropogenic changes have been detected globally in indices of extremely warm nights, although with

some indications that the model overestimates the observed warming (*Christidis et al.* 2005). However other recent studies show that the *regional responses* of observed trends in temperature and precipitation extremes can also largely be driven by large scale processes which might not be adequately simulated in global climate models (*Scaife et al.* 2008; *Meehl et al.* 2004; *Meehl et al.* 2005). On regional scales (*e.g. Sillmann and Roekner* 2008 for Europe; *Meehl and Tebaldi* 2004 and *Meehl et al.* 2007b for U.S.A.) while the modelled trends have been shown to capture observed trends reasonably accurately, the results are somewhat dependent on the extreme under consideration. To date no such analysis has been carried out for Australia.

Recent initiatives by the World Climate Research Programme (WCRP) in preparation for the Intergovernmental Panel on Climate Change (IPCC) Fourth Assessment Report (AR4) in 2007 have now made it possible to compare multiple model simulations with high quality observations of extremes. At the request of the Joint Scientific Committee (JSC)/CLIVAR Working Group on Coupled Models, coupled modelling groups worldwide submitted a standard set of 'extremes indices' to the WCRP's Coupled Model Intercomparison Project phase 3 (CMIP3) multi-model dataset at the Program for Climate Model Diagnosis and Intercomparison (PCMDI) in California (hereafter named the CMIP3 archive). Ten extremes indices, calculated from daily data and based on the definitions of *Frich et al.* (2002), were submitted with 5 temperature-based indices (*e.g.* heat wave duration, occurrence of frosts) and 5 precipitation-based indices (*e.g.* heavy precipitation events, consecutive dry days). *Tebaldi et al.* (2006) was the first study to analyse these indices for both the historical and future simulations on global and hemispheric scales. Global averages of the temperature-based indices were found to be dominated by trends in the Northern Hemisphere, with Southern Hemisphere trends much weaker. This is intuitively explained by the presence of a relatively stable ocean in close proximity to all Southern Hemisphere landmasses, sheltering them from extreme cold and warm air masses. However in that study observational datasets with which to compare the multi-model output were not yet adequate or available so an assessment of the models ability to reproduce observed trends in extremes was not possible. The Commission for Climatology (CCl)/CLIVAR/JCOMM Expert Team on Climate Change Detection and Indices (ETCCDI),initiated a project aimed at addressing gaps in observed data availability and analysis in previous global studies (*e.g. Frich et al.* 2002). Following on from this, *Alexander et al.* (2006) updated and extended the analysis of *Frich et al.* (2002) using the

best global observations available, gridding a total of 27 indices onto a regular latitude-longitude grid from 1951 to 2003.

The CMIP3 multimodel dataset and recently available high quality gridded datasets provide us with an unprecedented opportunity to directly compare observed trends in extremes over Australia with multiple model simulated trends and to compare projections in these extremes, both across models and across scenarios. In this study we first briefly discuss how the extremes indices are calculated from the observed and modelled datasets followed by a comparison of the models with observations and the future projections for the selected temperature and precipitation extremes across Australia.

5.2 Extremes indices data

The indices used in this study, based on the definitions of *Frich et al.* (2002), are given in **Table 5.1**. Nine annual indices are analysed (four derived from daily maximum and/or minimum temperature and five from daily precipitation) providing one value per gridbox per year per index. The indices chosen contain more robust statistical properties than could be expected from the analysis of more infrequent events and allow global climate models the possibility to adequately simulate these events. Therefore some of the indices may be viewed as not particularly 'extreme' but given their statistical properties and their availability in the CMIP3 archive we chose to use these definitions as the basis for our analysis. Note that the *Frich et al.* (2002) indices also contained a definition for *growing season length* which is not analysed here since it has little meaning in the Australian climate (*Collins et al.* 2000). *Frost days* are included in the analysis but note that this index is only meaningful for parts of southern Australia. There are some differences between the observed and model definitions for three of the indices (see **Table 5.1**) and the potential effects these could have on the results are discussed in Section 3.3. Model indices for which climatologies were required were calculated relative to each model's own climatology thus partially removing inherent model bias.

Table 5.1: Extremes indices used in this study.

Index name	**Index definitions**		**units**
	Model (Frich *et al.* 2002)	**Obs** (Alexander *et al.* 2006)	
Warm nights (**TN90)**	Percent of time Tmin > 1961-1990 90th percentile of daily minimum temperature	Percentile calculation differs from model definition in that the bootstrapping technique of *Zhang et al.* (2005) is used	%
Frost days (**FD)**	Total number of days with absolute minimum temperature < 0°C	As model	days
Extreme temperature range (**ETR)**	Difference between the highest and lowest temperature observation in a calendar year	As model	°C
Heat wave duration (**HWDI)**	Maximum period > 5 consecutive days with Tmax > 5°C above the 1961-1990 daily Tmax normal	Known as *warm spell duration index* (WSDI) – maximum period > 5 consecutive days with Tmax > 1961-1990 90th percentile of daily maximum temperature. Percentiles are calculated using the bootstrapping technique of *Zhang et al.* (2005) and spells can continue across calendar years	days
Heavy precipitation days (**R10)**	Number of days with precipitation ≥ 10mm	As model	days
Maximum 5-day precipitation (**R5D)**	Maximum precipitation total over a 5-day period	As model	mm
Simple daily intensity (**SDII)**	Ratio of annual total precipitation to number of days ≥ 1mm	As model	mmd^{-1}
Consecutive dry days (**CDD)**	Maximum number of consecutive days < 1mm	Basic definition is the same as model except a spell can continue across calendar years	days
Very heavy precipitation contribution (**R95T)**	Fraction of annual total precipitation due to events exceeding the 1961-1990 95th percentile	As model	%

5.2.1 Observations

High quality daily maximum and minimum temperature (*Trewin* 2001) and daily precipitation (*Haylock and Nicholls* 2000) data composed the Australian contribution to the *Alexander et al.* (2006) study which created 2.5 degrees of latitude by 3.75 degrees of longitude gridded datasets (HadEX) of observed extremes indices for the globe (data available from www.hadobs.org). Extremes indices were first calculated for each station

and then were transformed to the grid. For this study we extract from this dataset those grid boxes which cover the Australian continent for each extremes index from **Table 5.1**. *Alexander et al.* (2006) used a distance weighting method which required that at least 3 stations be within a pre-defined search radius from the centre of a gridbox in order for an extreme to be calculated for that gridbox. Because Australia is large but sparsely populated, high quality observations tend to be lacking in more remote areas. This means that for some of the indices (especially the precipitation indices which have small decorrelation length scales) there is little or no coverage in inland or northern areas. Other indices such as *warm nights* however, provide almost complete observational coverage over the country.

5.2.2 Model data

Extremes indices from nine models were available for inclusion in the IPCC 4th Assessment Report (AR4), as analysed by *Tebaldi et al.* (2006) and presented in the AR4 by *Meehl et al.* (2007a). As noted above, each modelling group calculated the indices based on the definitions of *Frich et al.* (2002) and submitted them to the CMIP3 archive at PCMDI (http://www-pcmdi.llnl.gov). There were four models from the U.S.A. (CCSM3, PCM, GFDL-CM2.0, GFDL-CM2.1), three from Japan (MIROC3.2 (medres), MIROC3.2 (hires), MRI-CGCM2.3.2), one from France (CNRM-CM3) and one from Russia (INM-CM3.0). Simulations of the climate of the twentieth century (20C3M) and three Special Report on Emissions Scenarios (SRES) experiments, B1 (low-range emissions), A1B (mid-range) and A2 (high-range) were available for most models. Each model varies in resolution but the indices from each of the nine models were interpolated here onto the observational grid *i.e*. 2.5 degrees of latitude by 3.75 degrees of longitude so that a direct comparison between the observations and the model simulations could be made. Multiple ensemble members were submitted for five out of the nine models (PCM, GFDL-CM2.0, GFDL-CM2.1, MIROC3.2 (medres) and MRI-CGCM2.3.2) with single runs available for the remaining four. In total there were 22 20C3M simulations from the nine models. The multi-model mean values shown here are the average across all ensemble members and then across all models.

5.3 Comparison between observed and modelled extremes over Australia

5.3.1 Spatial and temporal comparison

To compare the modelled and observed indices, trends were calculated between 1957 and 1999 for each grid box with available data. The start date was chosen as the date from when high quality temperature station data are available for Australia (*Trewin* 2001) and the end date chosen was based on when some of the model groups end their climate of the 20th Century simulations. Trends in precipitation indices were also calculated over this period for consistency even though high quality station data exist prior to this (*Haylock and Nicholls* 2000). In all cases, for computational efficiency, trends are calculated using ordinary least squares (OLS) regression and trend significance is calculated at the 5% level using a non-parametric Mann-Kendall test (*Mann* 1945; *Kendall* 1975). However because OLS is sensitive to outliers in the series which may be present in the extremes indices analysed here, an additional non-parametric iterative technique to estimate trends and significance (*Wang and Swail* 2001) was used in some cases to test the robustness of OLS results. This method makes no assumptions about the distribution of the timeseries residuals and is robust to the effect of outliers in the series. Our general conclusions however remain unchanged irrespective of the trend calculation method used. Trends were only calculated in gridboxes if at least 40 out of the 43 years of observed indices data were available. In order that comparable analyses could be performed, the model output was masked by the regions where observed trend data exist. In addition to trend calculation, timeseries were produced for each of the nine indices using areally averaged data from the masked gridboxes in order to compare the magnitude and interannual variability of observed and simulated extremes and these are plotted in **Fig. 5.1**. Average trends for Australia and associated significance for the observations and multi-model ensemble are given in **Table 5.2** while ensemble mean trends for each individual model are given in **Table 5.3**. To assess the uncertainty in the multi-modelled trends we provide confidence intervals using a bootstrapping technique described in section 3.2 with all 22 model runs. The associated uncertainties in the trend calculation method for the observations are given as two standard errors using Restricted Maximum Likelihood (*Trenberth et al.* 2007). Spatial trend patterns of the observations and multi-model simulations for each of the nine extremes indices were compared for temperature (**Fig. 5.2**) and precipitation (**Fig. 5.3**).

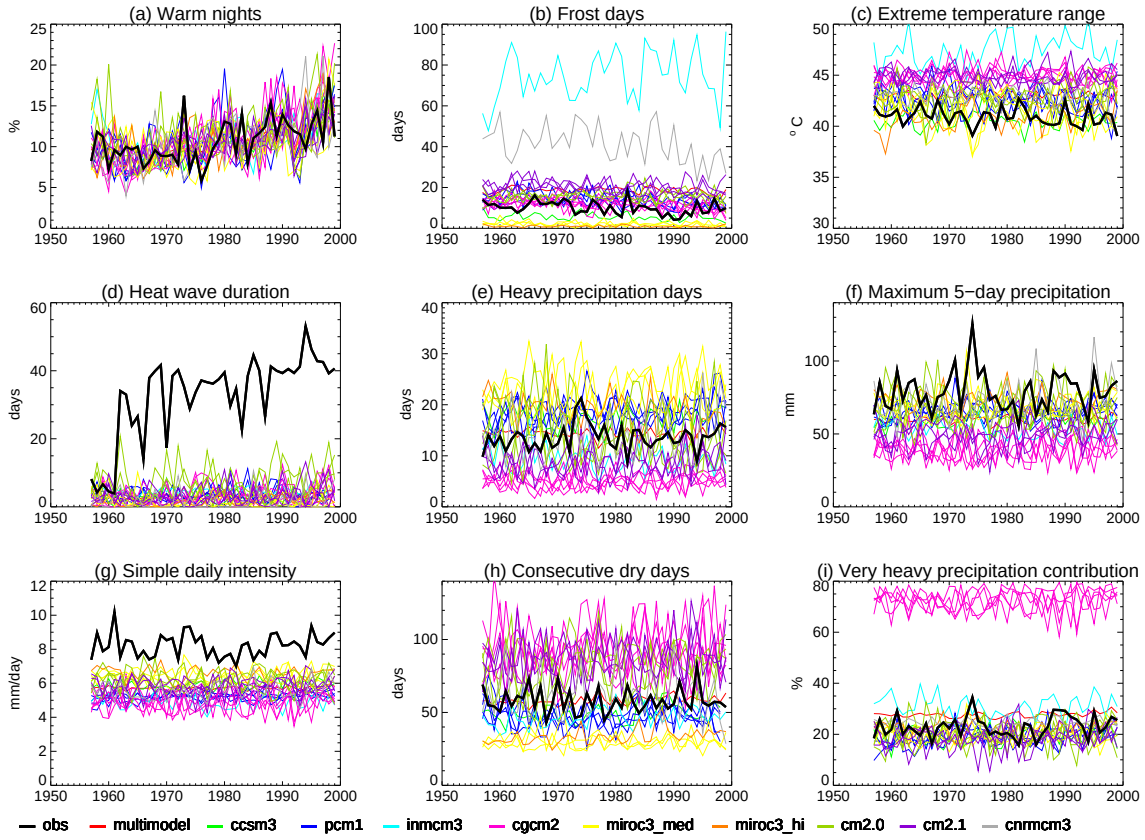

Fig. 5.1: Observed (black line) and modelled (coloured lines) timeseries of areally averaged extremes indices (*Frich et al.* 2002) from 1957 - 1999 using grid boxes in Australia with observed data.

5.3.1.1 Temperature extremes

Trends for the observed and multi-model simulation are given in **Table 5.2** while the mean trends associated with each of the nine models used in this study are given in **Table 5.3**. **Table 5.2** shows that all of the observed trends for the four temperature indices are statistically significant and commensurate with warming. The majority of models (**Table 5.3**) and individual model runs (not shown) obtain the correct sign of trend for each temperature index when averaged across Australia. In fact 21 of the 22 model runs exhibit a statistically significant increasing trend in *warm nights*; the multi-model trend of 1.15 %/decade is comparable to the observed trend of 1.11 %/decade. Eight of the nine models and the multi-model ensemble produce trends in *frost days* of the same sign as the observed trends. Five of the nine models agree with the observations that *extreme*

temperature range is decreasing on average and seven of the nine models show increases in *heat wave duration* in agreement with observed trends. However the confidence intervals for these two indices compared to *warm nights* and *frost days* shows that there is much greater uncertainty both within and between models as to the sign of the trend over the latter part of the 20th century. Moreover, while the sign of the temperature trends was correct, the magnitude was generally very different from the observed values. *Warm nights* is the only index where the confidence intervals in all models and multi-model ensemble do not overlap with zero indicating that there is very good consensus between the models that the recent trend in *warm nights* over Australia is positive. The lowest resolution model, INM-CM3.0, is the only model which shows an increase in *frost days* while the highest resolution model, MIROC3 (hires), is the only model which shows a significant increase in *extreme temperature range* contrary to the observed trends. **Fig. 5.1** shows that the models also do reasonably well at simulating the amount and variability of the temperature extremes. This is particularly true of *warm nights.* However, no one model is consistently "best" across all indices. **Fig. 5.1a** and **Table 5.3** show that all models are particularly good at simulating the amount, interannual variability and trend of this index. It is obvious however that some models are overestimating the actual value of some of the temperature extremes indices. In addition to showing increased trends in *frost days*, INM-CM3.0 (**Table 5.3**) also vastly overestimates the amount of frosts that actually occur in Australia (**Fig. 5.1b**) and this is likely to contribute to its overestimate of *extreme temperature range* (**Fig. 5.1c**). Similarly the CNRM-CM3 model also overestimates the amount of *frost days* and *extreme temperature range* although it gets the right sign of trend for both indices. It is likely that the vastly different amounts of and magnitude of trends in *heat wave duration* (**Fig. 5.1d; Table 5.2 & 5.3**) are related to the different definitions of this index between the model and observations (see **Table 5.1**) and this is discussed in Section 3.3. In addition, this index definition is statistically 'volatile' (*e.g.* it contains a lot of zeros and no values between one and five) and is particularly sensitive to missing data. Given that we allow a maximum of three years of missing data before a trend can be calculated and most of the missing data occurs early on in the record, this creates an apparent inhomogeneity in the observations near the beginning of the timeseries (**Fig. 5.1d**). It is likely therefore that the observed trend in *heat wave duration* is smaller than indicated in **Table 5.2**. However, we chose not to remove this index from the study since the models may be doing a reasonable job using this definition and future changes in this index may have pronounced societal impacts.

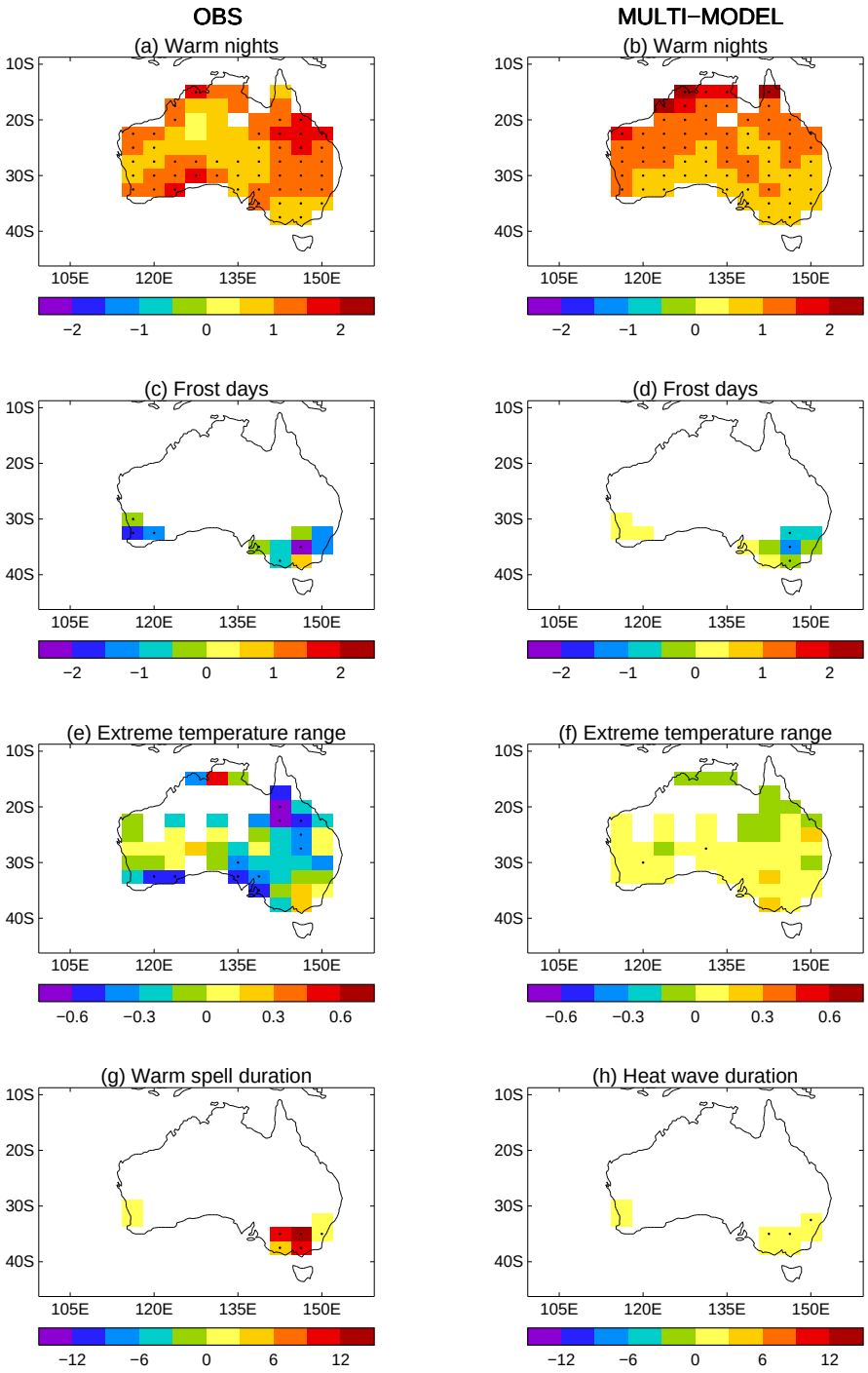

Fig. 5.2: Observed and modelled decadal trends calculated between 1957 and 1999 for extreme temperature indices (**Table 5.1**) for Australia. Model data are masked with gridboxes which have observed data. Stippling indicates trend significance at the 5% level. Units as **Table 5.1** (per decade).

The spatial trend patterns of temperature extremes across Australia for the observations and multi-model are shown in **Fig. 5.2**. As noted the majority of models are able to simulate the observed sign of change in the temperature indices when averaged across Australia however it is clear from **Fig. 5.2** that the regional trend pattern is less well captured by the models. While there is an observed increase in *warm nights* across northwest Australia over the period studied, it is small and mostly non-significant (**Fig. 5.2a**). Indeed if the analysis is extended beyond 1999 we see a non-significant decrease in *warm nights* over the northwest region (*Alexander et al.* 2006) and this is consistent with a cooling in mean minimum temperatures annually but particularly associated with a decrease in minimum temperatures between December and August (*Alexander et al.* 2007). **Fig. 5.2a** and **Fig. 5.2b** show the multi-model ensemble is overestimating the observed trends in *warm nights* in the northwest and underestimating the observed trends in this index in southern and eastern Australia. In fact there is very good consensus between the individual models (not shown) that the number of *warm nights* has increased significantly in the northwest region. However while there is some discrepancy in the magnitude and significance between the observed and multi-modelled trends, it is noteworthy that the sign of the simulated trend in *warm nights* is consistent with the sign of the observed trend in every grid box across Australia. While there are few regions of Australia where *frost days* can be measured (**Fig. 5.2c**) almost all grid boxes show a consistent and mostly significant decline. **Fig. 5.2d** indicates that the multi-model gets the opposite sign of trend to the observations in southwest Western Australia and southwestern Victoria and there can be large differences between the observed and modelled response. Overall the multi-model ensemble underestimates the observed trend in *frost days* but the ensemble average from several individual models such as PCM and MRI-CGCM2.3.2 get very good approximations to the observed trend (-0.92 and -0.91 days/decade respectively). The observed pattern of trends for *extreme temperature range* (**Fig. 5.2e**) is generally not well simulated (**Fig. 5.2f**). The trend pattern for *heat wave duration* is well simulated by the multi-model although trend magnitudes are underestimated in each grid box (**Fig. 5.2g - Fig. 5.2h**), which as noted previously is likely to be related to definitional differences between the observations and models.

Table 5.2: Observed and simulated decadal OLS trends calculated over the 1957 to 1999 period for each index (**Table 5.1**) averaged across Australia using grid boxes containing observations from **Fig. 5.2** and **Fig. 5.3**. Bold signifies trends are significant at 5% level. Observations are shown with 2 standard errors in the trend calculation estimated using Restricted Maximum Likelihood (*Trenberth et al.* 2007) while 10 to 90% confidence intervals are shown in brackets for the model data by randomly resampling the bootstrapped trends (see text) across all model runs to give an estimate of the uncertainty from using multiple model simulations. Units as **Table 5.1** (per decade).

Index	Obs	Multi-model
Warm nights	**1.11** ±0.06	**1.15** (0.48/1.87)
Frost days	**-0.89** ±0.07	-0.19 (-1.46/0.22)
Extreme temperature range	**-0.19** ±0.02	0.04 (-0.29/0.31)
Heat wave duration	**7.05** ±0.33	**0.26** (-0.31/0.91)
Heavy precipitation days	0.28 ±0.06	-0.06 (-0.79/0.89)
Maximum 5-day precipitation	0.42 ±0.33	0.32 (-1.37/2.32)
Simple daily intensity	0.04 ±0.02	0.02 (-0.06/0.13)
Consecutive dry days	-0.14 ±0.15	**1.04** (-1.68/3.36)
Very heavy precipitation contribution	0.60 ±0.12	0.26 (-0.58/1.23)

5.3.1.2 Precipitation extremes

There are no significant observed trends in the precipitation indices (**Table 5.2**) which is perhaps not surprising given that precipitation extremes are less well spatially correlated and have larger interannual variability over Australia than temperature extremes (*Alexander et al.* 2007). Also it is clear from **Table 5.2 and 5.3** that there are generally wider confidence intervals on the simulated trends of precipitation extremes than temperature extremes. Precipitation is also not expected to respond as consistently or strongly to greenhouse gas forcing as temperature (*e.g. Lambert et al.* 2005). Given this we might expect that it would be more difficult for climate models to capture observed trends in precipitation extremes. So it is encouraging to find that the majority of models match the sign of the observed trend for four out of the five precipitation extremes. The exception is *consecutive dry days* where six out of the nine models and the multi-model average have trends of opposite sign to the observations. **Fig. 5.1** shows that the models also do reasonably well at simulating the amount and variability of the precipitation extremes (**Fig.**

5.1e - Fig. 5.1i). In addition all models underestimate the actual amount of observed *simple daily intensity* (**Fig. 5.1g**) while most models also underestimate *maximum 5-day precipitation* amount (**Fig. 5.1f**) although the trend averaged over Australia from the multiple model simulations is close to the observed trend (**Table 5.2**). The observations of *heavy precipitation days* (**Fig. 5.1e**), *consecutive dry days* (**Fig. 5.1h**) and *very heavy precipitation contribution* (**Fig. 5.1i**) sit within the range of values for those indices simulated by the full suite of models. However, the model ranges are very large.

The spatial trend maps for the precipitation indices (**Fig. 5.3**) show that it is mostly southern Australia that is covered by observational data. Even so, this corresponds to the region with the highest population density so it provides useful information for future studies which relate climate extremes to impacts. Unfortunately no observed high quality precipitation extremes data exist for the northwest region although current work at the Bureau of Meteorology is aimed at addressing this (personal communication Dörte Jakob). This is unfortunate since there is a well established increase in mean precipitation in this region since the 1950s, the reason for which is still being debated in current literature (*e.g.* *Rotstayn et al.* 2007; *Shi et al.* 2008; *Wardle and Smith* 2004). However most models (not shown) simulate a decrease in *heavy precipitation days* over the northwest region but a mixed response regarding the trends in *simple daily intensity*.

As noted the multi-modelled trend for *maximum 5-day precipitation* is close to the observed trend but **Fig. 5.3c – Fig. 5.3d** show there are some differences in regional response. The multi-modelled trend in *simple daily intensity* also fails to capture some of the strong spatial gradients shown in the observations *e.g.* Victoria in south-east Australia exhibits increasing trends in the western part of the state and decreasing trends in the east (**Fig. 5.3e**) whereas the multi-model shows uniform increases in precipitation intensity across the region (**Fig. 5.3f**). Observed trends in *consecutive dry days* (**Fig. 5.3g**) have not been as uniformly increasing as simulated trends might suggest (**Fig. 5.3h**), the overall trend across those parts of Australia with observed data shows that the simulated multi-model trend is significantly increasing (1.04%/decade) contrasting with the observed decreasing trend of -0.14%/decade (**Table 5.2**). Also, as with *heavy precipitation days*, it is the models INM-CM3.0, MIROC3.2 (hires) and GFDL-CM2.1 with statistically significant increases in *consecutive dry days* which are largely influencing this temporal trend (**Table 5.3**). Southwestern Western Australia has seen a significant and well documented decline

in precipitation since the mid-1970's (*IOCI* 2002) and this agrees with an increase in *consecutive dry days* in the region (**Fig. 5.3g**). However the observed increase is not as large or statistically significant as the models suggest (**Fig. 5.3h**). In general, the simulated and observed spatial distributions of trends of *very heavy precipitation contribution* (**Fig. 5.3i** and **Fig. 5.3j**) are not in good agreement. However given that precipitation is a much less spatially coherent variable than temperature and that precipitation extremes could depend on specific convection or storm events, models would be expected to have a more difficult time simulating patterns of precipitation extremes than temperature extremes. Given this fact it is quite impressive that the models capture some of the observed trends and trend patterns.

In the next section measures of trend uncertainty are estimated for observed and modelled temperature and precipitation extremes to provide objective comparison of the temporal and spatial similarity between observed and modelled trends.

5.3.2 Measuring trend uncertainty

For each index objective measures were calculated to assess the models' ability to reproduce 1) observed area averaged trends (temporal similarity) and 2) spatial patterns of observed trends (spatial similarity) over Australia. In each case a bootstrapping technique was employed to assess the uncertainty associated with the modelled trend estimates over Australia during the latter part of the 20th century. To assess the uncertainty associated with temporal similarity, the modelled timeseries from **Fig. 5.1** are used to calculate the lines of best fit and associated residuals for each index. Next, a moving block bootstrap resampling (following the method of *Wilks* 1997) was used to randomly resample the residuals in blocks of two years to maintain some of the temporal correlation in the timeseries. This procedure is performed 1000 times, adding the line of best fit back each time to the resampled residuals and recalculating the trend. Essentially this produces a distribution of probable or 'plausible' climate trends for Australia. The same bootstrapping method is followed independently for each of the model simulation index timeseries from **Fig. 5.1**. Probability distribution functions (PDFs) are then created using the 1000 bootstrapped trends for each index so that the observations and models can be compared. PDFs are centred on the original model trend and models with multiple simulations are

combined into one PDF and centred on the ensemble mean trend. **Fig. 5.4** shows the temporal similarity PDFs for each index.

Table 5.3: As **Table 5.2** but showing OLS trends and 10% and 90% confidence intervals for each model used in this study. For models where the ensemble mean is calculated from multiple simulations, the confidence intervals are calculated using all ensemble members.

Temperature extremes

	Warm nights	Frost days	Extreme temperature range	Heat wave duration
CCSM3	**1.41** (1.11/1.71)	-0.47 (-0.73/-0.18)	-0.02 (-0.16/0.12)	0.02 (-0.24/0.30)
PCM	**1.22** (0.60/1.91)	**-0.92** (-1.58/-0.01)	**-0.19** (-0.40/0.03)	-0.09 (-0.50/0.30)
INM-CM3.0	**0.81** (0.34/1.24)	2.44 (0.46/4.44)	0.31 (0.06/0.54)	0.10 (-0.09/0.27)
MRI-CGCM2.3.2	**1.71** (1.13/2.60)	**-0.91** (-1.33/-0.45)	0.02 (-0.18/0.23)	0.30 (-0.17/0.77)
MIROC3.2(med)	**0.78** (0.30/1.26)	**-0.19** (-0.38/-0.04)	**-0.22** (-0.55/0.08)	-0.18 (-0.52/0.17)
MIROC3.2 (hi)	**1.37** (0.96/1.78)	-0.04 (-0.12/0.03)	**0.48** (0.30/0.67)	**0.62** (0.41/0.81)
GFDL-CM2.1	**0.85** (0.33/1.31)	-0.07 (-0.52/0.42)	0.14 (-0.06/0.35)	**0.75** (0.11/1.51)
GFDL-CM2.0	**0.78** (0.50/1.08)	**-0.78** (-1.48/-0.10)	-0.02 (-0.17/0.13)	**0.39** (-0.06/0.83)
CNRM-CM3	**1.59** (1.16/2.01)	**-2.91** (-4.27/-1.62)	-0.17 (-0.32/-0.01)	0.37 (-0.07/0.83)

Precipitation extremes

	Heavy precipitation days	Maximum 5-day precipitation	Simple daily intensity	Consecutive dry days	Very heavy precipitation contribution
CCSM3	0.01 (0.33/0.36)	0.25 (-0.89/1.23)	0.06 (0.02/0.09)	1.20 (0.05/2.18)	0.15 (-0.41/0.63)
PCM	**0.51** (-0.03/1.43)	**1.31** (0.19/2.41)	**0.05** (-0.01/0.12)	-0.27 (-1.82/1.59)	**0.83** (0.30/1.45)
INM-CM3.0	-0.41 (-0.78/-0.03)	**-1.54** (-2.48/-0.63)	-0.04 (-0.11/0.02)	**1.65** (0.67/2.63)	-0.25 (-0.92/0.39)
MRI-CGCM2.3.2	0.08 (-0.32/0.48)	0.58 (-0.79/2.00)	**0.05** (-0.07/0.17)	0.64 (-2.79/5.02)	0.26 (-0.56/1.13)
MIROC3.2(med)	0.33 (-0.36/0.97)	0.31 (-1.41/2.70)	0.03 (-0.04/0.09)	-0.07 (-0.79/0.62)	0.15 (-0.53/0.86)
MIROC3.2 (hi)	**-1.07** (-1.52/-0.64)	-0.04 (-1.25/1.19)	-0.03 (-0.09/0.04)	**1.95** (1.12/2.80)	0.08 (-0.47/0.60)
GFDL-CM2.1	**-0.70** (-1.64/0.14)	-0.42 (-3.11/2.0)	-0.02 (-0.13/0.09)	**2.58** (-0.15/5.16)	0.04 (-0.98/1.07)
GFDL-CM2.0	0.25 (-0.16/0.68)	1.01 (-0.29/2.42)	0.05 (-0.03/0.13)	0.80 (-1.09/2.76)	0.51 (-0.25/1.34)
CNRM-CM3	0.89 (0.21/1.56)	2.95 (0.99/5.03)	0.07 (-0.01/0.16)	-1.18 (-3.53/1.11)	0.15 (-0.10/0.38)

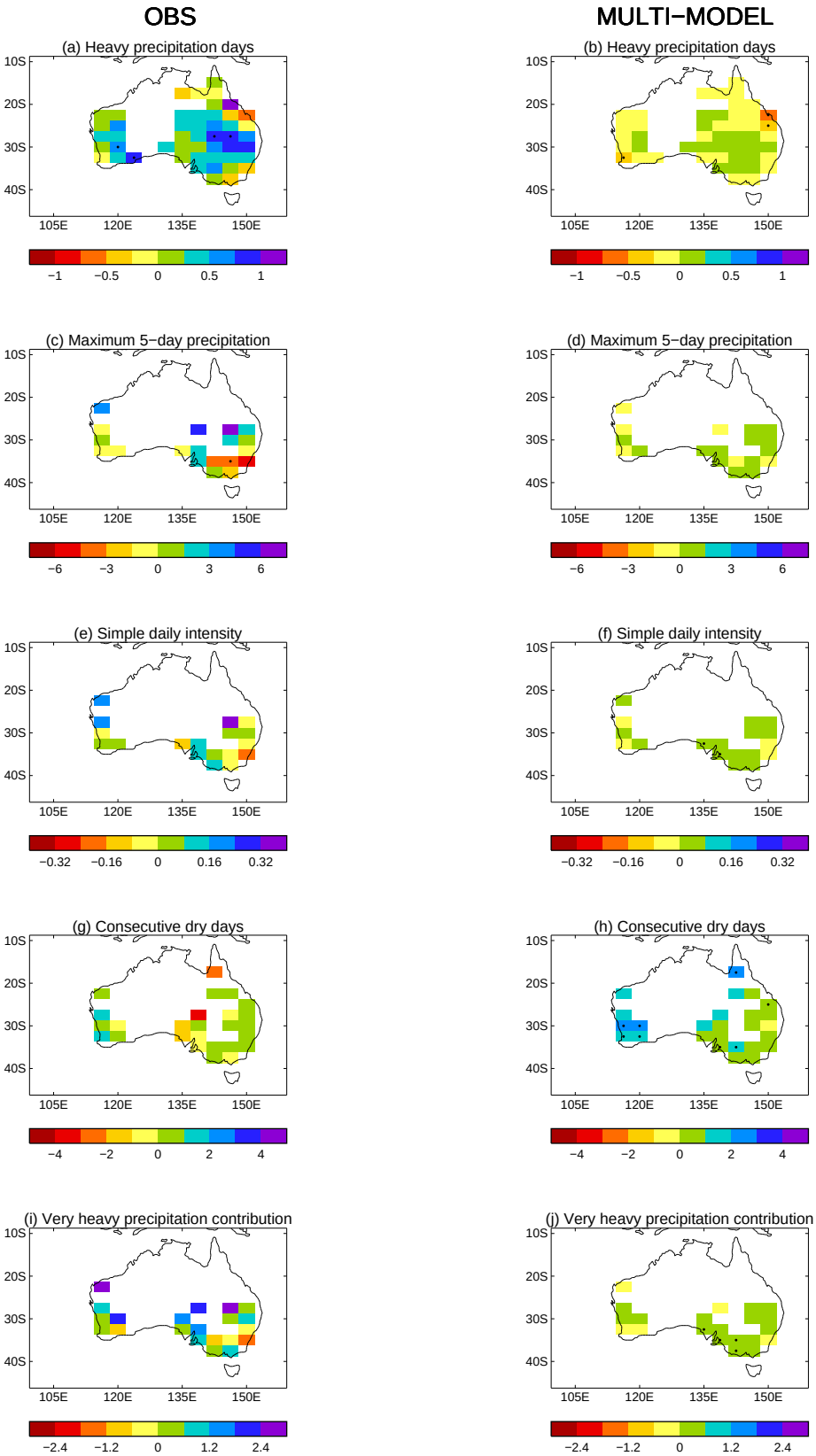

Fig. 5.3: As **Fig. 5.2** but for extreme precipitation indices (**Table 5.1**).

In most cases the spread of plausible model trends overlaps with the observations. *Heat wave duration* (**Fig. 5.4d**) is the only index where none of the PDFs of modelled trends overlap with the observed trends and this is probably associated with the different definitions used (see Section 3.3). For *warm nights* all models support a warming trend and indeed there is very little overlap of any of the model PDFs with zero (**Fig. 5.4a**). This is also supported by the positive confidence intervals on the multi-model trend estimates in **Table 5.2**. Trends in the other temperature indices, *frost days* (**Fig. 5.4b**) and *extreme temperature range* (**Fig. 5.4c**) are generally less well simulated than *warm nights* although for instance the median value of the PCM model PDF for both *frost days* and *extreme temperature range* is centred around the observed trend. Some other models do a relatively poor job of simulating these indices. For instance the highest resolution model, MIROC3.2 (hires), and the lowest resolution model, INM-CM3.0, exhibit little or no overlap with the observations for both *frost days* and *extreme temperature range*. Note also that two of the models, CNRM-CM3 and INM-CM3.0, have a much larger spread than the rest of the models for trends in frost days (**Fig. 5.4b**). Both these models have only one ensemble member, but the greater variance of the PDFs is most likely due to the larger interannual variability of simulated frost days by these models as shown in **Fig. 5.1b**.

To assess the uncertainty associated with spatial trend patterns *i.e*. in order to determine the spatial similarity of trends between the observations and models, the bootstrapping technique is again employed but this time timeseries are randomly resampled at each grid point to calculate trends. The bootstrapping is done synchronously at all locations to maintain the spatial coherence of the trends. This produces 1000 gridded fields of plausible spatial trend patterns for the observations and models to reflect the uncertainty associated with natural climate variability. From these 1000 fields a spatial correlation statistic is calculated as follows. We randomly select an observed trend pattern and independently a model trend pattern. The area-weighted uncentred spatial correlation between these two patterns is calculated (this measure is similar to the congruence statistic described by *Kiktev et al.* 2007). The procedure is repeated 2500 times and the resulting distribution of spatial correlation values is used to create PDFs for each model run and index. To ensure that the bootstrapped PDFs are measuring the uncertainty around the models' "best estimate", the medians were centred on the original values of pattern similarity between the observed and modelled trend fields. The resulting PDFs are shown in **Fig. 5.5**. In general the higher the median value of the PDF, the better a model is at simulating the observed

pattern of trends for that index. The null hypothesis that the models have no significant skill at reproducing observed spatial trend patterns is tested and rejected if a zero correlation falls within the lower 5% tail of the PDF. Very few of the individual model runs (**Fig. 5.5**) and none of the ensemble means (not shown) from the nine models showed significant skill at reproducing the observed pattern of trends over Australia for any of the indices. Indeed only the pattern of *maximum 5-day precipitation* (**Fig. 5.5f**) is significantly well simulated by one run from each of the PCM and MRI-CGCM2 models. However, interestingly the multi-model ensemble did show significant skill at simulating the trend pattern for *heavy precipitation days* even though there was no significant skill in any of the contributing models (not shown).

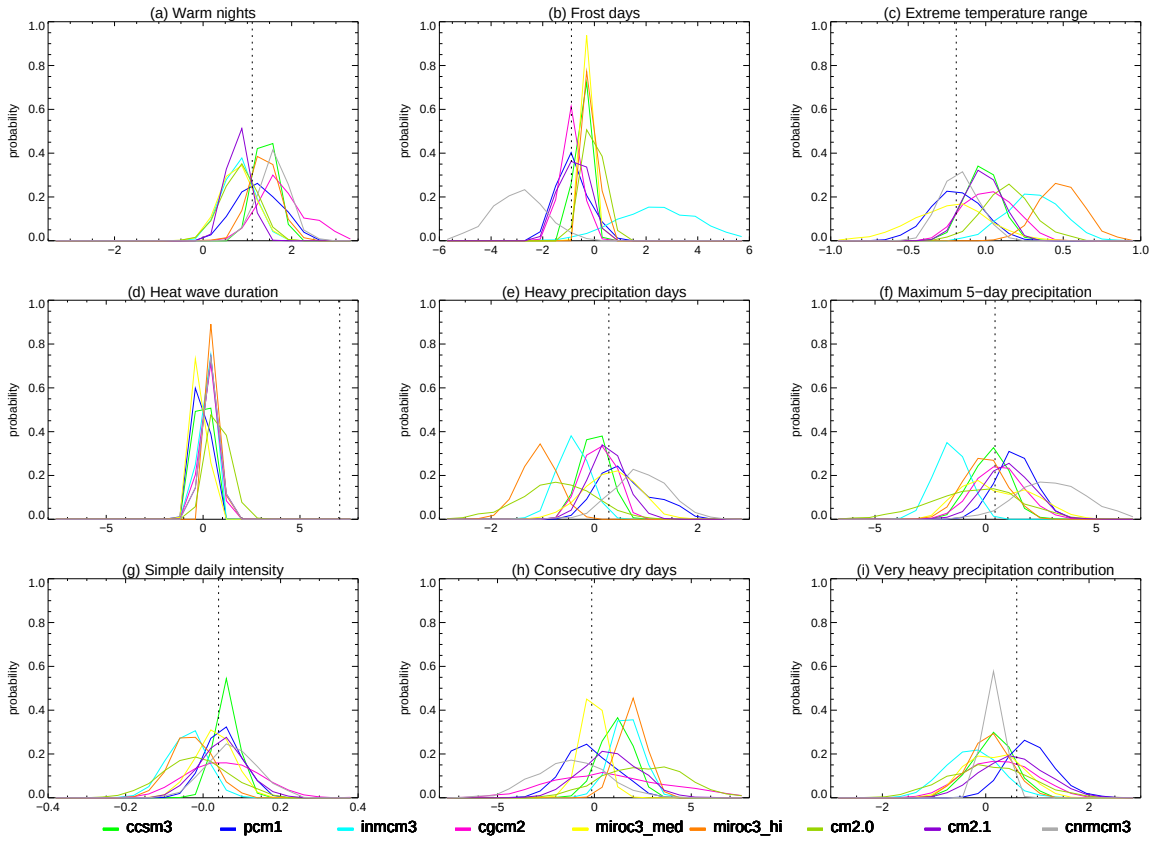

Fig. 5.4: PDFs of plausible areally averaged OLS trends (1957 to 1999) over Australia using each of the nine climate models in the CMIP3 archive. PDFs are calculated using the 'temporal similarity' bootstrapping technique described in the text. Where there are multiple ensemble members, PDFs are centred on the ensemble mean trend. The dashed lines represent where the observed trends lie over the same period. Units on x-axes as **Table 5.1** (per decade).

5.3.2.1 Natural versus anthropogenic forcings

Two out of the nine models (CCSM3 and PCM) are also available for analysis using natural-only and anthropogenic-only as well as all-forcings runs. The natural-only runs include only forcing from volcanic aerosols and solar variability while anthropogenic-only runs include only forcing from greenhouse gases, sulphate aerosols, black carbon aerosols (CCSM3 only) and stratospheric ozone depletion. The natural and anthropogenic forcings for PCM and CCSM3 are described in more detail in *Meehl et al.* (2004) and *Meehl et al.* (2006), respectively. Again the variability in the trends for each of the model runs is calculated using the bootstrapping procedure described above to measure both the temporal and spatial similarity between observed and modelled trends. The resulting PDFs of temporal similarity are again analysed to assess how well the different forcings runs simulate the observed trends during the latter part of the 20th century for each index. In most cases the PDFs for the different forcings runs overlapped with the observed trend indicating that in these cases at least there was no discernible difference in the models performance between the natural and all-forcings runs.

Fig. 5.6 shows the PDFs using the different forcings from both the PCM and CCSM3 models for *warm nights* and *very heavy precipitation contribution*. For *warm nights,* the PDFs for the natural-only forcings do not overlap (or overlap less than 5% in the case of the PCM model) with the observed trends. **Fig. 5.6a** and **Fig. 5.6b** show that it is only when anthropogenic forcings are included that the models are able to adequately simulate the observed trend in warm nights. The precipitation extremes do not show any significant differences between the natural, anthropogenic and all-forcings runs although **Fig. 5.6c** and **Fig. 5.6d** shows that there does appear to be some separation between the natural-only and all-forcings runs for *very heavy precipitation contribution*. However, when the PDFs of spatial similarity are compared with the observations there is no significant skill in either the PCM or CCSM3 model in reproducing the spatial trend pattern of any index irrespective of which forcings are used (not shown). **Fig. 5.6** however does highlight that the observed trends in at least one of the temperature extremes during the latter half of the 20th century when averaged over Australia is unlikely to have been produced from natural forcings alone.

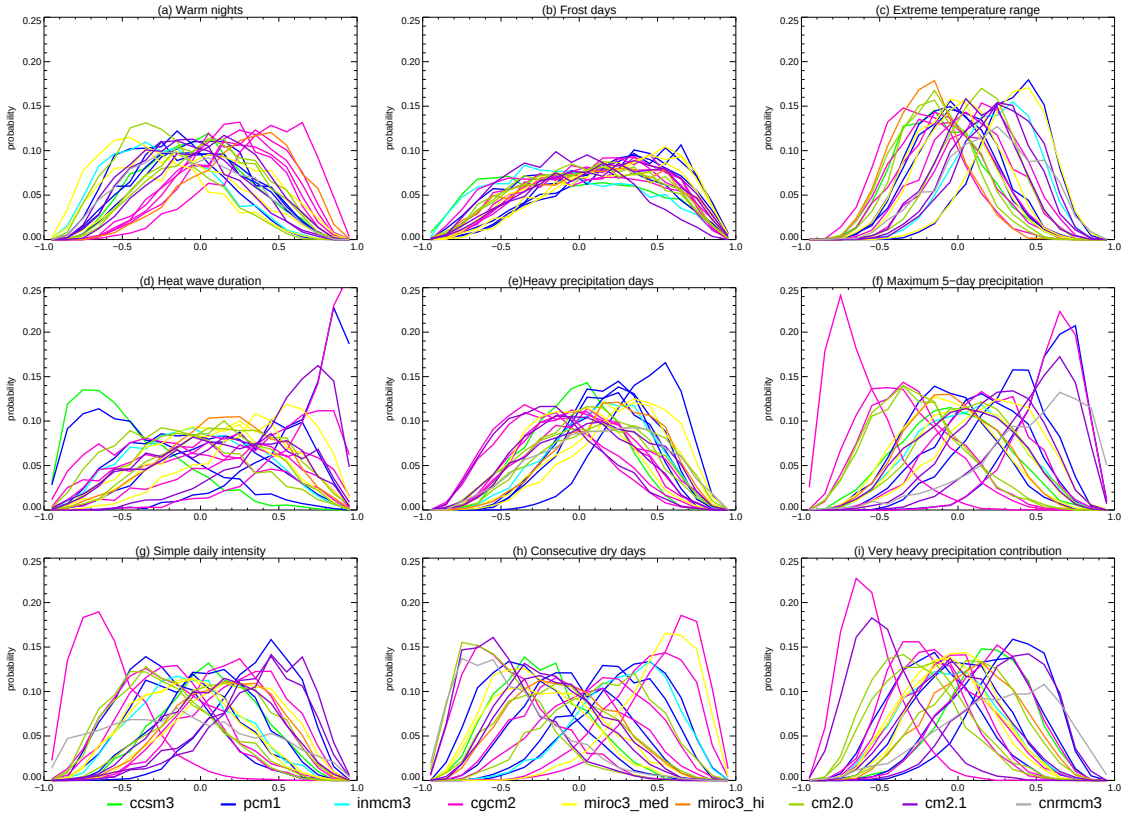

Fig. 5.5: PDFs of the spatial trend correlations (calculated over 1957 – 1999) between observations and 22 runs from the nine CMIP3 models available for this study over Australia. PDFs are calculated using the 'spatial similarity' bootstrapping technique described in the text. PDFs are not shown for CNRM-CM3 *frost days* and *heat wave duration* due to the masking applied to this model at source which reduces the number of gridboxes available for the spatial correlation calculation.

5.3.3 Differences in index definitions

Potential errors or differences amongst the model results could be due to potentially different computational techniques used by each group. Another complication in comparing the modelled and observed indices is that when the *Frich et al.* (2002) analysis was updated by *Alexander et al.* (2006) some of the definitions using the observed data had to be redefined since statistical inconsistencies were discovered when the original definition was used. Three of the indices in this study have been affected by this update (**Table 5.1**). In particular it was shown that the original simple threshold calculation for the 90th percentile of minimum temperatures (*warm nights*) contained an inhomogeneity at the start and end of the 1961-1990 base period (*Zhang et al.* 2005). Unfortunately these inconsistencies were discovered after the extremes indices had been submitted to the

CMIP3 archive so they could not be re-calculated without access to the original daily model data. To try and assess how these definitional differences would affect our comparison, we plotted trends in the original station data for Australia that were used in *Frich et al.* (2002) with trends in the same stations using the *Alexander et al.* (2006) definitions. **Fig. 5.7** shows the comparisons for *heat wave duration*, *warm nights* and *consecutive dry days* which are the indices where differences in definition occur. *Heat wave duration* has the lowest correlation between the two methods (0.17) and the biggest difference in the trends (the slope of 0.28 of the line of best fit using total least squares regression indicates that in general the trends in *heat wave duration* from *Frich et al.* (2002) are much larger than the *warm spell duration* defined by *Alexander et al*. (2006)). *Warm nights* are reasonably well spatially correlated between the two methods (0.45) but the slope of the line of best fit (0.5) indicates that using the *Frich et al.* (2002) definition produces trends about twice as large as those using the *Alexander et al.* (2006) definition when averaged across Australia. *Consecutive dry days* are highly spatially correlated between the two methods (0.77) and the slope of the line of best fit is close to 1.0 indicating that the trends are reasonably comparable between the *Frich et al.* (2002) and *Alexander et al.* (2006) definitions.

We judge that to adjust for these changes would not be feasible particularly since bias corrections would probably have to be calculated regionally and our station sample size is simply not large enough to do this rigorously. The best option would obviously be to recalculate these indices using the daily output from the nine climate models. However at present the model data are not available for us to do this so the differences discussed above should be considered when assessing the projected future changes in extremes presented in the next section.

5.4 Discussion

It is encouraging to note that the majority of global climate models (GCM) analysed in this study were able to generally simulate the sign of the observed trend and to some extent the associated variability of temperature and precipitation extremes when averaged over Australia. This gives us some confidence in the projected changes presented in *Alexander and Arblaster* 2008 which indicate substantial increases in w*arm nights* and *heat wave*

duration and decrease in *frost days* by the end of this century. However the results also showed that GCMs may not be adequately simulating the spatial trend patterns of extremes across the continent during the late 20th century.

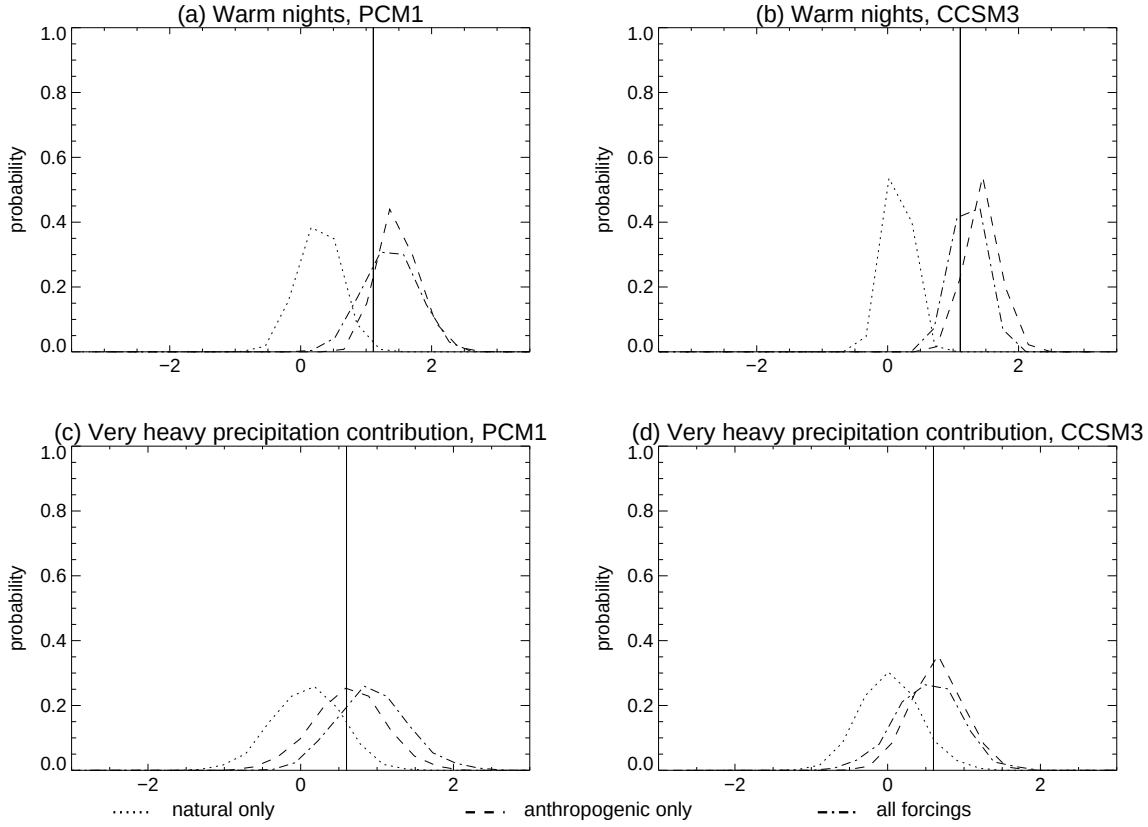

Fig. 5.6: PDFs of annual OLS trends (1957 to 1999) in *warm nights* for (a) PCM and (b) CCSM3 and *very heavy precipitation contribution* for (c) PCM and (d) CCSM3 over Australia for natural only (dotted), anthropogenic only (dashed) and all forcings (dotted dashed). PDFs are centred on the ensemble mean trend. The solid lines represent where the observed trends lie over the same period. PDFs are calculated using the 'temporal similarity' bootstrapping technique described in the text and trends are calculated as **Fig. 5.4**.

Previous studies (*e.g.* *Kiktev et al.* 2003; *Christidis et al.* 2005; *Kharin et al.* 2007) show that climate models are generally skilful at reproducing global trend patterns of temperature extremes but have little skill in reproducing trend patterns of precipitation extremes. *Hegerl et al.* (2004) also find that patterns of change in precipitation extremes are more heavily influenced by internal variability of the climate system when compared to temperature extremes. The detection of trends in climate variables is a signal to noise problem, and the noise associated with temperatures at regional scales is greater than at

larger continental or global scales (*Karoly and Wu* 2005). So perhaps we cannot expect regional trend patterns to be well simulated particularly if variations in extremes in Australia are driven primarily by local influences. Furthermore, the strong influence of ENSO on the Australian climate (as discussed in **Section D** and **Chapter 4**), which improves predictability on seasonal timescales, also enhances the variability, making attribution on climate scales more difficult.

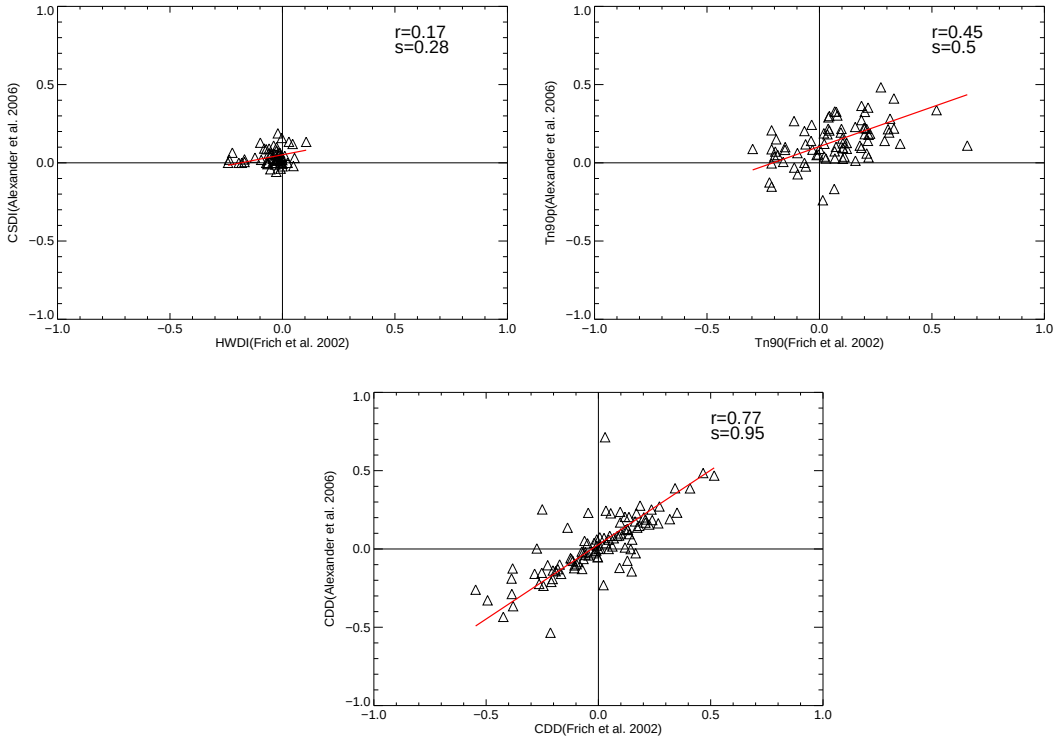

Fig. 5.7: The relationship between two different definitions of the *heat wave duration*, *warm nights* and *consecutive dry days* indices (**Table 5.1**) across Australia. Each triangle represents the annual trend calculated between 1957 and 1996 for each index at Australian stations. The red line represents the line of best fit using total least squares regression, s is the slope of the line and r is the spatial correlation between all points.

In this study, model resolution appears not to be critical. While the lowest resolution model, INM-CM3.0, gets the wrong sign of trend of all the precipitation indices and two temperature indices, the highest resolution model, MIROC3 (hires), also does not fare well for four of the five precipitation indices and one of the temperature indices. *Perkins et al.* (2007) find that it is possible to discriminate between models in their ability to simulate daily temperature and precipitation distributions over Australia, but the findings here

suggest that no one model is particularly good or bad at reproducing the observed trends or spatial patterns in the extremes of the two variables. In addition *Chen and Knutson* (2008) suggest that the way in which the observed precipitation indices are gridded prohibits a fair comparison between models and observations.

Given that changes in climate extremes will have much larger societal and ecological impacts than mean change (*Easterling et al.* 2000) we need to be confident in our ability to simulate future changes in extremes if we are to adequately assess their impacts. This study shows that while we can have some confidence in a general sense when assessing simulated extremes from coupled climate models over Australia, uncertainties in the patterns of future projections need to be considered when assessing changes on regional scales.

5.5 Conclusions

In this study objective measures have been used to analyse the ability of an ensemble of multiple global climate models to simulate observed trends in climate extremes over Australia and to assess projected changes in these extremes at the end of the 21st Century. In general the models capture the sign of observed trends in both temperature and precipitation extremes but no one model is consistently good at reproducing all indices. In spite of some differences in definition, the amount, interannual variability and trend of the *warm nights* index is particularly well represented by all models analysed. A pattern correlation technique however has shown that none of the models are skilful at simulating important trend patterns on regional scales, only the multi-model ensemble showing any significant skill at modelling trend patterns of *heavy precipitation days*. This may imply that some regional and/or large-scale process or processes over Australia are not well modelled or resolved, or that unforced variability is contributing largely to these changes.

More work would be required to determine to what degree recent changes in climate extremes over Australia are due to human causes, and more international cooperation is essential to ensure that the modelling and observational groups derive consistent extremes indices. However, it has been important to document the models' ability to reproduce 20th century changes. As the driest inhabited continent with marginal agricultural climate and

unique and vulnerable societies and ecosystems, stakeholders and policymakers in Australia urgently need information regarding climate extremes. We highlight here both the agreement and uncertainty around model simulations.

6. Concluding remarks

The main aim of this thesis was to identify and analyse key mechanisms driving observed changes in climate extremes in Australia. This was done by answering three primary questions:

1. How have climate extremes of temperature, precipitation and storminess changes in Australia during the observational record?

Using high quality daily temperature and precipitation data for Australia, it was shown that trends in extremes of both temperature and precipitation were very highly correlated with mean trends. Annually, the spatial correlation between trends in extremes and trends in the mean was stronger for maximum temperature than for minimum temperature. However, this relationship was reversed in winter, when minimum temperatures showed the stronger correlations. Analysis of the rate of change of extremes and means across Australia as a whole showed most stations have greater absolute trends in extremes than means. There was also some evidence that the trends of the most extreme events of both temperature and precipitation are changing more rapidly in relation to corresponding mean trends than are the trends for more moderate extreme events. The annual relationships between means and extremes of precipitation in Australia were consistent with all other global regions studied. It was also shown that severe storms at Cape Otway in south-eastern Australia have significantly declined in frequency over the past 150 years.

2. Are interactions between and changes in large-scale mechanisms driving observed trends in climate extremes?

Using the method of Self-Organizing Maps (SOMs), daily synoptic pressure patterns were produced for Australia from a combination of a high quality daily dataset of *in-situ* mean sea level pressure and ERA-40 reanalysis data for the period 1907 to 2006. Changes in the frequencies of these patterns revealed that there has been a significant reduction in the rain bearing systems affecting southern Australia since the beginning of the 20th century. This reduction has significantly impacted the frequency of severe storms in south-east Australia but there were more complex changes related to rainfall extremes at four major Australian

cities. There are also links between large scale pressure patterns and cloud regimes but again the impact of changes in cloud regimes across southern Australia appears to be different depending on the region.

SOMs were also used to categorise sea surface temperature (SST) patterns of variability for both observations and two experiments from a state of the art global climate model. The patterns were used to investigate the global response of extreme temperature and precipitation indices from the HadEX dataset to different nodes of SST variability. Results showed very strong statistically significant opposite responses from strong La Niña patterns when compared to strong El Niño patterns. Extreme maximum temperatures were significantly cooler during strong La Niña events than strong El Niño events over Australia, southern Africa, India and Canada while the converse was true for USA and north-eastern Siberia. Even intermediate patterns representing a move from weak El Niño to a weak La Niña phase also produced statistically significant increases in warm nights and warm days particularly across Scandinavia and north-west Russia. While the response of precipitation extremes to global SST patterns was less spatially coherent there were large areas across North America and central Europe which showed statistically significant differences in the response to opposite phases of ENSO. The results indicate that the variability of global SST anomalies is important for the modulation of extreme temperature and precipitation globally. Even weak phases of ENSO can have significant impacts on extreme events across large regions and this is particularly evident in high latitudes. An atmosphere-only global climate model (CAM3) forced with observed SSTs was used to investigate whether state of the art models could reproduce some of the significant responses that have been observed over Australia. Results showed that the model obtained the opposite response to that which was observed. This may indicate that some important atmospheric processes are not well captured by the model.

A further two global climate models (CCSM3 and PCM1) with output from different forcings showed however that the observed trends in *warm nights* over Australia was consistent with an anthropogenic response but was inconsistent with natural-only forcings.

3. Can state of the art climate models adequately represent observed changes in climate extremes?

Multiple simulations from nine global coupled climate models were assessed for their ability to reproduce observed trends in a set of indices representing temperature and precipitation extremes over Australia. Observed trends over the 1957 to 1999 period were compared with individual and multi-modelled trends calculated over the same period. When averaged across Australia the magnitude of trends and interannual variability of temperature extremes were well simulated by most models particularly for the *warm nights* index. The majority of models also reproduced the correct sign of trend for precipitation extremes although there was much more variation between the individual model runs. A bootstrapping technique was used to calculate uncertainty estimates and also to verify that most model runs produce plausible trends when averaged over Australia. Although very few showed significant skill at reproducing the observed spatial pattern of trends, a pattern correlation measure showed that spatial noise could not be ruled out as dominating these patterns.

There are still many unanswered questions and avenues for further research. Climate model projections are becoming increasingly important for the study of the impact that changes in climate extremes might have on *e.g.* health, biodiversity, infrastructure etc. The results presented here suggest that while climate models can reproduce variability and trends in climate extremes in a general sense, the response in Australia to important mechanisms such as the atmospheric response to global SST variability appear not to be well represented in state of the art climate models. If we could have confidence in these models they would show that future projections of the indices presented in **Chapter 5** indicate substantial increases in w*arm nights* and *heat wave duration* and decreases in *frost days* by the end of this century under the best emissions scenario estimates produced by the IPCC (*Alexander and Arblaster* 2008). The precipitation indices *simple daily intensity*, *consecutive dry days* and *very heavy precipitation contribution* are also set to more than double within the next 100 years although the uncertainty estimates across multiple climate simulations are large. *Alexander and Arblaster* (2008) also note that the magnitude of changes in both temperature and precipitation indices were found to scale with the strength of emissions. This could mean that the future anthropogenic climate change signal may eventually swamp some of the natural variations that have been important to the

modulation of Australian climate extremes in the past. Alternatively it may indicate that global climate models under-represent important aspects of natural climate variability. For this reason, the validation of climate models should remain a top priority for further research into climate extremes if we are to give useful advice to policymakers about their potential future changes and impacts.

References

Aguilar E, Peterson TC, Ramírez Obando P, Frutos R, Retana JA, Solera M, González Santos I, Araujo RM, Rosa Santos A, Valle VE, Brunet India M, Aguilar L, Álvarez L, Bautista M, Castañón C, Herrera L, Ruano E, Siani JJ, Obed F, Hernández Oviedo GI, Salgado JE, Vásquez JL, Baca M, Gutiérrez M, Centella C, Espinosa J, Martínez D, Olmedo B, Ojeda Espinoza CE, Haylock M, Núnez R, Benavides H, Mayorga R. 2005. Changes in precipitation and temperature extremes in Central America and Northern South America, 1961-2003. *Journal of Geophysical Research-Atmospheres* **110**: D23107, doi:10.1029/2005JD006119

Alexander LV, Arblaster JM. 2008. Assessing trends in observed and modelled climate extremes over Australia in relation to future projections. *International Journal of Climatology* DOI: 10.1002/joc.1730

Alexander LV, Hope P, Collins D, Trewin B, Lynch A, Nicholls N. 2007. Trends in Australia's climate means and extremes: a global context. *Australian Meteorological Magazine* **56**: 1-18

Alexander LV, Tett SFB, Jonsson T. 2005. Recent observed changes in severe storms over the United Kingdom and Iceland. *Geophysical Research Letters* **32**: L13704

Alexander LV, Zhang X, Peterson TC, Caesar J, Gleason B, Klein Tank AMG, Haylock M, Collins D, Trewin B, Rahim F, Tagipour A, Kumar Kolli R, Revadekar JV, Griffiths G, Vincent L, Stephenson DB, Burn J, Aguilar E, Brunet M, Taylor M, New M, Zhai P, Rusticucci M, Vazquez Aguirre JL. 2006. Global observed changes in daily climate extremes of temperature and precipitation. *Journal of Geophysical Research - Atmospheres* **111**: D05109. DOI:10.1029/2005JD006290

Alexandersson H, Tuomenvirta H, Schmith T, Iden K. 2000. Trends of storms in NW Europe derived from an updated pressure data set. Climate Research **14**: 71-73

Allan R, Tett S, Alexander LV. 2008. Fluctuations in autumn-winter severe storms over the British Isles: 1920 to present. *International Journal of Climatology*. DOI: 10.1002/joc.1765

Allen MR, Tett SFB. 1999. Checking for model consistency in optimal fingerprinting. *Climate Dynamics* **15**: 419-434

Anderberg MR. 1973. Cluster analysis for applications. 359pp., Elsevier, New York

Ansell TJ, Jones PD, Allan RJ, Lister D, Parker DE, Brunet M, Moberg A, Jacobeit J, Brohan P, Rayner NA, Aguilar E, Alexandersson H, Barriendos M, Brandsma T, Cox NJ, Della-Marta PM, Drebs A, Founda D, Gerstengarbe F, Hickey K, Jonsson T, Luterbacher J, Nordli O, Oesterle H, Petrakis M, Philipp A, Rodwell MJ, Saladie O, Sigro J, Slonosky V, Srnec L, Swail V, Garcia-Suarez AM, Tuomenvirta H, Wang X, Wanner H, Werner P, Wheeler D, Xoplaki E. 2006. Daily mean sea level pressure reconstructions for the European-North Atlantic region for the period 1850-2003. *Journal of Climate* **19**: 2717-2742

Bärring L, Fortuniak K. 2008. Multi-indices analysis of southern Scandinavian storminess 1780 – 2005 and links to inter-decadal variations in the NW Europe - North Sea region. *International Journal of Climatology* DOI: 10.1002/joc.1842

Bärring L, von Storch H. 2004. Scandinavian storminess since about 1800. *Geophysical Research Letters* **31**: L20202

Barsugli JJ, Shin SI, Sardeshmukh PD. 2005. Sensitivity of global warming to the pattern of tropical ocean warming. *Climate Dynamics* **27**: 483-492

Bates BC, Hope P, Ryan B, Smith I, Charles S. 2008. Key findings from the Indian Ocean Climate Initiative and their impact on policy development in Australia. *Climatic Change* doi 10.1007/s10584-007-9390-9

Bengtsson L, Hodges KI, Roekner E. 2006. Storm tracks and climate change. *Journal of Climate* **19**: 3518-3543

Bonan GB, Oleson KW, Vertenstein M, Levis S, Zeng X, Dai Y, Dickinson RE, Yang Z-L. 2002. The land surface climatology of the Community Land Model coupled to the NCAR Community Climate Model. *Journal of Climate* **15**: 3123-3149

Boville, B.A., P.J. Rasch, J.J. Hack, and J.R. McCaa, 2006: Representation of clouds and precipitation processes in the Community Atmosphere Model (CAM3). *Journal of Climate* **19**: 2184-2198

Caesar J, Alexander L, Vose R. 2006. Large-scale changes in observed daily maximum and minimum temperatures: Creation and analysis of a new gridded data set. *Journal of Geophysical Research* **111**: D05101, doi:10.1029/2005JD006280

Cai W, Cowan T. 2006. SAM and regional rainfall in IPCC AR4 models: Can anthropogenic forcing account for southwest Western Australian winter rainfall reduction? *Geophysical Research Letters* **33**: L24708, doi:10.1029/2006GL028037

Cai W, Shi G, Li Y. 2005. Multidecadal fluctuations of winter rainfall over southwest Western Australia simulated in the CSIRO Mark 3 coupled model. *Geophysical Research Letters* **32**: L12701, doi:10.1029/2005GL022712

Cassano JJ, Uotila P, Lynch AH. 2006. Changes in synoptic weather patterns in the polar regions in the 20th and 21st centuries, Part 1: Arctic. *International Journal of Climatology* **26**(8): 1027-1049

Cavazos T. 2000. Using self-organizing maps to investigate extreme climate events: An application to wintertime precipitation in the Balkans. *Journal of Climate* **13:** 1718-1732

Chambers LE. 2006. Associations between climate change and natural systems in Australia. *Bulletin of the American Meteorological Society* **87**: 201-206

Chambers LE, Griffiths GM. 2008. The changing nature of temperature extremes in Australia and New Zealand. *Australian Meteorological Magazine* **57**: 13-35

Chen C-T, Knutson T. 2008. On the verification and comparison of extreme rainfall indices from climate models. *Journal of Climate* **21**: 1605-1621

Christidis N, Stott PA, Brown S, Hegerl GC, Caesar J. 2005. Detection of changes in temperature extremes during the second half of the 20th century. *Geophysical Research Letters* **32**: L20716. DOI:10.1029/2005GL023885

Collins DA, Della-Marta PM, Plummer N, Trewin BC. 2000. Trends in annual frequencies of extreme temperature events in Australia. *Australian Meteorological Magazine* **49**: 277-292

Collins WD, Rasch PJ, Boville BA, Hack JJ, McCaa JR, Williamson DL, Briegleb BP, Bitz CM, Lin SJ, Zhang MH. 2006a. The formulation and atmospheric simulation of the Community Atmosphere Model version 3 (CAM3). *Journal of Climate* **19**: 2144-2161

Collins WD, Bitz CM, Blackmon ML, Bonan GB, Bretherton CS, Carton JA, Chang P, Doney SC, Hack JJ, Henderson TB, Kiehl JT, Large WG, McKenna DS, Santer BD, Smith RD. The Community Climate System Model version 3 (CCSM3). 2006b. *Journal of Climate* **19**: 2122-2143

CSIRO (Commonwealth Scientific and Industrial Research Organisation). 2001. Climate Projections for Australia. *CSIRO Atmospheric Research*, Melbourne, 8 pp., http://www.dar.csiro.au/publications/projections2001.pdf

CSIRO-Bureau of Meteorology. 2007. Climate Change in Australia, *CSIRO*, 148 pp

Della-Marta PM, Collins DA, Braganza K. 2004. Updating Australia's high quality annual temperature dataset. *Australian Meteorological Magazine* **53**: 75-93

Deser C, Wallace JM. 1987. El Niño events and their relation to the Southern Oscillation: 1925–1986. *Journal of Geophysical Research* **92:** 189–196

Deser C, Wallace JM. 1990. Large-scale atmospheric circulation features of warm and cold episodes in the tropical pacific. *Journal of Climate* **3:** 1254–1281

Easterling DR, Meehl GA, Parmesan C, Changnon SA, Karl TR, Mearns LO. 2000. Climate extremes: Observations, modeling, and impacts. *Science* **289**: 2068-2074

Emanuel K. 2005. Increasing destructiveness of tropical cyclones over the past 30 years. *Nature* **436**: 686-688, doi:10.1038/nature03906

Fitzharris B, Hennessy K, Bates B, Hughes L, Howden M, Salinger J, Harvey N, Warrick R. 2007. In: Climate Change 2007: Impacts, Adaptation and Vulnerability. Working Group II contribution to the Intergovernmental Panel on Climate Change Fourth Assessment Report. Cambridge University Press: Cambridge UK and New York USA, 1032 pp

Folland CK, Karl TR, Christy JR, Clarke RA, Gruza GV, Jouzel J, Mann ME, Oerlemans J, Salinger MJ, Wang SW. 2001. Observed climate variability and change. In: Climate Change 2001: The Scientific Basis. Contribution of Working Group I to the Third Assessment Report of the Intergovernmental Panel on Climate Change. Cambridge University Press, Cambridge UK and New York USA, 881 pp

Foullet A, Rey G, Laurent F, Pavillon G, Bellec S, Guihenneuc-Jouyaux C, Clavel J, Jougla E, Hemon D. 2007. Excess mortality related to the August 2003 heat wave in France, *International Archives of Occupational and Environmental Health* **80**: 16-24

Frederiksen JS, Frederiksen CS. 2007. Interdecadal changes in southern hemisphere winter storm track modes. *Tellus Series A-Dynamic Meteorology and Oceanography* **59**: 599-617

Frich P, Alexander LV, Della-Marta P, Gleason B, Haylock M, Klein Tank AMG, Peterson T. 2002. Observed coherent changes in climatic extremes during the second half of the twentieth century. *Climate Research* **19**: 193-212

Gallant AJE, Hennessy KJ and Risbey J. 2007. Trends in rainfall indices for six Australian regions: 1910-2005. *Australian Meteorological Magazine* **56**: 223-239

Golub G, Van Loan CF. 1996. Matrix Computations - Third Edition. Baltimore: The Johns Hopkins University Press. p. 53. ISBN 0-8018-5413-X

Green D, Alexander L, McInnes K, Church J, Nicholls N. 2009. Will climate change force Torres Strait Islanders to be the first 'internally displaced' Australians? *Climatic Change* (submitted).

Griffiths GM, Chambers LE, Haylock MR, Manton MJ, Nicholls N, Baek H.-J, Choi Y, Della-Marta PM, Gosai A, Iga N, Lata R, Laurent V, Maitrepierre L, Nakamigawa H, Ouprasitwong N, Solofa D, Tahani L, Thuy DT, Tibig L, Trewin B, Vediapan K, Zhai P. 2005. Change in mean temperature as a predictor of extreme temperature change in the Asia-Pacific region. *International Journal of Climatology* **25**: 1301-1330

Groisman PY, Knight RW, Easterling DR, Karl TR, Hegerl GC, Razuvaev VAN. 2005. Trends in Intense Precipitation in the Climate Record. *Journal of Climate* **18**:1326–1350

Hack JJ. 1994. Parameterization of moist convection in the NCAR Community Climate Model, CCM2. *Journal of Geophysical Research* **99**: 5551-5568

Hack JJ, Caron JM, Yeager SG, Oleson KW, Holland MM, Truesdale JE, Rasch PJ. 2006. Simulation of the global hydrological cycle in the CCSM Community Atmosphere Model version 3 (CAM3): Mean features. *Journal of Climate* **19**: 2199-2221

Halpert MS, Ropelewski CF. 1992. Surface temperature patterns associated with the Southern Oscillation. *Journal of Climate* **5**: 577-593

Haylock M, Nicholls N. 2000. Trends in extreme rainfall indices for an updated high quality data set for Australia, 1910-1998. *International Journal of Climatology* **20**: 1533-1541

Haylock MR. Peterson T, Abreu de Sousa JR, Alves LM, Ambrizzi T, Baez J, Barbosa JI, Barros VR, Berlato MA, Bidegain M, Coronel G, Corradi V, Grimm AM, Jaildo dos Anjos R, Karoly D, Marengo JA, Marino MB, Meira PR, Miranda GC, Molion L, Moncunill DF, Nechet D, Ontaneda G, Quintana J, Ramirez E, Rebello E, Rusticucci M, Santos JL, Varillas IT, Villanueva JG, Vincent L, Yumiko M. 2006. Trends in total and extreme South America rainfall 1960-2000 and links with sea surface temperature. *Journal of Climate* **19**: 1490-1512

Hegerl GC, Zwiers FW, Stott PA, Kharin VV. 2004. Detectibility of anthropogenic changes in annual temperature and precipitation extremes. *Journal of Climate* **17**: 3683-3700

Hennessy KJ, Suppiah R, Page CM. 1999. Australian rainfall changes, 1910-1995. *Australian Meteorological Magazine* **48**: 1-13

Hewitson BC, Crane RG. 2002. Self-organizing maps: applications to synoptic climatology. *Climate Research* **22**: 13-26

Hope PK. 2006. Projected future changes in synoptic systems influencing southwest Western Australia. *Climate Dynamics* **26**: 751-764

Hope PK, Drosdowsky W, Nicholls, N. 2006. Shifts in the synoptic systems influencing southwest Western Australia. *Climate Dynamics* **26**: 751-764

Hoyos CD, Agudelo PA, Webster PJ, Curry JA. 2006. Deconvolution of the factors contributing to the increase in global hurricane intensity. *ScienceExpress* doi:10.1126/science.1123560

Hughes TP, Baird AH, Bellwood DR, Card M, Connolly SR, Folke C, Grosberg R, Hoegh-Guldberg O, Jackson JBC, Kleypas J, Lough JM, Marshall P, Nystrom M, Palumbi SR, Pandolfi JM, Rosen B, Roughgarden J. 2003. Climate change, human impacts, and the resilience of coral reefs. *Science* **301**: 929-933

Hurrell JW, Hack JJ, Phillips AS, Caron J, Yin J. 2006. The dynamical simulation of the Community Atmosphere Model version 3 (CAM3). *Journal of Climate* **19**: 2162-2183

Hurrell JW, Hack JJ, Shea D, Caron JM, Rosinski J. 2008. A new sea surface temperature and sea ice boundary dataset for the Community Atmosphere Model. *Journal of Climate* **21**: 5145-5153

Intergovernmental Panel on Climate Change (IPCC) 2001. Climate Change 2001: The Scientific Basis: Contribution of Working Group I to the Third Assessment Report of the

Intergovernmental Panel on Climate Change, edited by J. T. Houghton et al., 881 pp., Cambridge Univ. Press, New York

Intergovernmental Panel on Climate Change (IPCC) 2007. Climate Change 2007 - The Physical Science Basis: Contribution of Working Group I to the Fourth Assessment Report of the IPCC, edited by S. Solomon et al., ISBN 978 0521 88009-1 Hardback; 978 0521 70596-7 Paperback, Cambridge Univ. Press, New York

Indian Ocean Climate Initiative (IOCI). 2002. Climate variability and change in south west Western Australia. Indian Ocean Climate Initiative Panel, Perth, 34 pp

Indian Ocean Climate Initiative (IOCI). 2005. IOCI reports key findings of recent research in south-western climate. IOCI Bulletin 6. http://www.ioci.com.au

Jakob C, Tselioudis G. 2003. Objective identification of cloud regimes in the Tropical Western Pacific, *Geophysical Research Letters* **30**: doi:10.1029/2003GL018367

Jones DA. 1998. The prediction of Australian land surface temperatures using near global sea surface temperature patterns. *BMRC Research Report 70*, Bureau of Meteorology, Melbourne

Jones DA, Trewin BC. 2000. On the relationships between the El Niño-Southern Oscillation and Australian land surface temperature. *International Journal of Climatology* **20**: 697-719

Kalnay E, Kanamitsu M, Kistler R, Collins W, Deaven D, Gandin L, Iredell M, Saha S, White G, Woollen J, Zhu Y, Chelliah M, Ebisuzaki W, Higgins W, Janowiak J, Mo KC, Ropelewski C, Wang J, Leetmaa A, Reynolds R, Jenne R, Joseph D. 1996. The NCEP/NCAR 40-year reanalysis project. *Bulletin of the American Meteorological Society* **77**: 437-471

Karoly DJ, Wu QG. 2005. Detection of regional surface temperature trends. *Journal of Climate* **18**: 4337-4343

Kato S, Hinkelman LM, Cheng AN. 2006. Estimate of satellite-derived cloud optical thickness and effective radius errors and their effect on computed domain-averaged irradiances. *Journal of Geophysical Research* **111**: D17201

Katz RW. 1999. Extreme value theory for precipitation: sensitivity analysis for climate change. *Advances in Water Resources* **23**: 133-139

Katz RW, Brown BG. 1992. Extreme events in a changing climate: Variability is more important than averages. *Climatic Change* **21**: 289-302

Kendall MG. 1975. Rank Correlation Methods, Griffin, London

Kenyon J, Hegerl GC. 2008. Influence of modes of climate variability on global temperature extremes. *Journal of Climate* **21**: 3872-3889

Kharin VV, Zwiers F, Zhang X, Hegerl GC. 2007. Changes in temperature and precipitation extremes in the IPCC Ensemble of Global Coupled Model Simulations. *Journal of Climate* **20**: 1419-1444

Kiem AS, Franks SW, Kuczera G. 2003. Multi-decadal variability of flood risk. *Geophysical Research Letters* **30**: 1035

Kiktev D, Caesar J, Alexander LV, Shiogama H, Collier M. 2007. Comparison of observed and multimodeled trends in annual extremes of temperature and precipitation. *Geophysical Research Letters* **34**: L10702.DOI:10.1029/2007GL029539

Kiktev D, Sexton DMH, Alexander L, Folland CK. 2003. Comparison of modelled and observed trends in indices of daily climate extremes. *Journal of Climate* **16**: 3560-3571

Kiladis GN, Diaz HF. 1987. Global climatic anomalies associated with extremes in Southern Oscillation. *Journal of Climate* **2:** 1069–1090

Kistler R, Kalnay E, Collins W, Saha S, White G, Woollen J, Chelliah M, Ebisuzaki W, Kanamitsu M, Kousky V, van den Dool H, Jenne R, Fiorino M. 2001. The NCEP-NCAR

50-year reanalysis: Monthly means CD-ROM and documentation. *Bulletin of the American Meteorological Society* **82**(2): 247-267

Klein Tank AMG, Peterson TC, Quadir DA, Dorji S, Xukai Z, Hongyu T, Santhosh K, Joshi UR, Jaswal AK, Kolli RK, Sikder A, Deshpande NR, Revadekar J, Yeleuova K, Vandasheva S, Faleyeva M, Gomboluudev P, Budhathoki KP, Hussain A, Afzaal M, Chandrapala L, Anvar H, Amanmurad D, Asanova VS, Jones PD, New MG, Spektorman T. 2006. Changes in daily temperature and precipitation extremes in Central and South Asia. *Journal of Geophysical Research* **111**: D16105, doi:10.1029/2005JD006316

Kohonen T. 2001. Self-organizing maps of massive databases. *Engineering Intelligent Systems for Electrical Engineering And Communications* **9**: 179-185

Lambert FH, Gillett NP, Stone DA, Huntingford C. 2005. Attribution studies of observed land precipitation changes with nine coupled models. *Geophysical Research Letters* **32**: L18704. DOI:10.1029/2005GL023654

Lavery BM, Kariko AP, Nicholls N. 1992. A high-quality historical rainfall data set for Australia. *Australian Meteorological Magazine* **40**: 33-39

Lavery B, Joung G, Nicholls N. 1997. An extended high-quality historical rainfall dataset for Australia. *Australian Meteorological Magazine* **46**: 27-38

Leloup JA, Lachkar Z, Boulanger JP, Thiria S 2007a. Detecting decadal changes in ENSO using neural networks. *Climate Dynamics* **28**: 147-162

Leloup J, Lengaigne M, Boulanger JP. 2007b. Twentieth century ENSO characteristics in the IPCC database. *Climate Dynamics* **30**: 277-291

Li Y, Cai W, Campbell EP. 2005. Statistical modelling of extreme rainfall in southwest Western Australia. *Journal of Climate* **18**: 852-863

Li G, Zhang GJ. 2008. Understanding biases in shortwave cloud radiative forcing in the national center for atmospheric research community atmosphere model (CAM3) during El Nino. *Journal of Geophysical Research* **113**: D02103

Lim EP, Simmonds I. 2007. Southern Hemisphere winter extratropical cyclone characteristics and vertical organization observed with ERA-40 data in 1979-2001. *Journal of Climate*, *20*, 2675-2690

Lynch AH, Brunner RD. 2007. Context and climate change: An integrated assessment for Barrow, Alaska. *Climatic Change* **82**: 93-111

Lynch A, Uotila P, Cassano JJ. 2006. Changes in synoptic weather patterns in the polar regions in the 20th and 21st centuries, Part 2: Antarctic. *International Journal of Climatology* **26**: 1181-1199

McBride JL, Nicholls N. 1983. Seasonal Relationships between Australian Rainfall and the Southern Oscillation. *Monthly Weather Review* **111**: 1998-2004

Malmgren BA, Winter A. 2000. Climate zonation in Puerto Rico based on principal components analysis and an artificial neural network. *Journal of Climate* **12**: 977-985

Mann HB. 1945. Nonparametric trends against test. *Econometrica* **13**: 245-259

Manton MJ, Della-Marta PM, Haylock MR, Hennessy KJ, Nicholls N, Chambers LE, Collins DA, Daw G, Finet A, Gunawan D, Inape K, Isobe H, Kestin TS, Lefale P, Leyu CH, Lwin T, Maitrepierre L, Ouprasitwong N, Page CM, Pahalad J, Plummer N, Salinger MJ, Suppiah R, Tran VL, Trewin B, Tibig I, Yee D. 2001. Trends in extreme daily rainfall and temperature in southeast Asia and the South Pacific: 1916-1998. *International Journal of Climatology* **21**: 269-284

Marchand R, Haynes J, Mace GG, Ackerman T, Stephens G. 2009. A comparison of simulated cloud radar output from the multiscale modeling framework global climate model with CloudSat cloud radar observations. *Journal of Geophysical Research* **114**: D00A20

Marshall AG, Lynch AH, Görgen K. 2009. A model intercomparison study of the Australian summer monsoon. Part I: General Characteristics. *Australian Meteorological Magazine* (submitted).

Matulla C, Schöner W, Alexandersson H, von Storch H, Wang, XL. 2008. European Storminess: Late 19th Century to Present. Climate Dynamics 31: 125-130. DOI: 10.1007/s00382-007-0333-y

Meehl GA, Arblaster JM, Tebaldi C. 2005. Understanding future patterns of precipitation extremes in climate model simulations. *Geophysical Research Letters* **32**: L18719. DOI: 10.1029/2005GL023680

Meehl GA, Stocker TF, Collins WD, Friedlingstein P, Gaye AT, Gregory JM, Kitoh A, Knutti R, Murphy JM, Noda A, Raper SCB, Watterson IG, Weaver AJ, Zhao Z.-C. 2007a. Global Climate Projections. In: Climate Change 2007: The Physical Science Basis. Contribution of Working Group I to the Fourth Assessment Report of the Intergovernmental Panel on Climate Change [Solomon, S., D. Qin, M. Manning, Z. Chen, M. Marquis, K.B. Avery, M. Tignor and H.L. Miller (eds.)]. Cambridge University Press, Cambridge, United Kingdom and New York, NY, USA

Meehl GA, Arblaster JM, Tebaldi C. 2007b. Contributions of natural and anthropogenic forcing to changes in temperature extremes over the U.S. *Geophysical Research Letters* **34**: L19709, doi:10.1029/2007GL030948

Meehl GA, Collins WD, Boville BA, Kiehl JT, Wigley TML, Arblaster JM. 2000. Response of the NCAR Climate System Model to Increased CO2 and the Role of Physical Processes. *Journal of Climate* **13**: 1879-1898

Meehl GA, Tebaldi C. 2004. More intense, more frequent and longer lasting heat waves in the 21st century. *Science* **305**: 994-997

Meehl GA, Tebaldi C, Nychka D. 2004. Changes in frost days in simulations of 21st century climate. *Climate Dynamics* **23**: 495-511

Meehl GA, Washington WM, Santer BD, Collins WD, Arblaster JM, Hu A, Lawrence DM, Teng H, Buja LE, Strand Jr. WG. 2006. Climate change projections for the 21st century and climate change commitment in the CCSM3. *Journal of Climate* **19**: 2597-2616

Menne MJ, Williams CN. 2005. Detection of undocumented change points: on the use of multiple test statistics and composite reference series. *Journal of Climate* **18:** 4271–86

Michaelides S, Pattichis CS, Kleovoulou G. 2001. Classification of rainfall variability by using artificial neural networks. *International Journal of Climatology* **21**: 1401-1414

Murphy BF, Timbal B. 2008. A review of recent climate variability and climate change in southeastern Australia. *International Journal of Climatology* **28**: 859-879

New M, Hewitson B, Stephenson DB, Tsiga A, Kruger A, Manhique A, Gomez B, Coelho B, Caio AS, Masisi DN, Kululanga E, Mbambalala E, Adesina F, Saleh H, Kanyanga J, Adosi J, Bulane L, Fortunata L, Mdoka ML, Lajoie R. 2006. Evidence of trends in daily climate extremes over Southern and West Africa. *Journal of Geophysical Research* **111**: D14102, doi:10.1029/2007GL030948

Nicholls N. 2003. Continued anomalous warming in Australia. *Geophysical Research Letters* **30**: 1370

Nicholls N, Alexander L. 2007. Has the climate become more variable or extreme? *Progress in Physical Geography* **32**: 1-11

Nicholls N, Alexander L, Macadam I. 2009. The use of proxy data to diagnose problems in the historical record of Australian region tropical cyclone numbers. *Journal of Climate* (submitted).

Nicholls N, Drosdowsky W, Lavery B. 1997. Australian rainfall variability and change. *Weather* **52**: 66-72

Nicholls N, Gruza G, Jouzel J, Karl T, Ogallo L, Parker D. 1996a. Observed Climate Variability and Change. Chapter 3 in Climate Change 1995: The Science of Climate

Change. JT Houghton, LG Meira Filho, BA Callander, N Harris, A Kattenberg, K Maskell (Eds). Cambridge University Press, Cambridge, UK. 132-192

Nicholls N, Lavery B, Frederiksen C, Drosdowsky W, Torok S. 1996b. Recent apparent changes in relationships between the El Niño - Southern oscillation and Australian rainfall and temperature. *Geophysical Research Letters* **23**: 3357-3360

Oleson KW, Dai Y, Bonan GB, Bosilovich M, Dickinson R, Dirmeyer P, Hoffman F, Houser P, Levis S, Niu G-Y, Thornton P, Vertenstein M, Yang Z-L, Zeng X. 2004. Technical description of the Community Land Model (CLM). *Technical Report NCAR/TN-461+STR*, National Center for Atmospheric Research, Boulder, CO. 80307-3000, 174 pp

Perkins SE, Pitman AJ, Holbrook NJ, McAneney J. 2007. Evaluation of the AR4 climate models' simulated daily maximum temperature, minimum temperature and precipitation over Australia using probability density functions. *Journal of Climate* **20**: 4356-4376

Peterson TC, Manton MJ. 2008. Monitoring changes in climate extremes: A tale of international collaboration. *Bulletin of the American Meteorological Society* **89**: 1266-1271. DOI:10.1175/2008BAMS2501.1

Philipp A, Della-Marta PM, Jacobeit J, Fereday DR, Jones PD, Moberg A, Wanner H. 2006. Long term variability of daily North Atlantic-European pressure patterns since 1850 classified by simulated annealing clustering. *Journal of Climate* **20**: 4065-4095

Pitman AJ, Narisma GT, Pielke Sr. RA, Holbrook NJ. 2004. Impact of land cover change on the climate of southwest Western Australia. *Geophysical Research Letters* **109**: Doi:10.1029/2003JD004347

Pitman AJ, Narisma GT. 2005. The role of land surface processes in regional climate change: a case study of future land cover change over south western Australia. *Meteorology and Atmospheric Physics* **89**: 235-249

Pittock B, Wratt D, Basher R, Bates B, Finlayson M, Gitay H, Woodward A. 2001. Australia and New Zealand. In: Climate Change 2001: Impacts, Adaptation and

Vulnerability. Contribution of Working Group II to the Third Assessment Report of the Intergovernmental Panel on Climate Change. Cambridge University Press, Cambridge UK and New York USA, 1032 pp

Plummer N, Salinger MJ, Nicholls N, Suppiah R, Hennessy KJ, Leighton RM, Trewin B, Page CM, Lough JM. 1999. Changes in climate extremes over the Australian region and New Zealand during the twentieth century. *Climatic Change* **42**: 183-202

Pezza AB, Simmonds I, Renwick JA. 2007. Southern Hemisphere cyclones and anticyclones: Recent trends and links with decadal variability in the Pacific Ocean. *International Journal of Climatology* **27**: 1403-1419

Power S, Sadler B, Nicholls N. 2005. The influence of climate science on water management in WA: lessons for climate scientists. *Bulletin of the American Meteorological Soc*iety **86**: 839-844

Power S, Tseitkin F, Torok S, Lavery B, Dahni R, McAvaney B. 1998. Australian temperature, Australian rainfall and the Southern Oscillation, 1910-1992: coherent variability and recent changes. *Australian Meteorological Magazine* **47**: 85-101

Rasmusson EM, Carpenter TH. 1982. Variations in tropical sea surface temperature and surface wind fields associated with the Southern Oscillation/El Niño. *Monthly Weather Review* **110:** 354–384

Rayner NA, Parker DE, Horton EB, Folland CK, Alexander LV, Rowell DP, Kent EC, Kaplan A. 2003. Global analyses of sea surface temperature, sea ice, and night marine air temperature since the late nineteenth century. *Journal of Geophysical Research - Atmospheres* **108**: D14 4407

Ropelewski CF, Halpert MS. 1986. North American precipitation and temperature patterns associated with the El Niño/ Southern Oscillation (ENSO). *Monthly Weather Review* **114:** 2352–2362

Ropelewski CF, Halpert MS. 1987. Global and regional scale precipitation patterns associated with El Niño/Southern Oscillation. *Monthly Weather Review* **115**:1606-1626

Rossow WB, Schiffer RA. 1991. ISCCP cloud data products. *Bulletin of the American Meteorological Society* **72**: 2-20

Rossow WB, Tselioudis G, Polak A, Jakob C. 2005. Tropical climate described as a distribution of weather states indicated by distinct mesoscale clod property mixtures. *Geophysical Research Letters* **32**: L21812, doi:10.1029/2005GL024584

Rotstayn LD, Cai W, Dix MR, Farquar GD, Feng Y, Ginoux P, Herzog M, Ito A, Penner JE, Roderick ML, Wang M. 2007. Have Australian rainfall and cloudiness increased due to the remote effects of the Asian anthropogenic aerosols? *Journal of Geophysical Research* **112**: D09202. DOI:10.1029/2006JD007712

Salinger MJ, Griffiths GM. 2001. Trends in New Zealand daily temperature and rainfall extremes. *International Journal of Climatology* **21**: 1437-1452

Samad T, Harp SA. 1992. Self-organization with partial data. *Network-Computations in Neural Systems* **3**: 205-212

Santer BD, Wigley TML, Gleckler PJ, Bonfils C, Wehner MF, AchutaRao K, Barnett TP, Boyle JS, Brüggemann W, Fiorino M, Gillett N, Hansen JE, Jones PD, Klein SA, Meehl GA, Raper SCB, Reynolds RW, Taylor KE, Washington WM. 2006. Forced and unforced ocean temperature changes in Atlantic and Pacific tropical cyclogenesis regions. *Proceedings of the National Academy of Sciences* **103**: 13905-13910. DOI:10.1073/pnas.0602861103

Scaife AA, Folland CK, Alexander LV, Moberg A, Knight JR. 2008. European climate extremes and the North Atlantic Oscillation. *Journal of Climate* **21**: 72-83

Schmidt H, von Storch H. 1993. German Bight storms analyzed. *Nature* **365**: 791

Shi G, Cai W, Cowan T, Ribbe J, Rotstayn L, Dix M. 2008. Variability and trend of the northwest Western Australia Rainfall: observations and coupled climate modelling. *Journal of Climate* **21**: 2938-2959

Sillmann J, Roekner E. 2008. Indices for extreme events in projections of anthropogenic climate change. *Climatic Change* **86**: 83-104

Simmonds I, Keay K. 2000. Mean southern hemisphere extratropical cyclone behavior in the 40-year ncep-ncar reanalysis. *Journal of Climate* **13**: 873-885

Smits A, Klein Tank AMG, Können GP. 2005. Trends in storminess over the Netherlands, 1962-2002. *International Journal of Climatology* **25**: 1331-1344

Tebaldi C, Hayhoe K, Arblaster JM, Meehl GA. 2006. Going to the extremes: An intercomparison of model-simulated historical and future changes in extreme events. *Climatic Change* **79**: 185-211 DOI:10.1007/s10584-006-9051-4

Tett SFB, Stott PA, Allen MR, Ingram WJ, Mitchell JFB. 1999. Causes of twentieth-century temperature change near the Earth's surface. *Nature* **399**: 569-572

Thompson DWJ, Solomon S. 2002. Interpretation of recent southern hemisphere climate change. *Science* **296**: 895-899

Timbal B, Arblaster JM, 2006. Land cover change as an additional forcing to explain the rainfall decline in the south west of Australia, *Geophysical Research Letters* **33**: L07717 doi:10.1029/2005GL025361

Timbal B, Arblaster JM, Power SB. 2006. Attribution of the late 20th century rainfall decline in South-West Australia. *Journal of Climate* **19**: 2046-2065

Torok SJ, Nicholls N. 1996. A historical annual temperature dataset for Australia. *Australian Meteorological Magazine* **45**: 251-260

Trenberth KE. 1991: Storm tracks in the Southern Hemisphere. *Journal of Atmospheric Science* **48**: 2159-2178

Trenberth KE, Jones PD, Ambenje P, Bojariu R, Easterling D, Klein Tank A, Parker D, Rahimzadeh F, Renwick JA, Rusticucci M, Soden B, Zhai P. 2007. Observations: Surface and Atmospheric Climate Change. In: Climate Change 2007: The Physical Science Basis. Contribution of Working Group I to the Fourth Assessment Report of the Intergovernmental Panel on Climate Change [Solomon, S., D. Qin, M. Manning, Z. Chen, M. Marquis, K.B. Averyt, M. Tignor and H.L. Miller (eds.)]. Cambridge University Press, Cambridge, United Kingdom and New York, NY, USA

Trewin BC. 2001. The development of a high-quality daily temperature data set for Australia. 11th Symposium on Meteorological Observations and Instrumentation, Albuquerque, New Mexico, 14-18 January 2001, 279-284

Tryhorn L, Risbey J. 2006. On the distribution of heat waves over the Australian region. *Australian Meteorological Magazine* **55**: 169-182

Ummenhofer CC, Sen Gupta A, Pook MJ, England MH. 2008. Anomalous rainfall over southwest Western Australia forced by Indian Ocean sea surface temperatures. *Journal of Climate* **21**: 5113-5134

Uppala SM, Kallberg PW, Simmons AJ, Andrae U, Bechtold VD, Fiorino M, Gibson JK, Haseler J, Hernandez A, Kelly GA, Li X, Onogi K, Saarinen S, Sokka N, Allan RP, Andersson E, Arpe K, Balmaseda MA, Beljaars ACM, Van De Berg L, Bidlot J, Bormann N, Caires S, Chevallier F, Dethof A, Dragosavac M, Fisher M, Fuentes M, Hagemann S, Holm E, Hoskins BJ, Isaksen L, Janssen PAEM, Jenne R, McNally AP, Mahfouf JF, Morcrette JJ, Rayner NA, Saunders RW, Simon P, Sterl A, Trenberth KE, Untch A, Vasiljevic D, Viterbo P, Woollen J. 2005. The ERA-40 re-analysis. *Quarterly Journal of the Royal Meteorological Society* 131: 2961-3012

Vernon-Kidd D, Kiem AS. 2008. On the relationship between large-scale climate modes and regional synoptic patterns that drive Victorian rainfall. *Hydrology and Earth System Science Discussions* **5**: 2791-2815

Vincent LA, Peterson TC, Barros VR, Marino MB, Rusticucci M, Carrasco G, Ramirez E, Alves LM, Ambrizzi T, Berlato MA, Grimm AM, Marengo JA, Molion L, Moncunill DF, Rebello E, Anunciação YMT, Quintana J, Santos J, Baez J, Coronel G, Garcia J, Trebejo I, Bidegain M, Haylock MR, Karoly D. 2005. Observed trends in indices of daily temperature extremes in South America 1960-2000. *Journal of Climate* **15**: 1322-1334

Viney NR, Bates BC. 2004. It never rains on Sunday: the prevalence and implications of untagged multi-day rainfall accumulations in the Australian high quality data set. *International Journal of Climatology* **24**: 1171-1192

Wang XL. 2008. Accounting for autocorrelation in detecting mean-shifts in climate data series using the penalized maximal t or F test. *Journal of Applied Meteorology and Climatology* **47**: 2423-2444

Wang XL, Swail VR. 2001. Changes in extreme wave heights in Northern Hemisphere oceans and related atmospheric circulation regimes. *Journal of Climate* **14**: 2204-2220

Wardle R, Smith I. 2004. Modelled response of the Australian monsoon to changes in land surface temperatures. *Geophysical Research Letters* **31**: L16205. DOI:10.1029/2004GL020157

WASA Group. 1998. Changing waves and storms in the northeast Atlantic? *Bulletin of the American Meteorological Society* **79**: 741–760

Webster PJ, Holland GJ, Curry JA, Change H–R. 2005. Changes in tropical cyclone number, duration, and intensity in a warming environment. *Science* **309**: 1844-1846, doi:10.1126/science.1116448

Wilks DS. 1997. Resampling hypothesis tests for autocorrelated fields. *Journal of Climate* **10**: 65-82

Wijngaard JB, Klein Tank AMG, Können GP. 2003. Homogeneity of 20th century European daily temperature and precipitation series. *International Journal of Climatology* **23**: 679–92

Zhang GJ, McFarlane NA. 1995. Sensitivity of climate simulations to the parameterization of cumulus convection in the Canadian Climate Centre general circulation model. *Atmosphere-Ocean* **33**: 407-446

Zhang GJ, Wang H. 2006. Toward mitigating the double ITCZ problem in NCAR CCSM3. *Geophysical Research Letters* **33**: L06709, doi:10.1029/2005GL025229

Zhang M. 2004. Cloud-climate feedback: How much do we know? *Observation, Theory, and Modeling of Atmospheric Variability,* X. Zhu et al., Eds., World Scientific Series on Meteorology of East Asia, Vol. 3, World Scientific Publishing, 161–183

Zhang X, Aguilar E, Sensoy S, Melkonyan H, Tagiyeva U, Ahmed N, Kutaladze N, Rahimzadeh F, Taghipour A, Hantosh TH, Albert P, Semawi M, Karam Ali M, Halal Said Al-Shabibi M, Al-Oulan Z, Zatari T, Al Dean Khelet I., Hammoud S, Demircan M, Eken M, Adiguzel M, Alexander L, Peterson T, Wallis T. 2005. Trends in Middle East Climate Extremes Indices during 1930-2003. *Journal of Geophysical Research* **110**: D22104, doi:10.1029/2005JD006181

Zhang XB, Hegerl G, Zwiers FW, Kenyon J. 2005. Avoiding inhomogeneity in percentile-based indices of temperature extremes. *Journal of Climate* **18**: 1641-1651

Zhang X, Vincent LA, Hogg WD, Niitsoo A. 2000. Temperature and precipitation trends in Canada during the 20th century. *Atmosphere-Ocean* **38**: 395–429

Zou X, Alexander LV, Parker DE, Caesar J. 2006. Variations in severe storms over China. *Geophysical Research Letters* **33**: L17701, doi:10.1029/2006GL026131.